UNIVERSIDADE ABERTA
www.uab.pt

Spherical tilings, GeoGebra contributions to their combinatorial and geometrical classification.

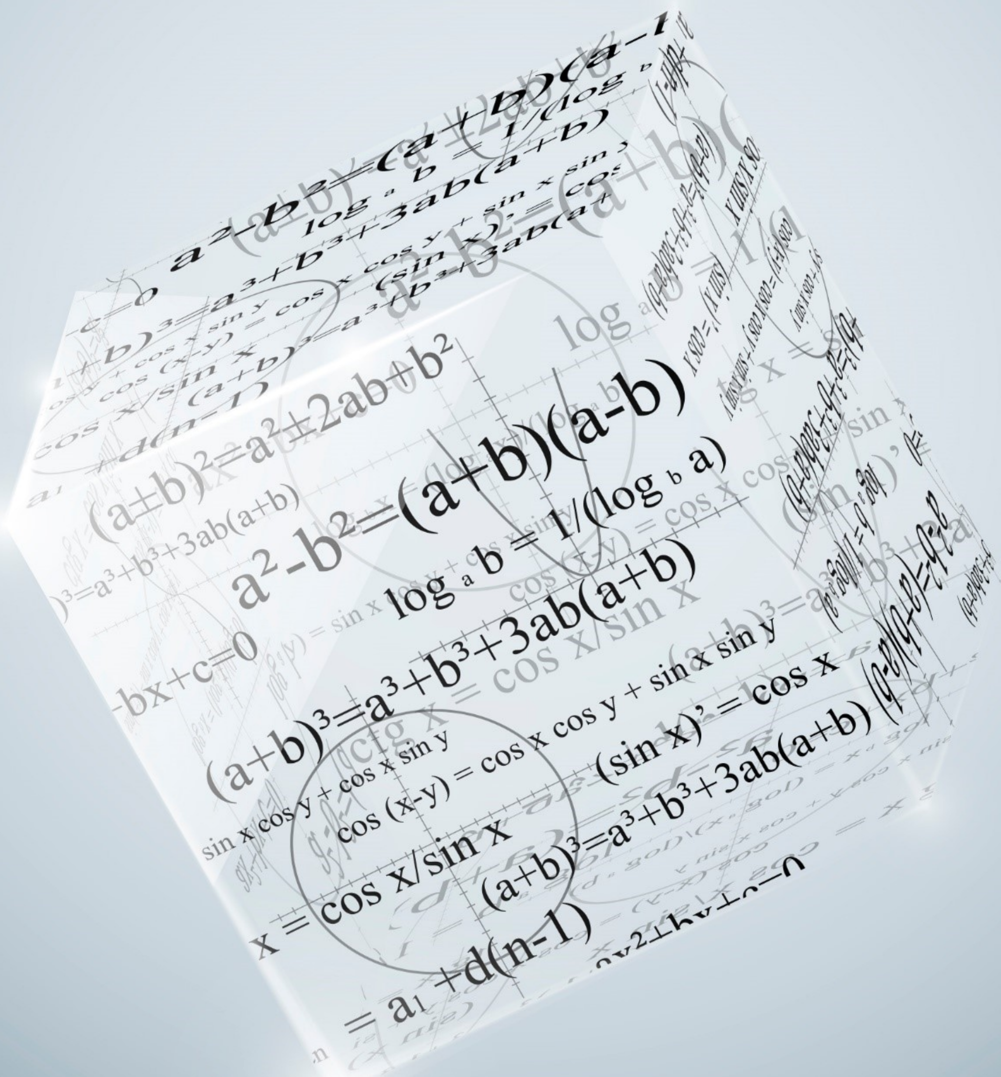

DOUTORAMENTO EM ÁLGEBRA COMPUTACIONAL | 2019

José Manuel Dos Santos Dos Santos

Spherical tilings, GeoGebra contributions to their combinatorial and geometrical classification.

José Manuel Dos Santos Dos Santos

Dissertation submitted in partial fulfillment for the degree of Doctor in Computational Algebra

Supervisors:

Prof. Dr. Ana Maria Reis D'Azevedo Breda

Prof. Dr. João Jorge Ribeiro Soares Gonçalves de Araújo

at

Universidade Aberta
Departamento de Ciências e Tecnologia

May 2019

Declaration of Authorship

I, *José Manuel Dos Santos Dos Santos* declares that this Dissertation, entitled - *Spherical tilings, GeoGebra contributions to their combinatorial and geometrical classification* - and the work presented in it, are my own. I confirm that:

- This work was entirely or mainly done while applying in candidature for a research degree at this University.
- Whenever any part of this dissertation has previously been submitted for a degree or any other qualification at this University or any other institution, this has been clearly stated.
- When I have consulted the published work of others, this was always clearly attributed.
- In cases of quotation from the work of others, the source is always given. With the exception of such quotations, this dissertation is entirely my own work.
- All main sources of help have been acknowledged.
- Whenever the dissertation involved joint work with others, it has been made clear what was done by others and what was contributed myself.
- According to the "regulamento do doutoramento em álgebra computacional" this dissertation includes the papers that have been already published or accepted for publication.

Signed:

Date: 10-05-2019

"Caminante, son tus huellas

el camino y nada más;

Caminante, no hay camino,

se hace camino al andar."

Antonio Cipriano José María Machado Ruiz

Abstract

The goal of this dissertation is to advance the classification of classes of spherical tilings: we find new ones and characterise new families. To do that we rely on theoretical considerations along with the interactive geometry, algebra, statistics and calculus software GeoGebra to which we produced new tools.

This research work comprises five papers, two published (see Chapters 3 and 4), two accepted (see Chapters 2 and 6) and one is submitted (see Chapter 5), being the chapter one reserved to the introduction.

In the second chapter we introduce the tools created in GeoGebra, the application of these tools to obtain some well known spherical tilings and provide illustrations of some new spherical tilings. In the following chapter, a new family of tilings of the sphere, $\widehat{\mathfrak{B}_{\frac{p}{q}}}$, $p, q \in \mathbb{N}$, are presented. This family contains the well known antiprismatic tilings, which is identified and obtained by a global action of a subgroup of spherical isometries. In Chapter 4, we study a monohedral family of tilings of the sphere, $\mathfrak{P}_{(\mathcal{C},\rho)}$, formed by four non-convex congruent spherical pentagons. In this case, the family is obtained by a local action of a subgroup of spherical isometries applied to $\mathcal{C}$, a set of spherical arcs concurrent in a point. In Chapter 5, the properties of the two families of spherical tilings, ${\mathfrak{P}^*}_{(\mathcal{C}_1,\tau^*)}$ and ${\mathfrak{P}^{**}}_{(\mathcal{C}_2,\tau^{**})}$, corresponding to dihedral tilings by pentagons are presented. The topological and combinatorial characterizations of each element of these families are given. In the folowing chapter we explore some new monohedral spherical tilings, $\mathfrak{H}_{(\mathcal{C}_3,\tau)}$, by six non-convex hexagons, and a new family of monohedral tiling by six spherical pentagons, $\mathfrak{P}_{(\mathcal{SC},\theta_1,\theta_2)}$, which arises as a degenerated case associated to the family $\mathfrak{H}_{(\mathcal{C},0)}$.

Finally, some conclusions driven from the work developed so far are presented and some considerations about the potential use of GeoGebra for research in this area will be given.

Keywords: Spherical Geometry, Spherical Tilings, GeoGebra.

Acknowledgements

I leave here an eternal thanks to Prof. Dr. Ana Maria D'Azevedo Breda, who besides being the supervisor of this dissertation, was the untiring friend who listened to me, appeased my anguish, and clarified my ideas.

I would like to thank the co-supervisor of the dissertation, Prof. Dr. João Jorge Ribeiro Soares Gonçalves de Araújo, for all the support provided from the beginning of the doctoral course to its end, which culminates in this work. I must mention his always unconditional support, full of optimism, even at times when I lacked the courage and the strength to continue.

I would also like to thank Prof. Dr. António João de Castilho Breda D'Azevedo for some of the conversations we had during the preparation of this dissertation.

To all the professors who accompanied me during the doctoral course, for what they taught me and for the suggestions given to improve my academic work, I leave my thanks and my appreciation.

Finally, I leave a special thanks to Professor Peter Jephson Cameron for all the care and dedication he has had in answering my requests.

Multas gratias tibi ago!

Contents

To my parents, all words of thanks would be insufficient. I dedicate this work to them, I leave my eternal gratitude ...

Chapter 1

Introduction

1.1 Main goal

In this work, we propose to explore and search new spherical tilings, subdivision of the unit sphere by spherical polygons, making use of GeoGebra [46], a well known free interactive mathematics software.

1.2 Some historical notes

The efficiency of arrangements and patterns (packaging, covering and coating) has been studied throughout the history of mathematics. The tilings of the sphere appear already in studies attributed to Pythagoras and in some Arab texts that influenced the elements of Euclid [11]. Euclid and Archimedes were already interested in this kind of question. In 1619, Johannes Kepler published the first classification of edge-to-edge regular monohedral spherical tilings, associated to the platonic solids, in Book II of *Harmonices Mundi* [50].

Crystallography studies, begun in the nineteen century by Hessel, Bravais, Möbius, Jordan, and Sohnck and others [49], have contributed to more knowledge about polyhedra and necessarily to associated spherical tilings. These studies were mainly based on geometric methods. Only later did Polya [61] and Maxwell [56] develop a more systematic work on the study of crystallographic groups, namely, using Coxeter's work [27–29].

It should be noted that from the crystallographic studies it was possible to first classify edge-to-edge tilings of the sphere produced by transitive actions of spherical isometry subgroups. Other studies arise from exclusively combinatorial properties, this is the case of the f-tilings [9, 13, 14, 25].

The first attempt to systematize classifications of spherical tilings begun with D. Sommerville who established, in [71], part of a classification of spherical tilings by isosceles triangles and analysed a very particular case by scalene triangles [33, p.467]. H. Davies, in [30], presents an incomplete classification of triangular monohedral tilings of the sphere. Besides, Davies has not provided sufficient evidence of his conclusions, omitting many details which were fixed later on.

Tilings of the sphere by right triangles were obtained by Yukako Ueno and Yoshio Agaoka in 1996 [76]. Later, in 2002, the same authors obtain the complete classification of monohedral edge-to-edge triangular spherical tilings [77]. It should be noted that monohedral spherical folding tilings were studied by Ana Breda and their classification was obtained in 1992, recognizing that their prototypes can only be spherical triangles, being as expected a subset of the set of triangular monohedral spherical tilings [13].

The classification of spherical tilings by triangles is not yet completed. In fact, little is known when the condition of being monohedral or edge-to-edge is dropped out. A systematised study to enumerate and classify all spherical tilings is far from being solved.

The classification of non monohedral spherical tilings by scalene triangles is an hard problem and only few developments are known [1]. The general classification remains open.

The regular dodecahedral spherical tiling is a well known tiling of the sphere by twelve regular pentagons. All edge-to-edge tilings of the sphere by 12 congruent convex pentagons have been classified by Honghao, Shi and Yan [40]. Recently, we have characterised a family of spherical monohedral tiles by four congruent non-convex spherical pentagons [22], using the tools presented in chapters 2 and 3.

Tilling problems, even in the plane, remained open for a long time. For instance the problem of the classification of all monohedral tilings of the plane by convex pentagons was only solved recently. In fact, in 2017, Michaël Rao [62] has presented a proof based on an exhaustive search, by means of computational methods, of all monohedral families of these class of tilings. His work revealed that there are no more than the 15 already known families. Up to 1985 only 13 monohedral such tilings were known. Rolf Stein [72] found a 14th monohedral tiling family in 1985 and the 15th monohedral tiling family was found, in 2015, by Mann, McLoud and Von Derau [55]. As expected not all families of monohedral tilings of the plane by convex pentagons are edge-to-edge.

It is not surprising that little is known about the classification of spherical tilings by convex and/or non convex polygons. This work intends to be an advance in the knowledge on this issue.

1.3 Some tilings applications

Tiling problems are interesting not only regarding theoretical aspects but also regarding several applications, among which are issues related with distribution of points on a sphere [67] with strong implications in the contemporary technology and in science in general. The facility location problems, spherical designs and minimal energy point configurations on spheres [10, 12] are other fields where the study of tilings can be used.

Walter Kohn report that the year 1984 brought a big surprise in the field of crystallography. He refers the work of:

> "D. Schechtman and co-workers that reported a beautiful x-ray pattern with unequivocal icosahedral symmetry for rapidly quenched AlMn compounds. The appropriate theory was independently developed by D. Levine and P. Steinhardt, who coined the words quasicrystal and quasiperiodic. Even more curious was the fact that R. Penrose (1984) had anticipated these concepts in purely geometric [terms], so-called Penrose tilings" [51, p. s70].

Findings of this kind reinforce the need to continue studying geometric patterns and their properties.

The study of spherical tiling has also applications to chemistry, for instance, in the study of periodic nanostructures [38]. The emerging of new forms of association of molecules, notably fullerenes [37], lead to the study of special classes of spherical tilings by triangles, squares, pentagons, and hexagons [63]. In the same line of reasoning, other tilings by heptagons[73] and heptagons and octagons [64] had emerged in a study done in a more rigorous way. Other research lines point to new possibilities for new molecular patterns [35, 78].

Namely, in the field of virology many applications of the spherical tilings arise. As Reidun Twarock state "tiles have a biological interpretation in terms of interactions between the proteins they encode, the viral tiling theory lends itself to various applications" [75]. Same studies have provided the evidence occurrence of tubular malformations in addition to spherical capsids[1] [69, 75], being necessary models of simulation of local actions [70]. The rearrangements due to these malformations lead to structures whose viral caspicides could be modelled by tiles with vertices of valence two.

Some of the aforementioned discoveries, which result from research in various branches of science, point to the analysis of configurations that can be modelled by geometric patterns. This is, among others, one of our motivations for our study. In fact, we will study spherical tilings whose prototypes are not necessarily convex spherical polygons.

1.4 Definitions

Let $S^2 = \{(x, y, z) \in \mathbf{R}^3 : x^2 + y^2 + z^2 = 1\}$ be the unit sphere in $\mathbf{R}^3$. A spherical polygon is a closed region limited by a set of spherical line segments (arcs obtained by the intersection of S^2 with planes passing through its centre), the edges of the polygon. The spherical segment joining A and B (for $A, B \in S^2$), will be denoted by AB.

A spherical tiling is called monohedral if all polygons of the subdivision are congruent among them. Any one of these polygons is called a prototile of the tiling.

A dihedral spherical tiling is a tiling in which every polygon of its division is congruent to one and only one of its two distinct prototiles.

The focus of this work are edge-to-edge spherical tilings, i.e., tilings where the intersection of two tiles is either a vertex or an entire edge.

1.5 Why using GeoGebra

There are many tools to work with spherical geometry, for instance Povray [34], and in an interactive way Sphaerica [39] and Spherical Easel [2]. While Povray [34] is a powerful tool to

[1]The protein coat or shell of a virus particle, surrounding the nucleic acid or nucleoprotein core. Origin of the word in late 19th century: from modern Latin Capsidae (plural), from Capsus (genus name).

illustrate objects in spherical geometry, Sphaerica and Easel present some potential to make constructions and explorations. For our purposes we need to work with more flexible tools and commands, in particular, we need to obtain in real time the orbit of a set of spherical points under the action of a (sub)group of spherical isometries.

GeoGebra [45] seems to be the best option for two crucial reasons: the widespread use of GeoGebra and the possibility of interaction with geometrical and algebraic representations simultaneously. In fact, GeoGebra has several geometrical representations in 2 and 3 dimensions allowing the interaction with spherical points in a diversity of ways. Besides, the algebraic capabilities of GeoGebra allow the study and the induction of some geometrical properties which may be visualized in real time. Among its many features GeoGebra allows the creation of new tools and commands, deals with sequences of several geometrical and algebraic objects and uses logic procedures and heuristics which, among other things, permits one, for instance, to certify the congruence of objects. There are other software as powerful as GeoGebra for work in three-dimensional geometry (for example, Archimedes Geo3D [41]), but they are not free, and this is, without any doubt, an added value to the choice of GeoGebra. Another interesting aspect of GeoGebra is that it allows us to obtain planar configurations of the spherical tilings in study, which are an important aid for the deduction procedures.

In all the results obtained in this work GeoGebra played an important role, see [15–19], in order to get: i) new GeoGebra tools and applications that allow the geometric development of new families of tilings; ii) algebraic descriptions for the geometrical features of the new family of tiling obtained by means of computer algebra system (*GeoGebra CAS*). The results obtained through *GeoGebra CAS* were confirmed manually and with the use of other software, namely Maple™, Wolfram Programming Lab [47] and SAGE [74]. It should be noted that, after obtaining all the algebraic definitions of the vertices of the tilings, new GeoGebra applications were constructed from the algebraic descriptions that confirmed the results obtained previously using the geometric tools created with GeoGebra.

Chapter 2

Spherical tiling with GeoGebra

New results, challenges and open problems [24]

In this paper our first goal was to show how to make use of GeoGebra to generate and visualise monohedral edge-to-edge triangular spherical tiling. We have also shown how to generate and visualise monohedral spherical tilings whose prototiles are polygons, not necessarily triangular or even convex.

Having these goals in mind, new GeoGebra tools for spherical geometry were created.

Besides the abstract and the introduction, the paper includes in the first section, GeoGebra resources which allow to build an octahedral spherical tiling, either using the command "surface" or combining this command with others related to $3D$ geometric isometries.

In the study of the spherical tilings, the angle measure plays a crucial role, being essential to construct tools, to define the edges of the polygons and to get the angle measure. This is the content of the second section. In the third section the way of obtaining the isometries of the sphere in GeoGebra is presented. They are relevant for the construction of patterns of spherical polygons that could end up in spherical tilings. In the fourth section, some applications of the spherical compass tool are given, namely in the construction of geometrical loci. In the fifth section, the equilateral spherical triangle tool is presented. This tool will be used to obtain regular spherical tilings starting from a net of equilateral triangles. GeoGebra will be also used to give the geometrical characterisation of these tilings, namely edge lengths and angle measures. Finally, in the sixth section, we present some spherical tilings as orbits of global or local actions of spherical isometries.

GENERAL ARTICLE

Spherical tiling with GeoGebra

New results, challenges and open problems.

Breda, Ana & Dos Santos, José

The theory of spherical tilings is an interesting and fruitful field, attracting, among other mathematician, biologists, physicists and engineers. It is a transverse topic crossing several mathematical areas such as geometry, algebra, topology and number theory, but it is also an object of interest for other scientific fields such as chemistry, physics, art and architecture. Here, making use of GeoGebra, we will establish some results, describing a class of monohedral spherical tilings and inferring some conjectures, showing how the use of this software was crucial for the construction of new knowledge in mathematics with applications in different areas of engineering.

Ana Maria D'Azevedo Breda is Associated Professor of the University of Aveiro, Portugal, Member of the Algebra and Geometry Group of the Center for Research and Development in Mathematics and Applications (CIDMA) and coordinator of the Thematic Research and Development Line GEOMETRIX.

José Manuel Dos Santos Dos Santos, professor of Mathematics of secondary education and teacher trainer, interested in Computational Algebra and in the use of GeoGebra for teaching and learning. Coordinates the GeoGebra Institute of Portugal since 2010.

Introduction

The efficiency of arrangements and patterns (packing, covering and tiling) have been the object of study of many generations of mathematicians. In fact, Euclid and Archimedes were already interested in this type of question.

The side by side spherical tilings by congruent polygons (monohedral tilings) has been extensively studied, being the triangular case completely classified, [9, 10].

There are many tools to work with spherical geometry in an interactive way, as Sphaerica [5], Spherical Easel [1], and POV-Ray [4]. However, for our purposes we need to work with more flexible tools and commands, in particular, we need to obtain in real time the orbit of a set of spherical points under the action of a (sub)group of spherical isometries. For that, GeoGebra [6] seems to be the best option for two crucial reasons: the widespread use of GeoGebra and the possibility of interaction with geometrical and algebraic representations simultaneously. In fact, GeoGebra has several geometrical representations in 2 and 3 dimensions allowing the interaction with spherical points in a diversity of ways. Besides, the algebraic capabilities of GeoGebra allows the study and the induction of some geometrical properties which may be visualized in real time. Among its many features, GeoGebra allows the creation of new tools and commands, dealing with sequences of various geometric and algebraic objects and using logical and heuristic procedures, permitting the certification of some properties of these same objects, as for example, to be congruent among them.

Our goal is, firstly, to use GeoGebra for the generation and visualisation of any regular triangular spherical tiling, followed by the generation and visualisation of monohedral spherical tilings whose prototile cell is a polygon, not necessarily triangular or even convex.

Within this goal, we have created new GeoGebra tools for spherical geometry.

1. Octahedral spherical tiling with GeoGebra and spatial geometric transformations

Using parametrizations we may color the eight octants corresponding to the eight spherical triangles that constitute the monohedral octahedral tilling of the sphere, see fig.1(a). One possibility is to make use of the lateral surface command, see fig.1(b), using this command eight times and coloring the spherical triangles with different colors.

Making use of spherical isometries, we may also construct an application to get what is illustrated in figure 1. Using two different colors for two adjacent spherical triangles, we obtain the other 6 by rotations and rotor-reflections of these two spherical triangles, see fig. 2(a).

In Figure 2(b), we see three great circles intersecting at right

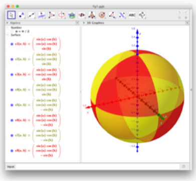

(a) Application view.

$\alpha = \frac{\pi}{2}$
s1=Surface(sin(a) cos(b), cos(a) cos(b), sin(b), a, 0, α, b, 0, α)
s2=Surface(sin(a) cos(b), cos(a) cos(b), sin(b), a, $\pi + \alpha$, $\pi + 2\alpha$, b, 0, α)
s3=Surface(sin(a) cos(b), cos(a) cos(b), sin(b), a, π, $\pi + \alpha$, b, 0, α)
s4=Surface(sin(a) cos(b), cos(a) cos(b), sin(b), a, α, π, b, 0, α)
s5=Surface(sin(a) cos(b), cos(a) cos(b), -sin(b), a, 0, α, b, 0, α)
s6=Surface(sin(a) cos(b), cos(a) cos(b), -sin(b), a, $\pi + \alpha$, 2π, b, 0, α)
s7=Surface(sin(a) cos(b), cos(a) cos(b), -sin(b), a, π, $\pi + \alpha$, b, 0, α)
s8=Surface(sin(a) cos(b), cos(a) cos(b), -sin(b), a, α, π, b, 0, α)

(b) Commands.

Figure 1: Octhaedral spherical tiling using parametizations in GeoGebra

angles, dividing the sphere into eight congruent, equilateral and right-angled spherical triangles.

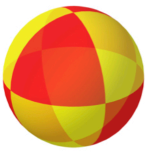

$\alpha = \frac{\pi}{2}$
s1=Surface(sin(a) cos(b), cos(a) cos(b), sin(b), a, 0, α, b, 0, α)
s2=Surface(sin(a) cos(b), cos(a) cos(b), sin(b), a, $\pi + \alpha$, $\pi + 2\alpha$, b, 0, α)
s3=Rotate(s1, 2α, zAxis)
s4=Rotate(s2, 2α, zAxis)
s5=Rotate(Reflect(s1, z = 0), α, zAxis)
s6=Rotate(Reflect(s2, z = 0), α, zAxis)
s7=Rotate(Reflect(s1, z = 0), 3α, zAxis)
s8=Rotate(Reflect(s2, z = 0), 3α, zAxis)

(a) Invariant by the group of rotor-reflections, of angle $\frac{\pi}{2}$, in the equator.

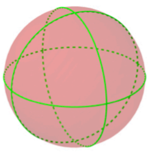

$\alpha = \frac{\pi}{2}$
s=Sphere((0, 0, 0), 1)
a1=CircularArc((0, 0, 0), (1, 0, 0), (0, 0, 1), xOyPlane)
a2=CircularArc((0, 0, 0), (1, 0, 0), (0, 1, 0), xOyPlane)
a3=CircularArc((0, 0, 0), (1, 0, 0), (0, 0, -1), xOyPlane)
E1=$\{a1, a2, a3\}$
Edges=Sequence(Rotate(E1, k α, zAxis), k, 0, 4)

(b) Invariant by the group of symmetries of the regular octahedron.

Figure 2: Octhaedral spherical tiling obtained by different ways of construction in GeoGebra

2. New tools in GeoGebra for spherical geometry

In spherical geometry the primitive elements "point" and "straight lines" are modelled, respectively, by points in the sphere , $S^2 = \{(x, y, z) \in \mathbf{R}^3 : x^2 + y^2 + z^2 = 1\}$, and great circles obtained by the intersection of S^2 with planes passing through the centre of S^2.

We assume, without loss of generality a sphere of radius 1 centered at the origin.

In GeoGebra, spherical points can be obtained making use of the point tool and the commands *A=Point[s]* .

Let *A* and *B* be two distinct spherical non antipodal points. Using the command *s=Sphere [(0,0,0),1]*, *s*, there is one and only one great circle, *r*, containing *A* and *B*. In GeoGebra the representation of the line *AB* will be given by:

```
r=Circle(Centre(s),A,Plane(Centre(s),A,B))
```

In accordance, the representation of the spherical segment *AB* would be:

```
AB=CircularArc(Centre(s),A,B,Plane(Centre(s),A,B))
```

A spherical polygon (concave or convex) corresponds to a spherical region bounded by spherical segments.

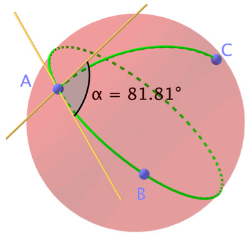

Figure 3: Points, straight lines, straight line segments, and angles in spherical geometry.

Another important element in spherical geometry is the angle defined by two spherical segments. Given three points *A*, *B* and *C* on the sphere the angle *BAC* corresponds to the angle defined by the tangent lines to the spherical segments *AB* and *AC* at the vertex *A*.

For the example illustrated in figure 3, the angle α was defined using the command:

```
Angle(Tangent(A,CircularArc(Centre(s),A,C,Plane(
    Centre(s),A,C))),Tangent(A,Circle(Centre(s),A,
    Plane(Centre(s),A,B))))
```

Following this way of thought for object construction we have created tools in GeoGebra, allowing the construction, in real time, of spherical segments and distances between points and angle measures, allowing the construction of different spherical configurations with control in angle and distance point measure enabling us a great deal of flexibility for the exploration of spherical patterns.

3. Spherical Isometries

As it is well known, the spherical isometries, transformations of the sphere onto itself preserving the spherical distance, are rotations about an axis passing through its center (fig. 4(a)); plane reflections passing through its center (fig. 4(b)); compositions of a reflection in a plane passing through its center followed by a rotation about an axis perpendicular to this plane passing through the center (fig. 4(c)) and any composition of the isometries already mentioned.

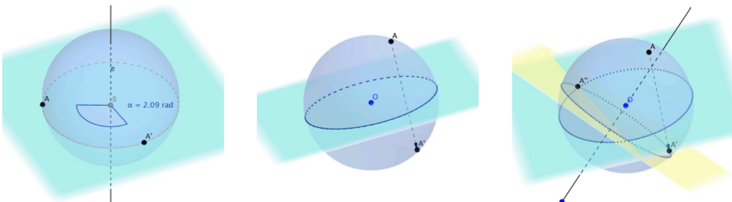

(a) Rotation. (b) Reflection. (c) Rotor-reflection.

Figure 4: Isometries of the sphere.

The image A', B', C' of 3 spherical points, A, B, C not belonging to the same large circle univocally determine a spherical isometry, f, satisfying, $f(A) = A'$, $f(B) = B'$, $f(C) = C'$.

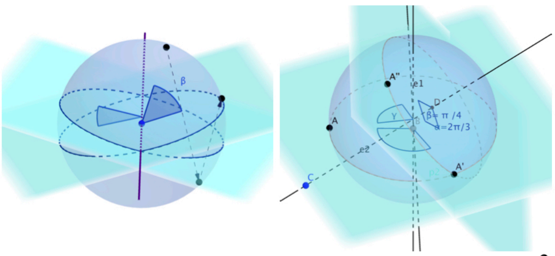

Figure 5: Composition of two reflections in S^2.

In figure 5, it can be visualised the composition of two reflections in planes passing through the center of the sphere, the rotation about the axis defined by the intersection of the two planes of reflection.

4. Locus in spherical geometry with spherical compass tool

In Euclidean geometry the constructions with ruler and compass play an important role. With the spherical compass GeoGebra tool, we can explore similar constructions in spherical geometry.

One of the simplest constructions in Euclidean geometry corresponds to the perpendicular bisector of a "straight line segment". In the sphere of center O and radius r, we may use the spherical compass tool to perform the same type of construction.

Considering two spherical points A and B and a distance l (controlled by a selector) and defining P by:

```
P=Intersect(SphereCompass(A,l,O,r),SphereCompass(B,l
    ,O,r))
```

P corresponds to the set of all spherical points equidistant from A and B, which is precisely the large circle perpendicular to the spherical segment AB (see figure 6(a)) passing through the midpoint of AB.

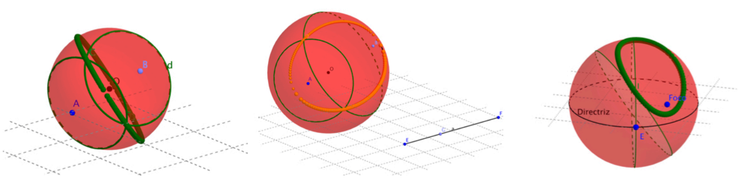

(a) Mediatrix of a spherical segment. (b) Spherical ellipse. (c) Spherical Parabola.

Figure 6: Locus on the Sphere.

GeoGebra can also help to obtain the locus equation using the *CAS View*.

Similarly, given two points A and B, on the sphere, and a distance l, we can use the spherical compass tool to construct the set of points P, on the sphere, such that $d_e(P,A) + d_e(P,B) = l$. This set of points corresponds to the "spherical ellipse" shown in Figure 6(b). The notions of straight lines and parabolas (unrestricted curves in the open set $\mathbf{R}^2$) and making use of the spherical compass tool it is easy to visualize the equivalent spherical notions, which correspond to the closed curves illustrated in fig. 6(c).

5. From the *STeqAB [A,B,O,r]* tool to the regular spherical tilings

Associated to the constructed spherical tool *Spherical Compass* is the command *STeqAB [A,B,O,r]* used to construct equilateral spherical triangles.

Using the *Spherical Compass* and starting from a net of n congruent equilateral triangles, depending on the initial points A and B, and moving these points around the sphere we can explore many configurations being some of them spherical tilings.

Using a set of n equilateral triangles	...in one hemisphere	Length of segment AB	...Closing around one vertex	Final length of segment AB
3	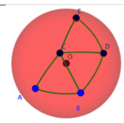	1,05 rad	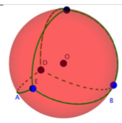	$\arccos(-1/3) = 2\arctan(\sqrt{2}) \approx$ $\approx 1.908 rad$
8	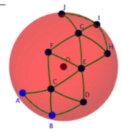	0,64 rad	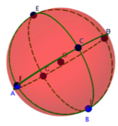	$\frac{\pi}{2} \approx 1.574 rad$
20	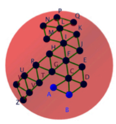	0,40 rad	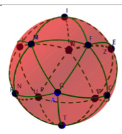	$2\arcsin(\frac{\sqrt{5-\sqrt{5}}}{\sqrt{10}}) \approx 1.107 rad$

Figure 7: Evolution of nets of equilateral and congruent triangles

In figure 7 we illustrate these procedure, using nets with three, eight and twenty triangles ending up in the tetrahedral, octahedral and icosahedral regular spherical tilings. Using the same strategy with another net of triangles, for example with common vertices or adjacent sides, and observing the evolution of the set according to the different positions of the initial points, we may explore the possibilities to obtain new spherical tilings, see fig.7.

6. Spherical tiling as global or local action of groups of spherical symmetries

In the previous sections we show how we can obtain regular tiling of the sphere, see figures 2(b) and 7, these are related to regular polyhedra and their symmetry groups. In these special cases, starting from a spherical triangle, it's orbit under the global action of a group of symmetries determine the spherical tiling.

Let us see another example obtained in a similar way.

Consider: i) an axis, e, of the sphere S; ii) a point A_1, such that $A_1 \in S$ and $A_1 \notin e$; iii) choose one point P, such that $P \in e \wedge S$; iv) angle $\alpha = \frac{2\pi}{n}, n \in \mathbf{N} \wedge n > 3$; v) let $\{A_n, n \in \mathbf{N}\}$ be the orbit of the point A_1 obtained by the action of the group of rotations of the sphere of angle α around the axis e. Under these conditions, we obtain a tiling of the sphere consisting of a spherical $n - gon$ and n congruent spherical triangles whose prototype is $[A_1A_2P]$. This tiling is generated by a cyclic group of order n. In the case of figure 8 we have as a group of symmetries the cyclic group of order 7, being the spherical tiling composed by eigth spherical polygons, one heptagon and seven triangles, this tiling is associated to a straight heptagonal pyramid.

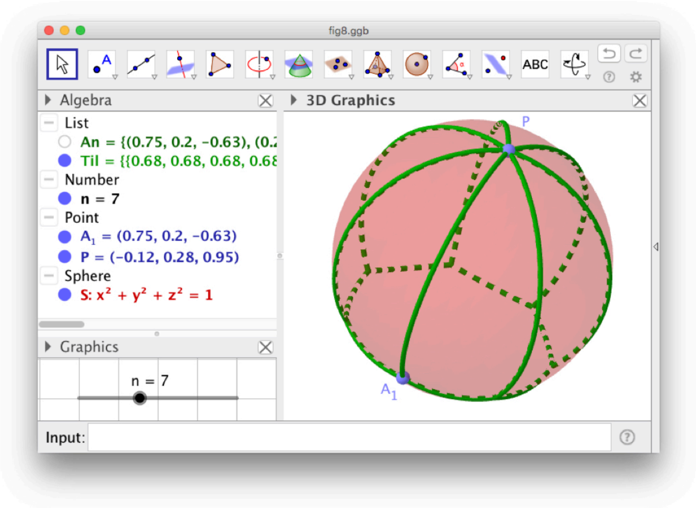

Figure 8: Application of GeoGebra to obtain a tiling of the sphere, invariant by a cyclic group of order equal to the value of selector n.

The basic idea for the construction of this type of tiling is to use the sequence command to model the set of the orbit points. To do that, we use a sequence of commands with a syntax similar to:

```
An=Sequence(Rotate(A_1,2$\pi$i/n,Line(Centre(S),P)),
    i,0,n,1)
```

On the other hand, to obtain the spherical segments, which are the sides of the tiling polygons, we use the list:

```
Til={Sequence(CircularArc(Centre(S),Element(An,i),
    Element(An,i+1)),i,1,n,1),Sequence(CircularArc(
    Centre(S),Element(An,k),P),k,1,n,1)}
```

There are many other spherical tilings that can be "found" by the local action of (sub) spherical isometry groups. These tilings are less well known requiring a systematic study approach.

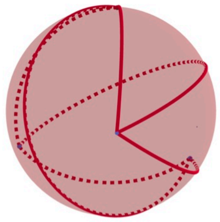

(a) With 4 congruent and non-convex triangles.

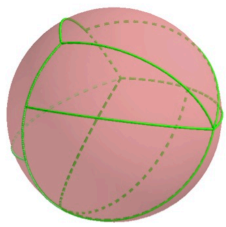

(b) With 8 triangles that are grouped two by two.

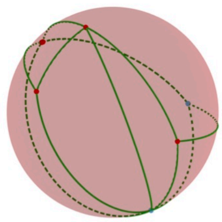

(c) Obtained with the *STAB*$\alpha\beta$ tool with six triangles, one quadrilateral, and ten different angles.

Figure 9: Other spherical tilings...

The tilings by non-convex spherical polygons (Fig.9(a)), specially the monohedral ones, is one of the cases that has not yet been studied so far. Also, the tilings that can integrate more than one type of spherical polygon (not necessarily regular (Fig.9(c)) and not necessarily convex) is another case that has not yet been explored.

In our recent work, using this tools, and from iteration of a set of points C from a set of spherical isometries, we found several classes of monohedral spherical tilings. In figure 10 we can see some of them: $\mathfrak{T}_{(C,\rho)}$, (fig. 10(a)), composed by four congruent triangles of area π; $\mathfrak{P}_{(C,\rho)}$, (fig. 10(b)), composed by four spherical pentagons of area π; two elements of $\mathfrak{H}_{(C,\rho)}$, in figure 10(c) the tiling have six spherical hexagons, however in figure 10(d) the tiling have six spherical pentagons, in both cases each tile has area $\frac{2\pi}{3}$.

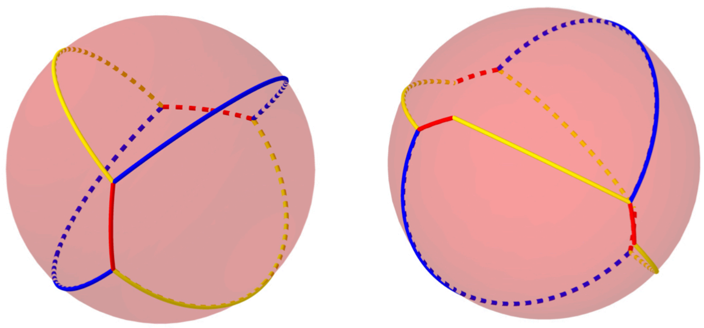

(a) Monohedral triangular spherical tiling, $\mathfrak{T}_{(C,\frac{\pi}{10})}$.

(b) Monohedral pentagonal spherical tiling, $\mathfrak{P}_{(C,\frac{\pi}{10})}$.

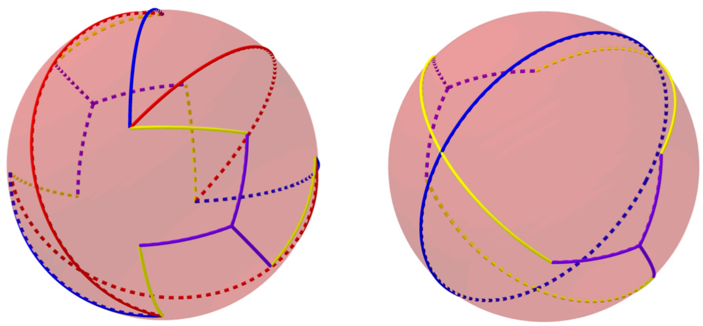

(c) Monohedral hexagonal spherical tiling, $\mathfrak{H}_{(C,\frac{7\pi}{6})}$.

(d) Monohedral hexagonal spherical tiling, $\mathfrak{H}_{(C,0)}$, end-up in a tiling with six congruents spherical pentagons.

Figure 10: Monohedral spherical tilings obtained iterating C under a set of local actions

The tiles of $\mathfrak{T}_{(C,\rho)}$, for $\rho > \frac{\pi}{2}$ are not convex spherical polygons. The convex case was already described by several other authors, see for instance Brooks and Strantzen [3]. However, the non-convex case, $\mathfrak{T}_{(C,\rho)}, \rho \in]\frac{\pi}{2}, \pi[$ as far as we know, is not mentioned in the literature. We only find a brief reference to $\mathfrak{T}_{(C,\arccos(-1/3))}$, in figure 9(a), by Gaiane in [8, 7]. As far as we know, the class of monohedral spherical tiling, $\mathfrak{P}_{(C,\rho)}$, by four spherical pentagons of area π, $\mathfrak{P}_{(C,\rho)}$ is a new one [2].

7. Conclusion

The GeoGebra applications built, so far, allow the visualisation and the establishment of relationships that can greatly contribute to the research in this topic. It is in the generation of such a great variety of spherical configurations / relationships that we believe GeoGebra can make a substantial contribution for the description and construction of spherical tilings not yet explored, besides being a resource of great utility in the study of spherical geometry, in general.

8. Acknowledgement

This work was supported in part by the Portuguese Foundation for Science and Technology (FCT — Fundação para a Ciência e a Tecnologia), through CIDMA — Centre for Research and Development in Mathematics and Applications, within project UID/MAT/04106/2013.

References

[1] D Austin and W Dickinson. *Spherical easel. A spherical drawing program.* Available online at http://merganser.math.gvsu.edu/easel/. 2009.

[2] Ana Maria d'Azevedo Breda and José Manuel Dos Santos Dos Santos. 'A new class of monohedral pentagonal spherical tilings with GeoGebra'. In: *Portugaliae Math* 74.3 (2018). In press, pp. 257–266.

[3] Jeff Brooks and John Strantzen. 'Spherical triangles of area π and isosceles tetrahedra'. In: *Mathematics Magazine* 78.4 (2005), pp. 311–314.

[4] Robert J MacG Dawson et al. 'Some New Tilings of the Sphere with Congruent Triangles'. In: *Renaissance Banff: Mathematics, Music, Art, Culture*. Bridges Conference. 2005, pp. 489–496.

[5] János Erdős. 'Sphaerica: Interactive Spherical Geometry Software'. In: *Proceedings of Bridges 2010: Mathematics, Music, Art, Architecture, Culture*. Ed. by George W. Hart and Reza Sarhangi. Available online at http://archive.bridgesmathart.org/2010/bridges2010-443.html. Phoenix, Arizona: Tessellations Publishing, 2010, pp. 443–446. ISBN: 978-0-98460-420-3.

[6] Markus Hohenwarter and Karl Fuchs. 'Combination of dynamic geometry, algebra and calculus in the software system GeoGebra'. In: *Computer Algebra Systems and Dynamic Geometry Systems in Mathematics Teaching Conference*. Available online at http://archive.geogebra.org/static/publications/pecs_2004.pdf. 2004.

[7] G Yu Panina. 'Pointed spherical tilings and hyperbolic virtual polytopes'. In: *Journal of Mathematical Sciences* 175.5 (2011), pp. 591–599.

[8] Gaiane Panina. 'Planar pseudo-triangulations, spherical pseudo-tilings and hyperbolic virtual polytopes'. In: *arXiv preprint math/0607171* (2006).

[9] DMY Sommerville. 'VI.—Division of Space by Congruent Triangles and Tetrahedra'. In: *Proceedings of the Royal Society of Edinburgh* 43 (1924), pp. 85–116.

[10] Yukako Ueno and Yoshio Agaoka. 'Tilings of the 2-dimensional sphere by congruent right triangles'. In: *Memoirs of the Faculty of Integrated Arts and Sciences, Hiroshima University. IV, Science reports: studies of fundamental and environmental sciences* 22 (1996). Available online at http://ir.lib.hiroshima-u.ac.jp/files/public/0/673/20141016120323365034/KJ00000197303.pdf, pp. 1–23.

Chapter 3

Spherical Geometry and Spherical Tilings with GeoGebra [21]

The classification of spherical tilings is a problem far from being solved. Here we show how to generate new families of antiprismatic spherical tilings using GeoGebra. Within the described proposal some spherical geometry capabilities of GeoGebra had to be extended. The outline of the algorithms behind some of the newly designed and implemented GeoGebra tools and applications will be given.

The research work described here has as its goal the generation in a systematic way of classes of spherical tilings and the search of new ones, making use of the GeoGebra computational capabilities. Our main result is the description of the combinatorial and geometrical characterisation of the two parameter spherical tiling family $\widehat{\mathfrak{B}_{\frac{p}{q}}}$, p, q in $\mathbb{N}$ with $gcd(p, q) = 1$, expanding the antiprismatic spherical tilings.

In the section 2 of this paper we present some tools, purposely created, to extend GeoGebra capabilities in a spherical geometry context. In the next section, we state and prove our main results, the combinatorial and geometrical characterisation of the family $\widehat{\mathfrak{B}_{\frac{p}{q}}}$. We also explain other procedures for obtaining spherical tilings, starting from a spherical triangle and submiting it to the local action of a (sub)group of spherical isometries, a strategy that may help to find new spherical tilings.

Journal for Geometry and Graphics
Volume 22 (2018), No. 2, 283-299.

Spherical Geometry and Spherical Tilings with GeoGebra

Ana Maria D'Azevedo Breda [1], José Manuel Dos Santos Dos Santos [2]

[1] *Departamento de Matemática, Universidade de Aveiro*
Campus Universitário de Santiago, 3810-193 Aveiro, Portugal
email:ambreda@ua.pt
[2] *Universidade Aberta*
Rua da Escola Politécnica 141-147, 1269-001 Lisboa, Portugal
email:dossantosdossantos@gmail.com

Abstract. The classification of spherical tilings is a problem far from being solved. Here we show how to generate new families of antiprismatic spherical tilings using *GeoGebra*, a well known free software commonly used as a tool to teach and learn mathematics. Within the described propose some spherical geometry capabilities of *GeoGebra* had to be extended. The outline of the algorithms behind some of the newly designed and implemented *GeoGebra* tools and applications will be given.

Key Words: Spherical Geometry, Spherical Tilings, *GeoGebra*.

MSC 2010: 51M20, 52C20, 05B45, 51N30, 97N80.

1. Introduction

The research work described here has as its main goal a systematic way to generate spherical tilings and to search for new ones by making use of computational capabilities. Our main result is the description of the combinatorial and geometric characterisation of the spherical tiling family $\widehat{\mathfrak{B}_{\frac{p}{q}}}$, p, q in $\mathbb{N}$ with $gcd(p, q) = 1$, which expands the antiprismatic spherical tilings.

The obtained results emerged by the new produced *GeoGebra* tools and the dynamic interaction capabilities of this software [18, 19], being the construction of an algorithm to get the orbit of a set of spherical points under the action of a (sub)group of spherical isometries (for the details see Section 2.4) as crucial point.

Let us consider the sphere centred at the point $O = (0, 0, 0)$, $S^2 = \{(x, y, z) \in \mathbb{R}^3 : d((x, y, z), (0, 0, 0)) = 1\}$. An element of S^2 is called a *spherical point*. Two spherical points are said to be *antipodal points* if the spherical distance between them is π.

Any two non–antipodal spherical points, A and B, define uniquely a great circle, a *spherical line* s, on the sphere such that $A, B \in s$. The spherical line s will be also denoted by AB. The smaller of the two great arc circles defined A and B is called a spherical segment and denoted by $[AB]$.

Given a spherical segment $[AB]$, its length, $|AB|$ is the measure of the angle $\angle AOB$, i.e., $|AB| = A\hat{O}B$. Given two spherical segments $[AB]$ and $[BC]$, they form a *spherical angle* $\widehat{ABC}$ defined by the angle defined by the tangent lines to the great circles AB and BC.

Considering three non-colinear spherical points on S^2, they define three spherical segments which bound two spherical regions. The smallest of these regions is the convex *spherical triangle* defined by the points; the other region is a concave spherical triangle. In this work we are only interested in convex spherical triangles. A spherical $n-gon$ is a closed polygonal spherical line

By a spherical tiling we mean a decomposition of the sphere by classes of congruent polygons (tiles). A *monohedral* spherical tiling is one in which all the tiles are congruent among them. In an monohedral spherical tiling any tile can be considered a prototile of the tiling. A *dihedral* spherical tiling is a tiling composed by two classes of congruent polygons, which means, a tiling made of two distinct prototiles. Similarly, $n-hedral$ tilings, $n \in \mathbb{N}$ and $n \geq 3$, are tilings with n distinct prototiles.

There are many tools to work with spherical geometry as *Povray* [11], and in an interactive way *Sphaerica* [17] and *Spherical Easel* [1]. While *Povray* [11] is a powerful tool to illustrate objects in spherical geometry, *Sphaerica* and *Easel* present some potential to make constructions and explorations. For our purposes we need to work with more flexible tools and commands, in particular, we need to obtain in real time the orbit of a set of spherical points under the action of a (sub)group of spherical isometries. For that, *GeoGebra* [20] seems the best option for two crucial reasons: the widespread use of *GeoGebra* and the possibility of interaction with geometrical and algebraic representations simultaneously. In fact, *GeoGebra* has several geometrical representations in 2 and 3 dimensions allowing the interaction with spherical points in a diversity of ways. Besides, the algebraic capabilities of *GeoGebra* allow the study and the induction of some geometrical properties which may be visualized in real time. Among its many features, *GeoGebra* allows the creation of new tools and commands [1], deals with sequences of several geometrical and algebraic objects and uses logic procedures and heuristics which, among other things, permits one, for instance, to certify the congruence of objects. There are other software as powerful as *GeoGebra* for work in three-dimensional geometry (for example, Archimedes Geo3D [2]), but they are not free, and this is, without any doubt, an added value to the choice of *GeoGebra*. It is worthwhile to mention that this methodology (making use of *GeoGebra* tools) was already implemented in the exploration of planar hyperbolic tilings, (see [26]).

The systematized study of of spherical tilings started with D. Sommerville [24] who has established part of the classification of spherical tilings by isosceles triangles having analyzed a very particular case by scalene triangles [12, p.467]. H. Davies, in [9], presents an incomplete classification of triangular monohedral tilings of the sphere [9] omitting many details which were fixed latter on.

Tilings of the sphere by right triangles were obtained by Yukako Ueno and Yoshio Agaoka

[1]For more details about tools in *GeoGebra* see [25, pp.89-94] and [28].
[2]http://spatialgeometry.com/drupal/en

in 1996 [29]. Later, in 2002, the same authors obtain a complete classification of monohedral edge-to-edge triangular spherical tilings [30]. Triangular spherical folding tilings were studied by Ana Breda and their classification was obtained in 1992, being these a subset of the triangular monohedral spherical tilings. [7]. Spherical tilings by isosceles and right triangles can be found in [10, 13]. Recently, the authors using the tools described here, characterised a family of spherical monohedral tiles by four congruent and non-convex spherical pentagons [4].

The classification of spherical tilings by triangles is not yet completed. In fact, little is known when the condition of being monohedral or edge-to-edge is dropped out. A systemized study to enumerate and classify all spherical tilings is far from been solved.

Being a rich research field with several distinct ways of approach, tiling problems are interesting not only regarding theoretical aspects but also regarding the innumerable applications about the distribution of points on a sphere [23] with strong implications to the contemporary technology and in science in general. The study of spherical tilings has also applications to chemistry, for instance, in the study of periodic nanostructures [16], emerging new forms of association of molecules, notably fullerenes [15], which lead to the study of spherical tilings by triangles, squares, pentagons, and hexagons [21]. In the same line of reasoning other tilings including heptagons[27] and heptagon and octagons[22] had emerged. Some other research points to new possibilities for new molecular patterns [31, 14]. The facility location problems and spherical designs and minimal energy point configurations on spheres [2, 3] are other fields where the study of tilings can be used for which we may give some contributions.

Next, we begin, in Section 2, by presenting some tools created that extend *GeoGebra* capabilities in spherical geometry. In section 3, we introduce and prove our main results. Also, we explain, in section 4, other ways of obtain spherical tilings, from a spherical triangle subject to the local action of a (sub) group of symmetries, strategy that may help to find new spherical tilings. Finally, in section 5, we present some of our conclusions about the use of *GeoGebra* in the study of spherical tilings.

2. GeoGebra tools for spherical geometry

GeoGebra gives the possibility of interacting, simultaneously, with graphic, algebraic and calculus views. It also gives the chance to create new tools and commands. In fact, the tools can be created from the combination of existing tools or commands. The new tool and the corresponding commands can be used in new constructions or may be integrated in the construction of new tools. We will use these functionality to construct useful tools and commands for spherical geometry. Next we will show how some of the new tools may be used.

2.1. Spherical geometry tools

Spherical *GeoGebra* tools were constructed among the purpose to explore, among others spherical tilings. Among these spherical tools, we mention the following ones: *Spherical Segment*, *Spherical Equidistant Points*, *Spherical Compass*, *Spherical Equilateral Triangle*. Here, by way of example, we describe how the Spherical Segment tool was constructed.

Given two non–antipodal spherical points A and B, the spherical segment joining them is a great circular arc bounded A and B. These spherical segment can be obtained in *GeoGebra* using the command $SphereSegment[A, B]$ described below (see Figure 1).

Tool Name	Spherical Segment
Command Name	SphericalSegment
Syntax	SphericalSegment[A,B]
Help	Given A,B and a spherical, s, draw the spherical segment joining A to B.
Icon	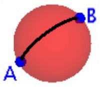
Script	s=Sphere[(0,0,0), 1] A=PointIn[s] B=PointIn[s] If[Distance[A,B]≠2,CircularArc[(0,0,0), A,B,Plane[(0,0,0),A,B]]]

Figure 1: Tool to construct a spherical segment

2.2. Spherical geometry tool to construct a spherical triangle given three angles

It is well known that we may use trigonometric relations to obtain the arc lengths of a spherical triangle given the measurements of its spherical angles.

Let A, B and C be the vertices of a spherical triangle and α, β, γ the measure of the corresponding spherical angles. Denoting by a the measure of the arc BC, $a = |BC|$, b the measure of AC, $b = |AC|$, and c the measure of the arc AB, $c = |AB|$, the following relations hold:

$$\cos(a) = \frac{\cos(\alpha) + \cos(\beta)\cos(\gamma)}{\sin(\beta)\sin(\gamma)}, \; \cos(b) = \frac{\cos(\beta) + \cos(\alpha)\cos(\gamma)}{\sin(\alpha)\sin(\gamma)}, \; \cos(c) = \frac{\cos(\gamma) + \cos(\alpha)\cos(\beta)}{\sin(\alpha)\sin(\beta)}. \quad (1)$$

Thus, we may obtain the measure of the arcs, as a function of the angles of the spherical triangle. Using the proprieties we may create the tool, following the steps described below.

(i) Definition of the unit sphere:
$O = (0, 0, 0);$
$S = Sphere[O, 1].$
(ii) Defining three angles of the spherical triangle.
$\alpha = pi/2;$
$\beta = pi/2;$
$\gamma = pi/2.$
(iii) Creating the vertices A, B and C:
A=Point[IntersectPath[z = 0, S]]
B=Rotate[A, acos((cos(γ) + cos(α) cos(β)) / (sin(α) sin(β))), Centre[S], z = 0]
C=Intersect[IntersectPath[PerpendicularPlane[Rotate[A, acos((cos(β) + cos(α) cos(γ)) / (sin(α) sin(γ))),Centre[S], z = 0], Line[Centre[S], A]], S], IntersectPath[PerpendicularPlane[Rotate[Rotate[A, acos((cos(γ) + cos(α) cos(β)) / (sin(α) sin(β))),Centre[S], z = 0], acos((cos(α) + cos(β) cos(γ)) / (sin(β) sin(γ))), Centre[S], z = 0], Line[Centre[S], Rotate[A, acos((cos(γ) + cos(α) cos(β)) / (sin(α) sin(β))), Centre[S], z = 0]]], S], 1]
(iv) Drawing the edges of spherical triangle:
Sa=CircularArc[O,B,C];
Sb=CircularArc[O,A,C];
Sc=CircularArc[O,A,B].
(v) Creating The tool

The final step is the creation of the *GeoGebra* tool hiding all the constructions presented in the algebraic view, as illustrated in Figure 2.

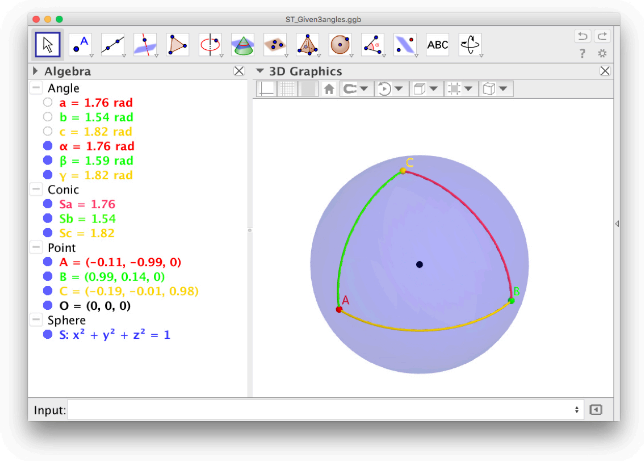

Figure 2: *GeoGebra* application to create a spherical triangle given tree angles

This tool is useful to find spherical tilings and search for new spherical patterns. This tool can be easily adapted to create tools to build any type of spherical triangles.

2.3. An application of the Equilateral Spherical Triangle Tool

One of the spherical tools constructed was the *Spherical Compass*. Using this tool we can easily construct equilateral spherical triangles.

Starting from a net of n congruent equilateral triangles, depending on initial points A and B, and moving these points around the sphere, we can explore many configurations where some of them are spherical tilings. In Figure 3 we illustrate these procedure, using nets with three, eight and twenty triangles ending up in the tetrahedral, octahedral and icosahedral regular spherical tilings. Using the same strategy with another net of triangles, for example with common vertices or adjacent sides, and observing the evolution of the set according to the different positions of the initial points, we may explore the possibilities to obtain new spherical tilings. The application presented above will be used and improved to develop some research in spherical tilings.

In the next section we show another way to find spherical tilings using spherical isometries.

2.4. Using spherical isometries to obtain spherical tilings by means of *GeoGebra*.

Let s be the sphere centred in $O = (0,0,0)$ and radius 1. Let e be a great circle of s and A and B two distinct points in c. Chose one point $C \in s$ such that $[ABC]$ defines an equilateral triangle.

Let $\mathfrak{B}_n, n \in \mathbb{N}$ be a band (closed net) of n congruent spherical equilateral triangles. Using the tool *equilateral spherical triangle*, *SEqT[A,B]*, we can construct an application to explore some properties of the band $\mathfrak{B}_n$. We will start with $n = 12$ (see Figure 4).

This application works in a similar way to that shown in Figure 3. Its use (exploration) reveals that for each position of the point B:

Using a set of n equilateral triangles	...in one hemisphere	...closing around one vertex	final length of segment AB
3	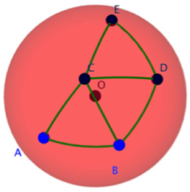	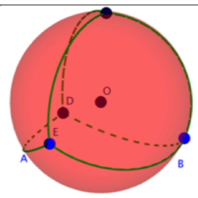	$\arccos(-\frac{1}{3}) =$ $= 2\arctan(\sqrt{2}) \approx$ $\approx 1.908\text{rad}$
8	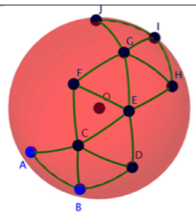	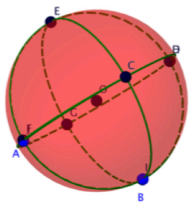	$\frac{\pi}{2} \approx 1.574\text{rad}$
20	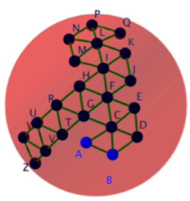	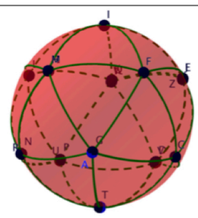	$2\arcsin(\frac{\sqrt{5-\sqrt{5}}}{\sqrt{10}}) \approx$ $\approx 1.107\text{rad}$

Figure 3: Evolution of nets of equilateral and congruent triangles (see [6]).

i) the orbits of the points A and C leave in the same plane, α;
ii) the orbits of the point B are in a plane, β, parallel to α;

```
s:Sphere[(0,0,0),1]
e:IntersectPath[z=0,s]
A=(1,0,0)
B=Point[e]
ABC={CircularArc[(0,0,0),A,B,Plane[(0,0,0),A,B]],CircularArc[(0,0,0),B,C,Plane
    [(0,0,0),B,C]],CircularArc[(0,0,0),C,A,Plane[(0,0,0),C,A]]}
CBD=SEqT[C,B]
CDE=SEqT[C,D]
EDF=SEqT[E,D]
EFG=SEqT[E,F]
GFH=SEqT[G,F]
GHI=SEqT[G,H]
IHJ=SEqT[I,H]
IJK=SEqT[I,J]
KJL=SEqT[K,J]
KLM=SEqT[K,L]
MLN=SEqT[M,L]
```

Figure 4: *GeoGebra* commands to explore the orbit of the equilateral triangles in band $\mathfrak{B}_{12}$.

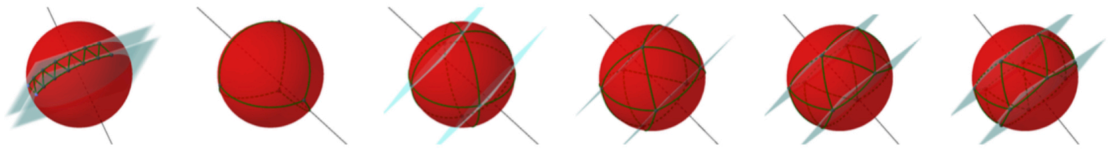

Figure 5: Band with 12 equilateral spherical triangles. Cases that end up in antiprismatic spherical tilings (see [5]).

iii) the distance between α and β is equal to the height of the spherical triangle $[ABC]$;

iv) for the values of the length of AB equal to $\frac{\pi}{2}+\arcsin(\frac{1}{3})$, $\frac{\pi}{2}$, $\arccos\left(\frac{2\sqrt{2}-1}{7}\right)$, $\arccos\left(\frac{\sqrt{5}}{5}\right)$, $\arccos\left(\frac{\sqrt{3}}{3}\right)$ we obtain, respectively, the spherical tilings induced by the antiprisms of 4, 6, 10, 12 and 14 faces. (see Figure 5)

The exploration of the above *GeoGebra* application revealed that the orbit of the triangle $[ABC]$ is generated by the action of a group of spherical rotations s an axis r, perpendicular to the planes α and β, passing through the center of s. Let P the point of intersection of α and r. Then the band $(\mathfrak{B}_n)_{n\in\mathbb{N}}$ is obtained by the rotation of the spherical triangle $[ABC]$ around the axis r by multiples of $\angle APB$.

For our purposes we are interested in knowing the conditions for which $\mathfrak{B}_n, n \in \mathbb{N}$ generates spherical tilings.

In order to construct a more accurate *GeoGebra* application to allow more generalized cases we consider:

i) the sphere s, the north pole P_N=(0,0,1);

ii) natural numbers p and q, $q < p$, defined by sliders;

iii) the point B_1, in the north hemisphere of s;

iv) the point B_2 obtained by the rotation of B_1 around the z–axis by an angle of $2\pi/\frac{p}{q}$;

v) the point A_1, a point in the bisector of the arc B_1B_2, which does not belong to this arc, that is, a point at the same spherical distance from B_1 and B_2 (note that A_1 belongs to the great circle defined by the plane $y = 0$);

vi) the point A_2, obtained by the rotation of A_1 around the z–axis by an angle of $2\pi/\frac{p}{q}$.

Under these conditions, $[B_1B_2A_1]$ defines an equilateral spherical triangle (see Figure 6). Denoting, respectively, by l and h the half of the length and the height of the spherical triangle $[B_1B_2A_1]$, chosen in the way described previously, one has

$$l = l\left(\frac{p}{q}\right) = \sqrt{2}\frac{\sqrt{cos\left(\pi/\frac{p}{q}\right)+2sin^2\left(\pi/\frac{p}{q}\right)+1}}{cos\left(\pi/\frac{p}{q}\right)+2sin^2\left(\pi/\frac{p}{q}\right)+1}, h = h\left(\frac{p}{q}\right) = \frac{\sqrt{\left(cos\left(\pi/\frac{p}{q}\right)+2sin^2\left(\pi/\frac{p}{q}\right)\right)^2-1}}{cos\left(\pi/\frac{p}{q}\right)+2sin^2\left(\pi/\frac{p}{q}\right)+1}.$$

Note that for l be well defined we need that $cos\left(\pi/\frac{p}{q}\right)+2sin^2\left(\pi/\frac{p}{q}\right)+1 \neq 0$ which correspond to $\frac{p}{q} \neq \frac{1}{2n+1}, n \in \mathbb{N}$ [3].

On the other hand, for h be well defined we need that

$$\left(cos\left(\pi/\frac{p}{q}\right) + 2sin^2\left(\pi/\frac{p}{q}\right)\right)^2 - 1 \geq 0.$$

[3]The application of *GeoGebra* show the tree points B_1, B_2 and A_1 coincidents

If $x = cos\left(\pi/\frac{p}{q}\right)$, then $(-2x^2+x+2)^2-1 \geq 0 \Leftrightarrow -\frac{1}{2} \leq x \leq 1$. Thus $-\frac{1}{2} \leq \cos\left(\pi/\frac{p}{q}\right) \leq 1$ then $0 < q \leq \frac{2}{3}p$. Hence, h is well defined if and only if $\frac{p}{q} \geq \frac{3}{2}$.

Accordingly,

$$B_1 = \left(l\left(\tfrac{p}{q}\right) cos\left(\pi/\tfrac{p}{q}\right),\ -l\left(\tfrac{p}{q}\right) sin\left(\pi/\tfrac{p}{q}\right), h\left(\tfrac{p}{q}\right)\right),$$
$$B_2 = \left(l\left(\tfrac{p}{q}\right) cos\left(\pi/\tfrac{p}{q}\right), l\left(\tfrac{p}{q}\right) sin\left(\pi/\tfrac{p}{q}\right), h\left(\tfrac{p}{q}\right)\right),\ A_1 = \left(l\left(\tfrac{p}{q}\right), 0, -h\left(\tfrac{p}{q}\right)\right).$$

Therefore $[B_1B_2A_1]$ is an equilateral triangle with side length equal to:

$$|B_1B_2| = |B_2A_1| = |A_1B_1| = \arccos\left(\frac{cos\left(\pi/\frac{p}{q}\right)+2\ \cos^2\left(\pi/\frac{p}{q}\right)-1}{cos\left(\pi/\frac{p}{q}\right)+2\ sin^2\left(\pi/\frac{p}{q}\right)+1}\right);$$
$$|B_1B_2| = |B_2A_1| = |A_1B_1| = \arccos\left(\frac{1-2\cos\left(\pi/\frac{p}{q}\right)}{2\cos\left(\pi/\frac{p}{q}\right)-3}\right);$$

and angle measure equal to:

$$\widehat{B_1B_2A_1} = \widehat{B_2A_1B_1} = \widehat{A_1B_1B_2} = \arccos\left(-\frac{1}{2}+\cos\left(\pi/\frac{p}{q}\right)\right).$$

The orbit of the equilateral triangle $[B_1B_2A_1] \bigcup A_1A_2$ by the the action of a group of rotations around the z–axis and of angle $2\pi/\frac{p}{q}$, can be obtained using the *GeoGebra* commands defined in figure 7.

The generated spherical patterns depends on the value of $\frac{p}{q}$. When $\frac{p}{q} \in \mathbb{N}$ and $\frac{p}{q} > 2$ the orbit defines spherical antiprisms associated to the $\frac{p}{q} - gon$ antiprism, all vertices have equal valence $(3, 3, 3, \frac{p}{q} = n)$, and the tiling has $2n$ vertices, $4n$ edges, $2n$ spherical triangles and

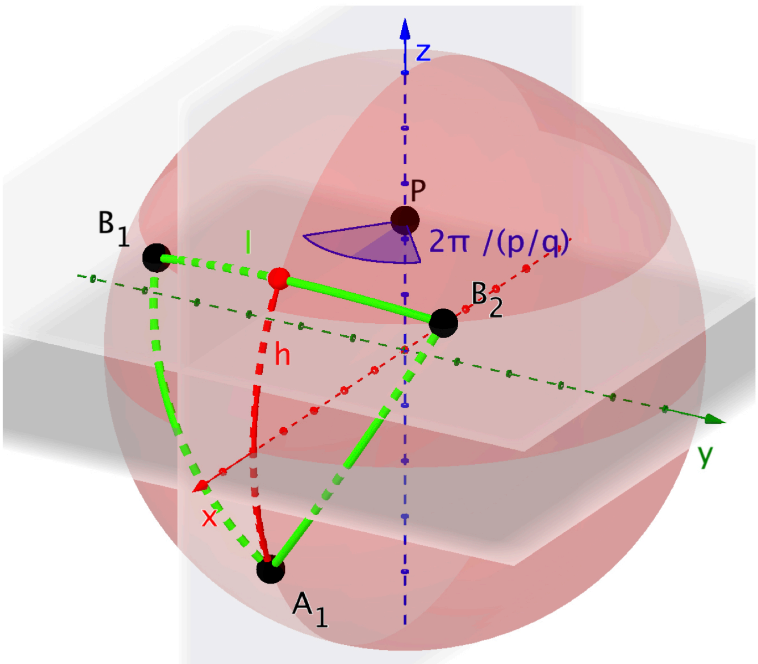

Figure 6: Spherical triangle $[B_1B_2A_1]$.

```
Sequence(Rotate(CircularArc((0,0,0),B1,B2,Plane((0,0,0),B1,B2)),k 2 pi/(p/q),
    zAxis),k,1,pq)
Sequence(Rotate(CircularArc((0,0,0),B2,A1,Plane((0,0,0),B2,A1)),k 2 pi/(p/q),
    zAxis),k,1,pq)
Sequence(Rotate(CircularArc((0,0,0),A1,B1,Plane((0,0,0),A1,B1)),k 2 pi/(p/q),
    zAxis),k,1,pq)
Rotate(Reflect(Sequence(Rotate(CircularArc((0,0,0),B_1,B_2,Plane[(0,0,0),B_1,
    B_2)),k 2 pi/(p/q),zAxis),k,1,pq),Plane(z=0)),pi/(p/q),zAxis)
```

Figure 7: *GeoGebra* commands for the generation of spherical tilings

2 spherical $n-gons$[4]. All the triangles have congruent angles of measure $\arccos\left(cos\left(\frac{\pi}{n}\right)-\frac{1}{2}\right)$. The spherical $n-gons$ has congruent angles and their measure is $2\pi - 3\arccos\left(cos\left(\frac{\pi}{n}\right)-\frac{1}{2}\right)$. All arcs of these tilings have measure $\arccos\left(\left(1-2\cos\left(\frac{\pi}{n}\right)\right)/\left(2\cos\left(\frac{\pi}{n}\right)-3\right)\right)$. All these tiling are invariant by the cycled group of order n and have central symmetry.

Analysing the behaviour of the maps h and l and considering their domain as the set of real numbers, we can prove in a straightforward way that $\lim_{x\to\infty} l(x) = 1$ and $\lim_{x\to\infty} h(x) = 0$ which corresponds to the construction of a tiling of the sphere by two hemispheres. Considering $x > \frac{3}{2}$ the function h have a maximum of $\frac{3}{5}$ and l have a minimum of $\frac{4}{5}$ at $x = \pi/\arccos\left(\frac{1}{4}\right)$, thus the minimum value of $2l$ is $8/5$, near of the arc length of the prototype of the tetrahedral spherical tiling, corresponding to the tiling of the sphere by equilateral triangles.

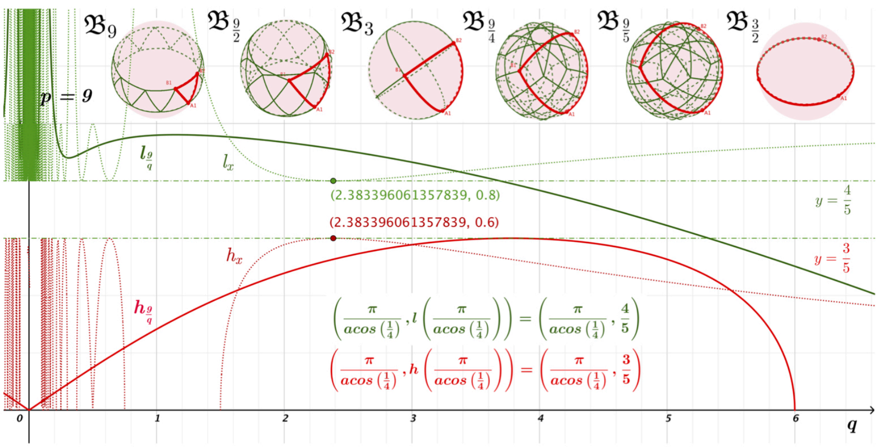

Figure 8: *GeoGebra* output of the graph behaviour of functions h and l, where $h_{\frac{9}{q}} = h(\frac{9}{q})$ and $l_{\frac{9}{q}} = l(\frac{9}{q})$.

If $\frac{3}{2} < x < \pi/\arccos\left(\frac{1}{4}\right)$ the corresponding side lengths B_1B_2 decrease to a minimum of $\frac{4}{5}$, while the sequence of heights of the corresponding triangles $[B_1B_2A_1]$ grow to a maximum value of $\frac{3}{5}$. Thus the generated bands, $\mathfrak{B}_x$, range from a set of two hemispheres to other bands whose "non-lateral" edges have their midpoints increasingly close to the poles (see Figure 8, $\mathfrak{B}_k, k \in \{\frac{3}{2}, \frac{9}{5}, \frac{9}{4}\}$).

[4]In this case the Euler formula, $F + V = E + 2$, is obviously satisfied, note that the tilings induce the anti-prism inscribed in the sphere.

Anti Prism Spherical tilings $\widehat{\mathfrak{B}_n}, n \in \mathbb{N}$	$\widehat{\mathfrak{B}_4}$ 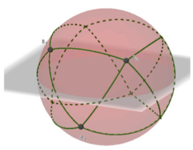	$\widehat{\mathfrak{B}_5}$ 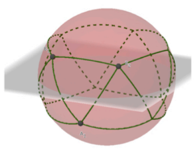	$\widehat{\mathfrak{B}_6}$ 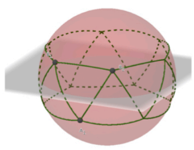
Planar Graph	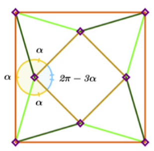	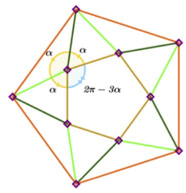	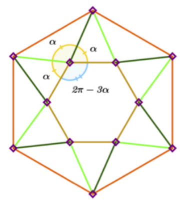
Vertices valence $(3,3,3,n)$	$(3,3,3,4)$	$(3,3,3,5)$	$(3,3,3,6)$
Angles around vertices $(\alpha;\alpha;\alpha;2\pi-3\alpha)$	$(\alpha;\alpha;\alpha;2\pi-3\alpha)$	$(\alpha;\alpha;\alpha;2\pi-3\alpha)$	$(\alpha;\alpha;\alpha;2\pi-3\alpha)$
$\alpha = \widehat{B_1B_2A_1}$ $\alpha = \arccos\left(cos\left(\frac{\pi}{n}\right)-\frac{1}{2}\right)$	$\arccos\left(\frac{\sqrt{2}-1}{2}\right)$	$\frac{2\pi}{5}$	$\arccos\left(\frac{1}{2}\ (\sqrt{3}-1)\right)$
$\arccos\left(\frac{1-2\cos\left(\frac{\pi}{n}\right)}{2\cos\left(\frac{\pi}{n}\right)-3}\right) = \lvert\widehat{B_1B_2}\rvert$	$\arccos\left(\frac{2\sqrt{2}-1}{7}\right)$	$\arccos\left(\frac{\sqrt{5}}{5}\right)$	$\arccos\left(\frac{\sqrt{3}}{3}\right)$
(Vertices, Edges, Faces) $(2n, 4n, 2n+2)$.	$(8,16,10)$	$(10,20,12)$	$(12,24,14)$

Figure 9: *n-gon* antiprism, $n \in \mathbb{N}$ and $n > 2$, obtained by rotations of a band of $2n$ equilateral triangles.

On the other hand, if $x > \pi/\arccos\left(\frac{1}{4}\right)$ the midpoints of the "non-lateral" edges of the band move away from the poles until the tiling pattern, associated with an regular n-agon antiprism is obtained (see Figure 8, $\mathfrak{B}_k, k \in \{3, \frac{9}{2}, 9\}$).

Figure 9 illustrates $\mathfrak{B}_n, n \in \{4,5,6\}$ and shows the arcs lengths, the angle measures and the planar configuration associated to the corresponding generated spherical tiling, from know on denoted by $\widehat{\mathfrak{B}_n}$. The angles and arcs measure of the triangles of the associated tilings can be obtained, dynamically, with the *GeoGebra* CAS.

By the use of *sequence* command the *GeoGebra* uncovers more complex tilings as the ones illustrated in figure 10, when we allow n to be the rational numbers $\frac{5}{q}$ with $q \in \{1,2,3\}$.

The tiling $\widehat{\mathfrak{B}_{\frac{5}{1}}}$ corresponds to the spherical pentagonal antiprism tiling described above. If $n = \frac{5}{2}$, the tiling $\widehat{\mathfrak{B}_n}$ has 25 vertices, 27 tiles from which two are spherical pentagons, ten are spherical triangle and fifteen are spherical quadrilaterals (five spherical rhombus and ten spherical kites). Finally, if $n = \frac{5}{3}$, the corresponding tiling, $\widehat{\mathfrak{B}_{\frac{5}{3}}}$, has 30 vertices defining 32 tiles (two spherical pentagons, ten spherical triangles, and twenty spherical kites).

In Figure 10 we may observe the tilings $\widehat{\mathfrak{B}_{\frac{5}{q}}}, q \in \{1,2,3\}$. This figure highlights the rotational symmetry of order 5 around the x–axis of all these tilings, the central symmetry of $\widehat{\mathfrak{B}_{\frac{5}{q}}}, q \in \{2,3\}$ and the reflection symmetry of $\widehat{\mathfrak{B}_{\frac{5}{2}}}$.

	$\widehat{\mathfrak{B}}_{\frac{5}{1}}$	$\widehat{\mathfrak{B}}_{\frac{5}{2}}$	$\widehat{\mathfrak{B}}_{\frac{5}{3}}$
Tilings	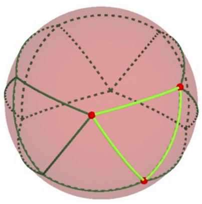	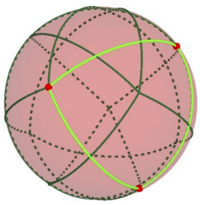	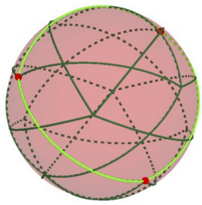
length of $\widehat{B_1B_2}$	$\arccos\left(\frac{\sqrt{5}}{5}\right)$	$\arccos\left(\frac{\sqrt{5}-4}{11}\right)$	$\arcsin\left(\frac{\sqrt{5}}{5}\right)+\frac{\pi}{2}$
Angles	$\frac{4\pi}{5};\frac{2\pi}{5}$	$\alpha=\arccos\left(\frac{1}{4}\left(\sqrt{5}-3\right)\right);2\pi-3\alpha$	$\frac{\pi}{3};\frac{2\pi}{5};\frac{2\pi}{3};\frac{4\pi}{5}$
Vertices: valence; angles; number.	$(3,3,3,5)$; $(\frac{2\pi}{5},\frac{2\pi}{5},\frac{2\pi}{5},\frac{4\pi}{5})$; 10.	$(3,4,3,5)$; $(3,4,4,4)$; $(4,4,4,4)$; $(3,4,4,4)$; $(3,4,3,5)$; 5 groups of 5 vertices each, in a total of 25.	$(3,4,3,5)$; $(\frac{\pi}{3},\frac{2\pi}{3},\frac{\pi}{3},\frac{2\pi}{3})$; $(3,4,4,4)$; $(\frac{2\pi}{5},\frac{2\pi}{5},\frac{4\pi}{5},\frac{2\pi}{5})$; $(4,4,4,4)$; $(\frac{\pi}{3},\frac{2\pi}{3},\frac{\pi}{3},\frac{2\pi}{3})$; $(4,4,4,4)$; $(\frac{\pi}{6},\frac{\pi}{3},\frac{\pi}{6},\frac{\pi}{3})$; $(3,4,4,4)$; $(\frac{2\pi}{5},\frac{2\pi}{5},\frac{4\pi}{5},\frac{2\pi}{5})$; $(3,4,3,5)$; $(\frac{\pi}{3},\frac{2\pi}{3},\frac{\pi}{3},\frac{2\pi}{3})$; 6 groups of 5 vertices each, in a total of 30.
Polyhedron	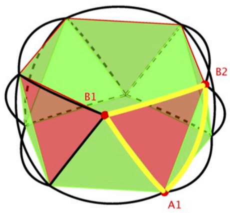	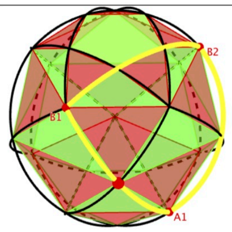	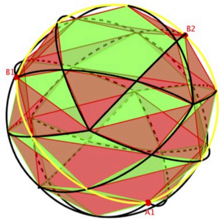
Faces Vertices Edges	12 Faces: 2, 5-gons; 2, 3-gons. 10 Vertices 20 Edges	37 Faces: 2, 5-gons; 30, 3-gons; 5, 4-gons. 25 Vertices 60 edges	42 Faces: 2, 5-gons; 40, 3-gons. 30 Vertices 70 edges

Figure 10: $\mathfrak{B}_{\frac{5}{q}}, q \in \{1,2,3\}$, combinatorial, geometric proprieties, and some of the associated polyhedra.

It should be noted that in this study we are not interested in the prismatic compound antiprisms, whose bases correspond to skew zig-zag polygons [8]. Although they appear in some cases, we emphasise that the tilings described above go beyond the class of tilings associated with those polyhedra. In our description there are tilings in which vertices of a given tile are not coplanar. This is the case of $\widehat{\mathfrak{B}}_{\frac{5}{2}}$ and $\widehat{\mathfrak{B}}_{\frac{5}{3}}$ (see Figure 10).

We may associate a polyhedron to these type of tilings, making use of triangulation of the non-coplanar tiles, but the process is not unique. The tiling $\widehat{\mathfrak{B}}_{\frac{5}{2}}$ has 27 spherical faces, 25 vertices and 40 edges; and we may associated to this tiling several polyhedra with 37 faces, 25 vertices and 60 edges (see row five in the table illustrated in Figure 10). It is worthwhile to mention that while tiling $\widehat{\mathfrak{B}}_{\frac{5}{2}}$ has two types of quadrangular faces, one with coplanar vertices and other with not coplanar vertices, the tiling $\widehat{\mathfrak{B}}_{\frac{5}{3}}$ has all quadrangular faces of a single type; its vertices are always not coplanar.

Let p and q be any two natural numbers, $p > q$. Observe that:

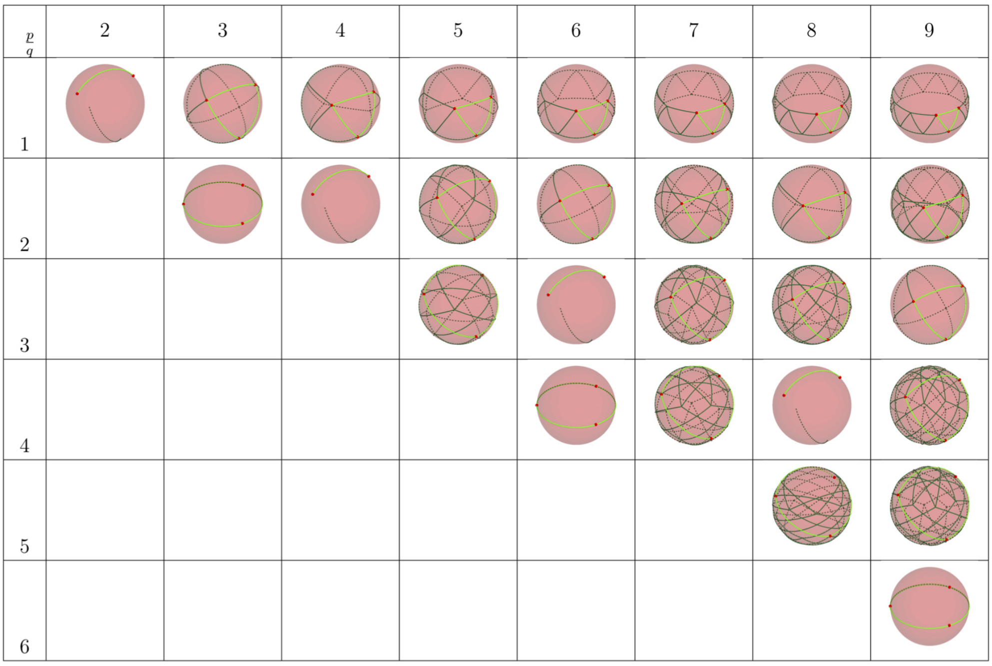

Figure 11: Configurations obtained with *GeoGebra* involving $\frac{p}{q} - agons$, with $p > q$.

- if $B_1 \neq B_2$ then $\frac{p}{q} \neq \frac{1}{n}, n \in \mathbb{N}$;
- if $\frac{p}{q} = \frac{3}{2}$, the points B_1, B_2 and A_3 are coplanar and $|B_1B_2| = |B_2A_1| = |A_1B_2| = \frac{2\pi}{3}$, and we have the sphere divided in two hemispheres. However these case corresponds to having A_1 in the arc $[B_1,B_2]$, which is not in consideration.
- the non trivial cases arise when $\frac{p}{q} > \frac{3}{2}$ and $gcd(p,q) = 1$.

3. Results

Theorem 3.1. *Let p and q be natural numbers such that $\frac{p}{q} > \frac{3}{2}$ and $gcd(p,q) = 1$. Let $k = min\{q, p-q\}$ and denote respectively by v, e and f, the number of vertices, edges and faces of the spherical tiling $\widehat{\mathfrak{B}_{\frac{p}{q}}}$, associate to $\mathfrak{B}_{\frac{p}{q}}$, then:*

- $v = p(2k+q-1)$;
- $e = 2p(2k+q-1)$;
- $f = p(2k+q-1)+2$;

Proof. The orbits of the points A_1 and B_1, as defined above, by the group of rotations about the z–axis through multiples of $2\pi/\frac{p}{q}$ generates two $\frac{p}{q}$ *spherical star-polygons*, Sp_T and Sp_D, about the points $(0,0,1)$ and $(0,0,-1)$, respectively.

Denote by T_j and D_j the vertices of Sp_T and Sp_D, with $j \in \{1,\dots,p\}$, respectively. These vertices of Sp_T and Sp_D are given by $T_j = Rot_{Oz}(B_1,(j-1)\frac{2\pi}{p})$ and $D_j = Rot_{Oz}(A_1,(j-1)\frac{2\pi}{p})$ with $j \in \{1,\dots,p\}$. The configurations of Sp_T, and Sp_D are the same as one corresponding to $\frac{p}{q}$ and $\frac{p}{p-q}$. Let $k = min\{q, p-q\}$. Thus, the number of vertices in Sp_T and Sp_D as part of $\widehat{\mathfrak{B}_{\frac{p}{q}}}$ is kp (see Figure 12).

Let us now see how to count the number of edges in Sp_T and Sp_D as part of $\widehat{\mathfrak{B}_{\frac{p}{q}}}$. Each arc T_iT_{i+q} (respectively D_iD_{i+q}) is divided into $2k-1$ arcs giving rise to $p(2k-1)$ edges. Thus, in total, Sp_T and Sp_D contribute with have $2p(2k-1)$ edges for the edges.of $\widehat{\mathfrak{B}_{\frac{p}{q}}}$.

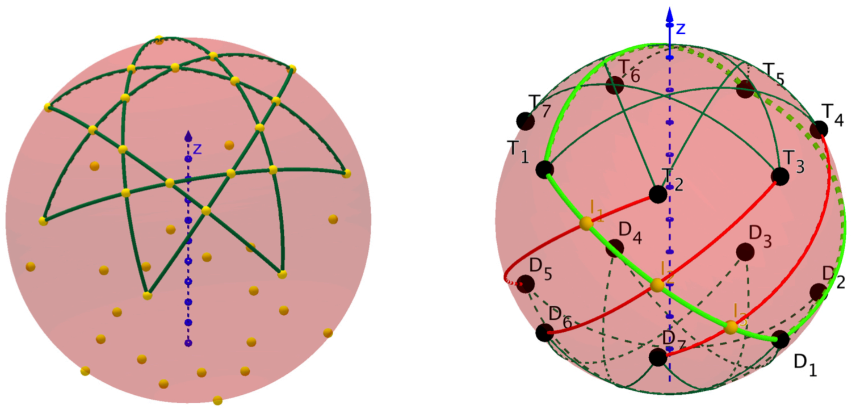

Figure 12: Vertices and cross points $\widehat{\mathfrak{B}_{\frac{p}{q}}}$.

The "lateral" edges [5] of $\widehat{\mathfrak{B}_{\frac{p}{q}}}$ joining the (external) vertices of Sp_T and Sp_D are the arcs corresponding to the orbit of the arcs T_1D_1 and D_1T_{1+q} by the cyclic group generated by the rotation of angle $\frac{2\pi}{p}$ around the z–axis. The arc T_1D_1 intersects the arcs $T_{1+j}D_{p-q+j}$ in $q-1$ cross points I_j with $j \in \{1, \ldots, q-1\}$. Therefore, the vertices T_1, D_1 and the cross points, $(I_j)_{j\in\{1,\ldots,q-1\}}$, define q edges $[T_1I_1], [I_1I_2], \ldots, [I_{j-1}I_j], [I_jD_1]$ of the $\widehat{\mathfrak{B}_{\frac{p}{q}}}$ tiling (see Figure 12). Thus the "lateral" net of $\widehat{\mathfrak{B}_{\frac{p}{q}}}$ has $p(q-1)$ vertices and pq edges.

Consequently $\widehat{\mathfrak{B}_{\frac{p}{q}}}$ has $v = p(2k+q-1)$ vertices, $e = 2p(2k+q-1)$ edges, and $f = p(2k+q-1)+2$ faces, being $(k-1)p$ triangles and $p(q+1)$ quadrilaterals.

□

Corollary 3.1.1. *If $\frac{p}{q} \in \mathbb{N}$ the family $\widehat{\mathfrak{B}_{\frac{p}{q}}}$ corresponds to the $\frac{p}{q}$−anti-prismatic tilings.*

Theorem 3.2. *Let p and q natural numbers such that $gcd(p,q) = 1$ and $\frac{p}{q} > \frac{3}{2}$. The tilings $\widehat{\mathfrak{B}_{\frac{p}{q}}}$*

- *are invariants by the cyclic group C_p;*
- *if q is a odd number then the tilings have central symmetry;*
- *if q is a even number then the tilings have reflection symmetry.*

Proof. The first and second statement are true having in consideration the construction of the band $\mathfrak{B}_{\frac{p}{q}}$ and the corresponding notation, given previously.

For the last statement it is enough to observe that

[5] In fact, the spherical segments that emerged between the vertices of Sp_T and Sp_D correspond to a helical polygon [8].

- the vertices $A_i \in 1, \dots p$ are in the orthogonal bisector of the arc segment B_iB_{i+1}. Thus, when q is an even number, the projections of the orbits of A_i and B_i in the plane $z = 0$ coincide;
- the edges of the the lateral net whose endpoints are not (external) vertices of Sp_T and Sp_D form an even number of edges of $\widehat{\mathfrak{B}_{\frac{p}{q}}}$ defining $q-1$ vertices of this tiling.

□

4. Exploring spherical tilings with GeoGebra

Here, we explore possible conjectures starting from a spherical triangle and its orbit under a local action of spherical reflections. We obtain a determined pattern by constructing a spherical triangle using the tools described in Section 2 and reflecting it in the planes containing its sides. We implemented this procedure in a *GeoGebra* application entitled "edge to edge" (see Figure 13 and Figure 14). Using this application and iterating it we get a sequence of spherical patterns as the one illustrated in Figure 13a. Since the initial triangle is not fixed it is expected that some of these patterns will end up in monohedral spherical tilings (see Figure 13b).

In figure 13b we illustrated this process beginning with the (fixed) spherical triangle $(\pi/2, \pi/2, \pi/3)$. As expected we end up with the hexagonal bypyramidal tiling. Using the same strategy but starting with the family of spherical triangles of angles $(\pi/2, \pi/2, 2\pi/n)$ we end up with the family of n-gons bypiramidal tiling.

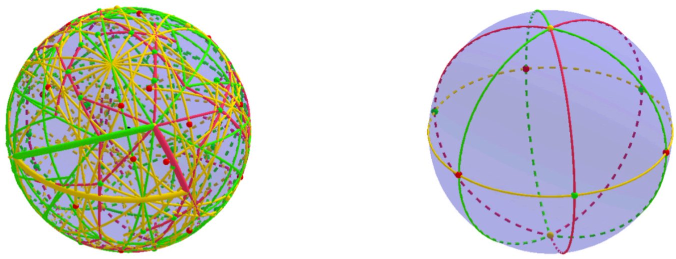

(a) Angles $\pi/5$,$2\pi/5$,and $3\pi/5$.

(b) Angles $\pi/2$, $\pi/2$, and $\pi/3$.

Figure 13: Spherical monohedral tilings, evolution to bi-pyramids tiling

Starting with the spherical triangle of angles $\pi/3$, $\pi/4$, and $\pi/2$ and using the same technique we end up with a spherical tiling with octahedral symmetry which corresponds to a polyhedron with 48 faces, the Catalan polyhedron disdyakis dodecahedron (see Figure 14a).

The spherical triangle of angles $\pi/5$, $\pi/3$, and $\pi/2$ gives rise to a spherical tiling with 120 congruent scalene triangles (see Figure 14b), with icosahedral symmetry, which corresponds to the Catalan polyhedron disdyakis triacontahedron.

Using the spherical triangle of angles $\pi/3$, $3\pi/4$, and $\pi/4$, we can we obtain a tiling by 12 congruent scalene spherical triangles, that corresponds a non-convex polyhedron with 12 triangular faces, 8 vertices and 18 edges (see Figure 14c). Continuing this process we end up always with a spherical tiling in which the starting triangle is not a tile of the achieved tiling but it is decomposed in tiles of the new tiling.

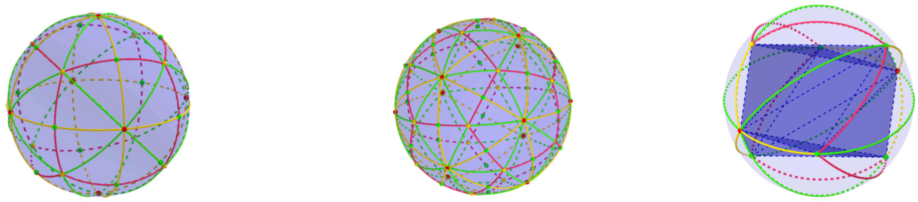

(a) Angles $\pi/3$, $\pi/4$, and $\pi/2$. (b) Angles $\pi/5$, $\pi/3$, and $\pi/2$ (c) Angles $\pi/3$, $3\pi/4$, and $\pi/4$.

Figure 14: Spherical monohedral tilings by triangles

The explorations carried out so far present some interesting results that need to be strengthened. It seems that using Schwarz triangles, this procedure seems to be able to provide a dynamic illustration of the polyhedral kaleidoscopes studied by Coxeter [8].

5. Conclusions

We have presented several new *GeoGebra* tools that may be used to explore spherical geometry and to explore spherical tilings. An important advantage of these applications is the interactivity and the visualisation of the created objects, promoting conjectures and the respective formal proofs. The conjectures can also be tested by the *GeoGebra* CAS capabilities.

Acknowledgements

This work was supported in part by the Portuguese Foundation for Science and Technology (FCT— Fundação para a Ciência e a Tecnologia), through CIDMA — Centre for Research and Development in Mathematics and Applications, within project UID/MAT/04106/2013. Special thanks to João Jorge Ribeiro Soares Gonçalves de Araújo for helpful comments and the reading of this paper.

References

[1] David Austin and Will Dickinson. *Spherical easel. A spherical drawing program.* 2002–2009. URL: http://merganser.math.gvsu.edu/easel/ (visited on 10/05/2018).

[2] Carlos Beltrán. ‘A facility location formulation for stable polynomials and elliptic Fekete points’. In: *Foundations of Computational Mathematics* 15.1 (Feb. 2015), pp. 125–157. ISSN: 1615-3383. DOI: 10.1007/s10208-014-9213-0. URL: https://doi.org/10.1007/s10208-014-9213- (visited on 10/05/2018).

[3] Johann S Brauchart and Peter J Grabner. ‘Distributing many points on spheres: minimal energy and designs’. In: *Journal of Complexity* 31.3 (2015), pp. 293–326. DOI: https://doi.org/10.1016/j.jco.2015.02.003. URL: http://www.sciencedirect.com/science/article/pii/S0885064X15000205 (visited on 10/05/2018).

[4] Ana M d'Azevedo Breda and José M Dos Santos Dos Santos. 'A new class of monohedral pentagonal spherical tilings with GeoGebra'. In: *Portugaliae Mathematica* 74.3 (2018), pp. 257–266. DOI: 10.4171/PM/2006. URL: https://ria.ua.pt/bitstream/10773/22148/1/PM_74-3_06%20257.pdf (visited on 10/05/2018).

[5] Ana M d'Azevedo Breda and José M Dos Santos Dos Santos. *Dihedral antiprismatic spherical Tilings*. 2018–. URL: https://ggbm.at/vybwsjm4 (visited on 25/11/2018).

[6] Ana M d'Azevedo Breda and José M Dos Santos Dos Santos. *Evolution of nets of equilateral spherical triangles*. 2018–. URL: https://ggbm.at/z6qsuwzj (visited on 25/11/2018).

[7] Ana MR Azevedo Breda. 'A class of tilings of S^2'. In: *Geometriae Dedicata* 44.3 (1992), pp. 241–253. ISSN: 1572-9168. DOI: 10.1007/BF00181393. URL: https://doi.org/10.1007/BF00181393 (visited on 10/05/2018).

[8] Harold Scott Macdonald Coxeter. *Regular complex polytope*. Cambridge University, 1974.

[9] HL Davies. 'Packings of spherical triangles and tetrahedra'. In: *Proc. Colloquium on Convexity (Copenhagen, 1965)*. 1967, pp. 42–51.

[10] Robert J MacG Dawson. 'An isosceles triangle that tiles the sphere in exactly three ways'. In: *Discrete & Computational Geometry* 30.3 (2003), pp. 459–466. URL: https://link.springer.com/article/10.1007/s00454-003-2777-0 (visited on 10/05/2018).

[11] Robert J MacG Dawson. 'Some New Tilings of the Sphere with Congruent Triangles'. In: *Renaissance Banff: Mathematics, Music, Art, Culture*. Bridges Conference. 2005, pp. 489–496. URL: https://archive.bridgesmathart.org/2005/bridges2005-489.pdf (visited on 10/05/2018).

[12] Robert J MacG Dawson. 'Tilings of the sphere with isosceles triangles'. In: *Discrete & Computational Geometry* 30.3 (2003), pp. 467–487. URL: https://link.springer.com/article/10.1007/s00454-003-2846-4 (visited on 10/05/2018).

[13] Robert J MacG Dawson and Blair Doyle. 'Tilings of the sphere with right triangles I: the asymptotically right families'. In: *The Electronic Journal of Combinatorics* 13.2 (2006), p. 48. URL: http://emis.ams.org/journals/EJC/Volume_13/PDF/v13i1r48.pdf (visited on 10/05/2018).

[14] Bart De Nijs et al. 'Entropy-driven formation of large icosahedral colloidal clusters by spherical confinement'. In: *Nature materials* 14.1 (2015), p. 56. URL: web.science.uu.nl/SCM/Articles/2015/de%20Nijs_NatureMater_2015.pdf (visited on 10/05/2018).

[15] Michel Deza et al. 'Fullerenes as tilings of surfaces'. In: *Journal of chemical information and computer sciences* 40.3 (2000), pp. 550–558. URL: http://citeseerx.ist.psu.edu/viewdoc/download?doi=10.1.1.105.5973&rep=rep1&type=pdf (visited on 10/05/2018).

[16] Mircea V Diudea and Csaba L Nagy. *Periodic nanostructures*. Vol. 7. Springer Science & Business Media, 2007.

[17] János Erdős. 'Sphaerica: Interactive Spherical Geometry Software'. In: *Proceedings of Bridges 2010: Mathematics, Music, Art, Architecture, Culture*. Ed. by George W. Hart and Reza Sarhangi. Phoenix, Arizona: Tessellations Publishing, 2010, pp. 443–446. ISBN: 978-0-98460-420-3. URL: http://archive.bridgesmathart.org/2010/bridges2010-443.pdf (visited on 10/05/2018).

[18] Markus Hohenwarter. 'Ein Softwaresystem für dynamische Geometrie und Algebra der Ebene'. MA thesis. Salzburg: Paris Lodron University, 2002. URL: http://archive.geogebra.org/static/publications/diplomarbeit_geogebra.pdf (visited on 10/05/2018).

[19] Markus Hohenwarter. *GeoGebra. Geometry and Algebra Software*. 2002–. URL: https://www.geogebra.org/ (visited on 10/05/2018).

[20] Markus Hohenwarter and Karl Fuchs. 'Combination of dynamic geometry, algebra and calculus in the software system GeoGebra'. In: *Computer Algebra Systems and Dynamic Geometry Systems in Mathematics Teaching Conference*. 2004. URL: http://archive.geogebra.org/static/publications/pecs_2004.pdf (visited on 10/05/2018).

[21] Ali Asghar Rezaei. 'Polygonal tiling of some surfaces containing fullerene molecules'. In: *Iranian Journal of Mathematical Chemistry* 5.2 (2014), pp. 99–105. URL: http://ijmc.kashanu.ac.ir/article_7375_490966fb9747f786985dfc15d4bc6a1a.pdf (visited on 10/05/2018).

[22] Ali Asghar Rezaei. 'Tiling Fullerene Surface with Heptagon and Octagon'. In: *Fullerenes, Nanotubes and Carbon Nanostructures* 23.12 (2015), pp. 1033–1036. DOI: 10.1080/1536383X.2015.1057817. eprint: https://doi.org/10.1080/1536383X.2015.1057817. URL: https://doi.org/10.1080/1536383X.2015.1057817 (visited on 10/05/2018).

[23] Edward B Saff and Amo BJ Kuijlaars. 'Distributing many points on a sphere'. In: *The mathematical intelligencer* 19.1 (1997), pp. 5–11. URL: https://perswww.kuleuven.be/~u0017946/publications/Papers97/art97a-Saff-Kuijlaars-MI/Saff-Kuijlaars-MathIntel97.pdf (visited on 10/05/2018).

[24] DMY Sommerville. 'VI.—Division of Space by Congruent Triangles and Tetrahedra'. In: *Proceedings of the Royal Society of Edinburgh* 43 (1924), pp. 85–116.

[25] Gerry Stahl. *Adventures in dynamic geometry*. Lulu. com, 2018. URL: http://gerrystahl.net/elibrary/topics/topics.pdf (visited on 17/11/2018).

[26] Lajos Szilassi. *A Bolyai geometria – szemléletesen*. 2018–. URL: https://www.geogebra.org/m/NSQ9meGe (visited on 17/11/2018).

[27] Yuan-Zhi Tan et al. 'Carbon arc production of heptagon-containing fullerene [68]'. In: *Nature communications* 2 (2011), ncomms1431. URL: https://www.nature.com/articles/ncomms1431.pdf (visited on 10/05/2018).

[28] GeoGebra Team. *Tutorial:Custom Tools and Customizing the Toolbar*. 2016–. URL: https://wiki.geogebra.org/en/Tutorial:Custom_Tools_and_Customizing_the_Toolbar (visited on 10/05/2018).

[29] Yukako Ueno and Yoshio Agaoka. 'Tilings of the 2-dimensional sphere by congruent right triangles'. In: *Memoirs of the Faculty of Integrated Arts and Sciences, Hiroshima University. IV, Science reports: studies of fundamental and environmental sciences* 22 (1996), pp. 1–23. URL: http://ir.lib.hiroshima-u.ac.jp/files/public/0/673/20141016120323365034/KJ00000197303.pdf (visited on 10/05/2018).

[30] Yukako Ueno, Yoshio Agaoka et al. 'Classification of tilings of the 2-dimensional sphere by congruent triangles'. In: *Hiroshima Mathematical Journal* 32.3 (2002), pp. 463–540. URL: http://www.math.sci.hiroshima-u.ac.jp/hmj/v32.3/P463-540.PDF (visited on 10/05/2018).

[31] Zhi Wang et al. 'Assembly of silver Trigons into a buckyball-like Ag180 nanocage'. In: *Proceedings of the National Academy of Sciences* 114.46 (2017), pp. 12132–12137. URL: http://www.pnas.org/content/pnas/114/46/12132.full.pdf (visited on 10/05/2018).

Received May 10, 2018; final from November 30, 2018

Chapter 4

A new class of monohedral pentagonal spherical tilings with GeoGebra [22]

Here, making use of GeoGebra, we show how to generate new classes of monohedral non-convex triangular and new non-convex pentagonal spherical tilings, changing the side gluing rules of the regular spherical tetrahedral tiling, by means of a local action of particular subgroups of spherical isometries. In both cases each polygon has π as area measure.

In relation to the new class of pentagonal tilings, we describe some of their geometrical and combinatorial properties and show the existence, in a special case, of an associated dihedral triangular spherical tiling.

These classes of spherical tilings have emerged as a result of an interative construction process, only possible by the use of the newly produced GeoGebra tools and the dynamic interaction capabilities of this software. In section 2 of this paper we begin by presenting a construction process of monohedral spherical tilings of area π, this procedure depends on the action of a subgroup of spherical isometries over a well chosen spherical set. We will end up with two one parameter new classes of spherical tilings $\mathfrak{T}_{(\mathcal{C},\rho)}$ and $\mathfrak{P}_{(\mathcal{C},\rho)}$.

The description of the one parameter family $\mathfrak{T}_{(\mathcal{C},\rho)}$, in which each one of its elements is composed by four triangles, is given in section 3 of this paper. Section 4 describes the one parameter family $\mathfrak{P}_{(\mathcal{C},\rho)}$, being that each one of its element is composed by four non-convex pentagons.

Portugal. Math. (N.S.)
Vol. 74, Fasc. 3, 2018, 257–266
DOI 10.4171/PM/2006

Portugaliae Mathematica

A new class of monohedral pentagonal spherical tilings with GeoGebra

Ana M. D'Azevedo Breda, José M. Dos Santos Dos Santos

(Communicated by João Araújo o and Peter J. Cameron)

Abstract. By a monohedral spherical tiling we mean a decomposition of the sphere by geodesic congruent polygons. Here, making use of GeoGebra, a well known free interactive mathematics software, we show how to generate new classes of monohedral non-convex triangular and new non-convex pentagonal spherical tilings, changing the side gluing rules of the regular spherical tetrahedral tiling, by means of a local action of particular subgroups of spherical isometries. In both cases each face has π as area measure.

In relation to the new class of pentagonal tilings, we describe some of their properties and show the existence, in a special case, of an associated dihedral triangular spherical tiling, that is, a tiling composed by two sets of congruent triangles.

These classes of spherical tilings have emerged as a result of an interative construction process, only possible by the use of newly produced GeoGebra tools and the dynamic interaction capabilities of this software.

Mathematics Subject Classification. 51L99; 58E40.

Keywords. Spherical Geometry, spherical tilings, GeoGebra

1. Introduction

In this paper our main result is the description of the combinatorial and geometric characterisation of a new one-parameter class of edge-to-edge spherical tilings, denoted by $\mathfrak{P}_{(\mathcal{C},\rho)\ \rho\in[0,\pi]}$, expanding the knowledge of monohedral spherical tilings by triangles and pentagons, that is, tilings of the sphere in which all spherical faces are congruent among them. This one-parameter class emerged as a result of an iterative construction process, starting from a particular subset of S^2 and particular sets of spherical isometries ruling the gluing side rules of the new constructed tilings (for details, see section 4), making use of new produced GeoGebra tools and the dynamic interaction capabilities of this software.

There are many tools to work with spherical geometry in an interactive way, as Sphaerica [8], Spherical Easel [1], and Povray [5]. However, for our purposes we need to work with more flexible tools and commands, in particular, we need to obtain in real time the orbit of a set of spherical points under the action of a (sub)group of spherical isometries. For that, GeoGebra [10] seems the best option for two crucial reasons: the widespread use of GeoGebra and the possibility of interaction with geometrical and algebraic representations simultaneously. In fact, GeoGebra has several geometrical representations in 2 and 3 dimensions allowing the interaction with spherical points in a diversity of ways. Besides, the algebraic capabilities of GeoGebra allow the study and the induction of some geometrical properties which may be visualized in real time. Among its many features, GeoGebra allows the creation of new tools and commands, dealing with sequences of various geometric and algebraic objects and using logical and heuristic procedures, it allows, to certify some properties of these same objects, for example, to be congruent with each other [7].

A systematic study of spherical tilings started with D. Sommerville [11] who has stablished part of the classification of spherical tilings by isosceles triangles having analysed a very particular case by scalene triangles [6, p.467]. H. Davies, in 1967, presents an incomplete classification of triangular monohedral tilings of the sphere [4] omitting many details which were fixed latter on.

Tilings of the sphere by right triangles were obtained by Yukako Ueno and Yoshio Agaoka in 1996 [14]. Later, in 2002, the same authors [15] obtain the complete classification of monohedral edge-to-edge triangular spherical tilings. It should be noted that triangular spherical folding tilings were studied by Ana Breda [2] and their classification was obtained in 1992, these being a subset of the triangular monohedral spherical tilings .

The regular dodecahedral spherical tiling is a well known tiling of the sphere by twelve regular pentagonal spherical polygons. More recently, all edge-to-edge tilings of the sphere by 12 congruent convex pentagons has been classified by Honghao, Shi and Yan [9].

The classification of spherical tilings by triangles is not yet completed. In fact, little is known when the condition of being monohedral or edge-to-edge is dropped out. A systematic study to enumerate and classify all spherical tilings is far from being complete.

In the next section 2, we begin by presenting a construction process of monohedral spherical tilings of area π, this process depends on a spherical set locally under the action of a subgroup of spherical isometries. We will end up with two classes. In section 3 we will describe the immersion of the class, $\mathfrak{T}_{(\mathcal{C},\rho)}$, of monohedral spherical tilings by four triangles, followed, in section 4, by the description of the finding of $\mathfrak{P}_{(\mathcal{C},\rho)}$, a class of monohedral spherical tiling by non-convex pentagons of area π. Finally, in section 5, we present our conclusions about the use of GeoGebra in the present work, as well as our proposals for upcoming research.

From now on, all the tilings in consideration are edge-to-edge, unless stated otherwise.

2. A class of monohedral tilings of the sphere of area π

Let S^2 be the sphere centred in $O = (0, 0, 0)$ and radius 1, c a great circle of S^2, and A and B two distinct points in c such that $\widehat{AOB} = \arcsin(\frac{1}{3}) + \frac{1}{2}\pi$. Chose one point $C \in S^2$ such that $[ABC]$ defines an equilateral triangle with angles $\frac{2\pi}{3}$. Let Q, R and S be the midpoints of the spherical segments $\widehat{AB}, \widehat{BC}$ and $\widehat{CA}$, respectively. Let $P \in \widehat{QC}$ such that $\widehat{QOP} = \rho$, $\rho \in [0, \pi]$. Let $\mathcal{C} = \{X \in S^2 : X \in \widehat{PS} \vee X \in \widehat{PR} \vee X \in \widehat{PQ}\}$. In order to obtain a spherical tiling, we use GeoGebra, applying spherical isometries to the set $\mathcal{C}$ (fig. 1(a)). All the isometries that will be applied to $\mathcal{C}$ fix the points of the set $\{A, B, C, Q, S, R\}$. In the case illustrated in figure 1(b), only the point P will be a vertex of the tiling and the points Q and R will be midpoints of edges of the tiling. In case of figure 1(c), the points Q, R will be vertices of the tiling and S will be the midpoint of an edge of the tiling. Since the points Q, S, R are midpoints of the spherical equilateral triangle ABC of angles $\frac{2\pi}{3}$, we have:

$$\widehat{QS} = \widehat{SR} = \widehat{RQ} = \frac{\pi}{2}, \quad \widehat{PS} = \widehat{PR}$$

$$\widehat{ABC} = \widehat{BCA} = \widehat{CAB} = \frac{2\pi}{3}, \quad \widehat{BSQ} = \widehat{SQB} = \widehat{QRA} = \widehat{AQR} = \frac{\pi}{4}.$$

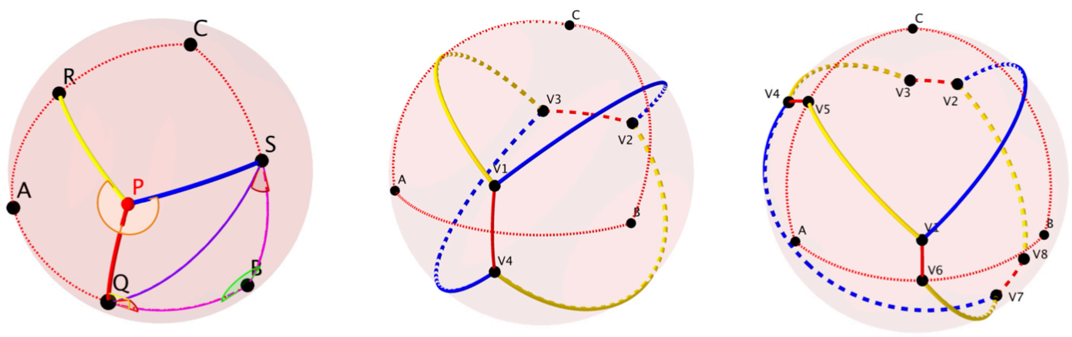

Figure 1. (a) Representation of the set $\mathcal{C}$. (b) monohedral triangular spherical tiling, $\mathfrak{T}_{(\mathcal{C}, \frac{\pi}{10})}$. (c) monohedral pentagons spherical tiling, $\mathfrak{P}_{(\mathcal{C}, \frac{\pi}{10})}$.

The lengths of the arcs in $\mathcal{C}$ (arcs emerging from P) and the angles around P are defined in function of ρ, using the spherical relations for triangles.

Accordingly, we have:

$$\widehat{PQ} = \rho, \quad \widehat{PR} = \widehat{PS} = \arccos\left(\tfrac{\sqrt{2}}{2}\sin(\rho)\right);$$

$$\widehat{QPS} = \widehat{QPR} = \arccos\left(\frac{-\cos(\rho)}{\sqrt{1+\cos(\rho)^2}}\right),$$

$$\widehat{PRA} = \widehat{PSB} = \tfrac{\pi}{4} + \arccos\left(\frac{\sqrt{2}\cos(\rho)}{\sqrt{1+\cos(\rho)^2}}\right).$$

In order to obtain the two classes of monohedral spherical tilings, $\mathfrak{T}_{(\mathcal{C},\rho)}$ and $\mathfrak{P}_{(\mathcal{C},\rho)}$,respectively by triangles and pentagons, see figure 1, we consider the rotations $\mathscr{R}_{(P,\rho)}$, about the axis OP, of angle ρ, $\rho \in [0,\pi]$, and two sets of spherical isometries $\mathfrak{I}_1$ and $\mathfrak{I}_2$ defined bellow.

Let $\mathfrak{I}_1 = \{\mathscr{R}_{(Q,\pi)}, \mathscr{R}_{(S,\pi)}, \mathscr{R}_{(R,\pi)}\}$ and $\mathfrak{I}_2 = \{\mathscr{R}_{(S,\pi)}, \mathscr{R}_{(C,2\pi/3)}\}$.

For each value of $\rho \in [0,\pi]$, the action of $\mathfrak{I}_1$ on $\mathcal{C}$ defines a class of spherical monohedral triangular tilings denoted by $\mathfrak{T}_{(\mathcal{C},\rho)}$.

On the other hand, for each value of $\rho \in [0,\pi]$, we may construct a new class of monohedral tilings by non-convex pentagons denoted by $\mathfrak{P}_{(\mathcal{C},\rho)}$.

In this case the four tiles of $\mathfrak{P}_{(\mathcal{C},\rho)}$ are obtained using $\mathfrak{I}_2$ and applying the procedure indicated bellow, see figure 1 (c).

Let

1. $\mathcal{C}_0 = \mathcal{C}$;
2. $\mathcal{C}_1 = \mathscr{R}_{(S,\pi)}(\mathcal{C})$;
3. $\mathcal{C}_2 = \mathscr{R}_{(C,2\pi/3)}(\mathcal{C}_1)$;
4. $\mathcal{C}_3 = \mathscr{R}_{(S,\pi)}(\mathcal{C}_2)$.

Then, $\mathfrak{P}_{(\mathcal{C},\rho)} = \cup_{i=0}^{3}\mathcal{C}_i$.

Let us see how GeoGebra had been used to generate the class of tilings $\mathfrak{T}_{(\mathcal{C},\theta)}$, $\theta \in [0,2\pi]$ and acted as support for some of the results presented here.

The first geometric construction was done starting from a point P in $\widehat{QC}$ and joinning P to the middle points of $\widehat{AC}$ and $\widehat{BC}$, giving rise to $\mathcal{C}$. Applying to $\mathcal{C}$ each one of the isometries in $\mathfrak{I}_1$, a spherical configuration emerges.

The code used for visualizing, for each value of θ, this configuration is shown in table 1.

If the obtained configuration is a spherical tiling, the CAS view is then used to obtain the algebraic expressions of the measures of: the arcs lengths; the angles surrounding each vertex and the coordinates of the vertices. Note that in the GeoGebra CAS view we do have all the vector and matrix operations needed to

Objects	3D View	CAS View
Parameter	θ=Slider(0, 2*pi,2*pi/100)	—
		Correspond one vector to each vertex
	C=(-1/3,-sqrt(2/9),sqrt(2/3))	vC:=C
	Q=(sqrt(3)/3,sqrt(2/3),0)	vQ:=Q
Points	S=((-sqrt(3))/3,sqrt(2/3)/2, sqrt(2)/2)	vS:=S
	R=(sqrt(3)/3,(-sqrt(2/3))/2,sqrt(2)/2)	vR:=R
	P=(cos(θ)*sqrt(3)/3,cos(θ)*sqrt(2/3),sin(θ))	vP:=(cos(ρ)*sqrt(3)/3,cos(ρ)*sqrt(2/3),sin(ρ))
	PQ=CircularArc((0, 0, 0),P,Q,Plane((0, 0, 0),P,Q))	arccos(vP*vQ)
Arcs	PS=CircularArc((0, 0, 0),P,S,Plane((0, 0, 0),P,S))	arccos(vP*vS)
	PQ=CircularArc((0, 0, 0),P,R,Plane((0, 0, 0),P,R))	arccos(vP*vR)
Cell	Ce={PQ,PS,PR}	—
$\mathscr{R}_{(Q,\pi)}$	I1Ce1=Rotate(Ce, pi, Ray((0,0,0), Q))	—
		For example, defining the rotation matrix,
		MSpi:= $\begin{pmatrix} -\frac{1}{3} & -\frac{\sqrt{2}}{3} & -\frac{\sqrt{6}}{3} \\ -\frac{\sqrt{2}}{3} & -\frac{2}{3} & 0 \\ -\frac{\sqrt{6}}{3} & \frac{1}{\sqrt{3}} & 0 \end{pmatrix}$
$\mathscr{R}_{(S,\pi)}$	I1Ce2=Rotate(Ce, pi, Ray((0,0,0), S))	applying the vector associated to a point,
		MSpi*vP
		and defining the image of a point.
		P"=(0,0,0)+MSpi*vP
$\mathscr{R}_{(R,\pi)}$	I1Ce3=Rotate(Ce, pi, Ray((0,0,0), R))	—

Table 1. GeoGebra commands to construct $\mathfrak{T}_{(\mathcal{C},\rho)}$ in 3D view and CAS view.

obtain the results presented in sections 3 and 4. Sometimes, we feel the need to use auxiliary applications and construct some macros. This was the case for the determination of the rotation matrices.

3. A class of monohedral spherical tilings by four triangles

The elements of $\mathfrak{T}_{(\mathcal{C},\rho)}$ are four congruent spherical triangles, but it should be pointed out that, for $\rho > \frac{\pi}{2}$ the tiles are not convex spherical polygons. The convex case was already described by several other authors, see for instance Brooks and Strantzen [3]. However, the non-convex case, $\mathfrak{T}_{(\mathcal{C},\rho)}, \rho \in]\frac{\pi}{2}, \pi[$ as far as we know, is not mentioned in the literature. We only find a brief reference to $\mathfrak{T}_{(\mathcal{C},\widehat{AOC})}$ by Gaiane in [12, 13].

The construction of $\mathfrak{T}_{(\mathcal{C},\rho)}, \rho \in]0, \pi[\setminus\{\frac{\pi}{2}\}$ is a family of four congruent triangles, all the vertices have the same valence surrounded by angles $(\alpha, \alpha, 2\pi - \alpha)$, with $\alpha(\rho) = \arccos\left(\frac{-\cos(\rho)}{\sqrt{1+\cos(\rho)^2}}\right)$.

The tiling $\mathfrak{T}_{(\mathcal{C},\arcsin(\frac{\sqrt{6}}{3}))}$ correspond to the tetrahedral spherical tilling. For some values of ρ ($\rho = 0, \frac{\pi}{2}, \pi$) we have spherical tilings by lunes (see figure 2). Note that allowing $\rho > \pi$ would lead to some arcs of $\mathcal{C}$ crossing others, revealing other types of spherical pattern.

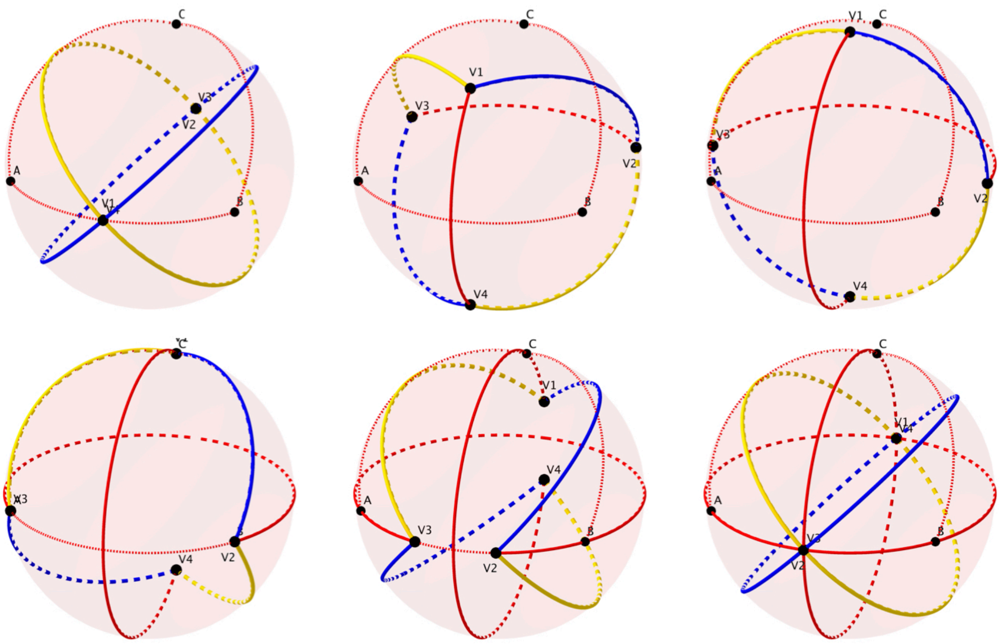

Figure 2. Representation of $\mathfrak{T}_{(\mathcal{C},0)}$,$\mathfrak{T}_{(\mathcal{C},arcsin(\frac{\sqrt{(6)}}{3}))}$,$\mathfrak{T}_{(\mathcal{C},\frac{\pi}{2})}$,$\mathfrak{T}_{(\mathcal{C},\widehat{AOC})}$, $\mathfrak{T}_{(\mathcal{C},\frac{7}{5}\widehat{AOC})}$, $\mathfrak{T}_{(\mathcal{C},\pi)}$.

4. A class of monohedral spherical tiling by four spherical pentagons of area π

Let us, now, present the details of the class of spherical monohedral tilings by four non-convex pentagons.

The procedure given previously applied to $\mathcal{C}$, already defined, is illustrated in figure 3. Observe that S and S' are antipodal points.

Let us summarise some of the geometric features of $\mathfrak{P}_{(\mathcal{C},\rho)} = \cup_{i=0}^{3}\mathcal{C}_i$.

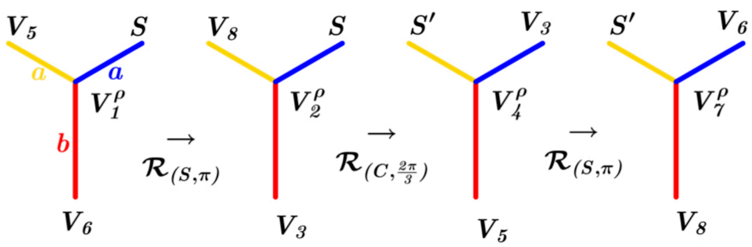

Points in $\mathcal{C}$	$\mathscr{R}_{(S,\pi)}(\mathcal{C})$	$\mathscr{R}_{(C,\frac{2\pi}{3})}(\mathscr{R}_{(S,\pi)}(\mathcal{C}))$	$\mathscr{R}_{(S,\pi)}(\mathscr{R}_{(C,\frac{2\pi}{3})}(\mathscr{R}_{(S,\pi)}(\mathcal{C})))$
$P = V_1^\rho$	V_2^ρ	V_4^ρ	V_7^ρ
$Q = V_6$	V_3	V_5	V_8
$R = V_5$	V_8	S'	S'
S	S	$V3$	V_6

Figure 3. Geometric features of $\mathfrak{P}_{(\mathcal{C},\rho)}$

Since we know how $\mathfrak{P}_{(\mathcal{C},\rho)}$ was built we may determine the coordinates of all its vertices. In fact,

$$P\left(\frac{\sqrt{3}}{3}\cos(\rho), \frac{\sqrt{6}}{3}\cos(\rho), \sin(\rho)\right), Q\left(\frac{\sqrt{3}}{3}, \frac{\sqrt{6}}{3}, 0\right),$$

$$R\left(\frac{\sqrt{3}}{3}, -\frac{\sqrt{6}}{6}, \frac{\sqrt{2}}{2}\right), S\left(-\frac{\sqrt{3}}{3}, \frac{\sqrt{6}}{6}, \frac{\sqrt{2}}{2}\right).$$

The $\mathfrak{I}_2$ isometries, namely, $\mathscr{R}_{(S,\pi)}$ and $\mathscr{R}_{(C,\frac{2\pi}{3})}$, may be defined, respectively, by the matrices:

$$\mathcal{R}_1 = \begin{pmatrix} -\frac{1}{3} & -\frac{\sqrt{2}}{3} & -\frac{\sqrt{6}}{3} \\ -\frac{\sqrt{2}}{3} & -\frac{2}{3} & 0 \\ -\frac{\sqrt{6}}{3} & \frac{1}{\sqrt{3}} & 0 \end{pmatrix}, \mathcal{R}_2 = \begin{pmatrix} -\frac{1}{3} & -\frac{\sqrt{2}}{3} & -\frac{\sqrt{6}}{3} \\ \frac{2\sqrt{2}}{3} & -\frac{1}{6} & -\frac{\sqrt{3}}{6} \\ 0 & -\frac{\sqrt{3}}{2} & \frac{1}{2} \end{pmatrix}.$$

.

Consequently, the coordinates of the vertices of $\mathfrak{P}_{(\mathcal{C},\rho)}$ are:

a) for the ones depending on ρ:

$V_2^\rho = \left(-\frac{\sqrt{3}}{3}\cos(\rho) - \frac{\sqrt{6}}{3}\sin(\rho), -\frac{\sqrt{6}}{3}\cos(\rho) + \frac{\sqrt{3}}{3}\sin(\rho), 0\right)$,

$V_4^\rho = \left(\frac{\sqrt{3}}{3}\cos(\rho), -\frac{\sqrt{6}}{6}\cos(\rho) - \frac{\sqrt{3}}{2}\sin(\rho), \frac{\sqrt{2}}{2}\cos(\rho) - \frac{1}{2}\sin(\rho)\right)$,

$V_7^\rho = \left(-\frac{\sqrt{3}}{3}\cos(\rho) + \frac{\sqrt{6}}{3}\sin(\rho), \frac{\sqrt{6}}{6}\cos(\rho) + \frac{\sqrt{3}}{6}\sin(\rho), -\frac{\sqrt{2}}{2}\cos(\rho) - \frac{1}{2}\sin(\rho)\right)$;

b) for the others:

$V_3 = \left(-\frac{\sqrt{3}}{3}, -\sqrt{\frac{2}{3}}, 0\right)$;

$V_8 = \left(-\frac{\sqrt{3}}{3}, \frac{\sqrt{6}}{6}, -\frac{\sqrt{2}}{2}\right)$.

A planar representation of the tiling $\mathfrak{P}_{(\mathcal{C},\rho)}$, is shown in figure 4. Accordingly, we have,

$$2\alpha_1 + \alpha_2 = 2\pi \text{ and } \alpha_3 + \alpha_4 = 2\pi,$$

where $\alpha_1(\rho) = \arccos\left(\frac{-\cos(\rho)}{\sqrt{1+\cos(\rho)^2}}\right)$, $\alpha_3(\rho) = \frac{3\pi}{4} + \arccos\left(\frac{\sqrt{2}\cos(\rho)}{\sqrt{1+\cos(\rho)^2}}\right)$.

The obtained configuration, see figure 4, defines a monohedral tiling of the sphere by four non convex pentagons if the points V_4^ρ, S', V_7^ρ belong to a same great circle. Obverve that the isometry $\mathscr{R}_{(S,\pi)}$ sends the point S, corresponding to the midpoint of $\widehat{V_1^\rho V_2^\rho}$, to itself. Besides,

$\overrightarrow{V_4^\rho S'} \otimes \overrightarrow{S' V_7^\rho} = \left(\frac{\sqrt{3}}{3}\cos(\rho) + \frac{\sqrt{6}}{6}\sin(\rho), \frac{\sqrt{6}}{3}\cos(\rho) - \frac{\sqrt{3}}{6}\sin(\rho), \frac{1}{2}\sin(\rho)\right)$,

and so, we may conclude that $\widehat{V_4^\rho V_7^\rho}$ is an edge of the tiling $\mathfrak{P}_{(\mathcal{C},\rho)}$.

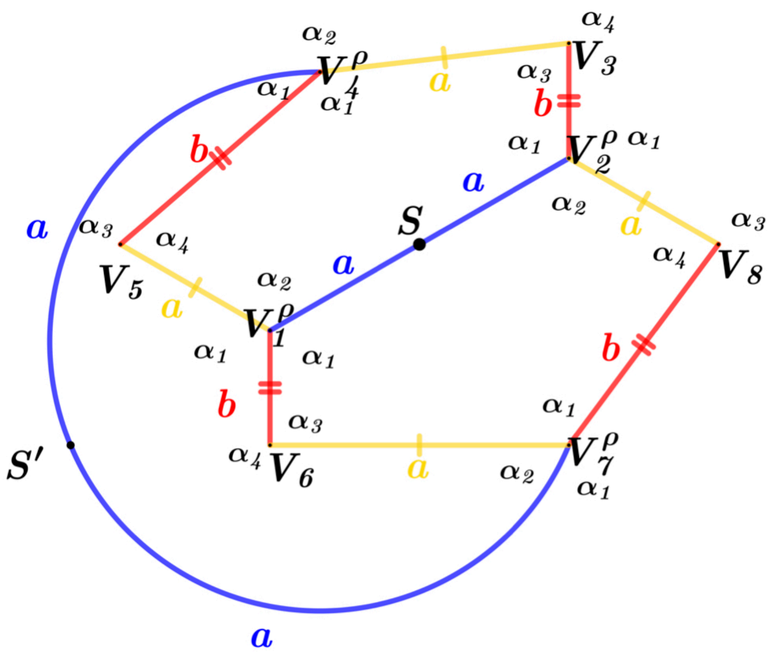

Figure 4. Planar representation of tiling $\mathfrak{P}_{(\mathcal{C},\rho)}$

The points $V_i, i \in \{1, \ldots, 8\}$, are then vertices of four non-convex congruent spherical pentagons, each one of area π, whose length edges are $(b, a, 2a, b, a)$ with $b = \rho$ and $a = \arccos\left(\frac{\sqrt{2}}{2}\sin(\rho)\right)$, see table 2.

T_1	T_2	T_3	T_4
$\widehat{V_1^\rho V_2^\rho} = 2a$	$\widehat{V_1^\rho V_2^\rho} = 2a$	$\widehat{V_2^\rho V_3} = b$	$\widehat{V_1^\rho V_6} = b$
$\widehat{V_2^\rho V_3} = b$	$\widehat{V_2^\rho V_8} = a$	$\widehat{V_3 V_4^\rho} = a$	$\widehat{V_6 V_7^\rho} = a$
$\widehat{V_3 V_4^\rho} = a$	$\widehat{V_8 V_7^\rho} = b$	$\widehat{V_4^\rho V_7^\rho} = 2a$	$\widehat{V_7^\rho V_4^\rho} = 2a$
$\widehat{V_4^\rho V_5} = b$	$\widehat{V_7^\rho V_6} = a$	$\widehat{V_7^\rho V_8} = b$	$\widehat{V_4^\rho V_5} = b$
$\widehat{V_5 V_1^\rho} = a$	$\widehat{V_6 V_1^\rho} = b$	$\widehat{V_8 V_2^\rho} = a$	$\widehat{V_5 V_1^\rho} = a$
$\widehat{V_5 V_1^\rho V_2^\rho} = \alpha 2$	$\widehat{V_6 V_1^\rho V_2^\rho} = \alpha 1$	$\widehat{V_8 V_2^\rho V_3} = \alpha 1$	$\widehat{V_5 V_1^\rho V_6} = \alpha 1$
$\widehat{V_1^\rho V_2^\rho V_3} = \alpha 1$	$\widehat{V_1^\rho V_2^\rho V_8} = \alpha 2$	$\widehat{V_2^\rho V_3 V_4^\rho} = \alpha 4$	$\widehat{V_1^\rho V_6 V_7^\rho} = \alpha 4$
$\widehat{V_2^\rho V 3 V 4} = \alpha 3$	$\widehat{V_2^\rho V_8 V_7^\rho} = \alpha 4$	$\widehat{V_3 V_4^\rho V_7^\rho} = \alpha 2$	$\widehat{V_6 V_7^\rho V_4^\rho} = \alpha 2$
$\widehat{V_3 V_4^\rho V_5} = \alpha 1$	$\widehat{V_8 V_7^\rho V_6} = \alpha 1$	$\widehat{V_4^\rho V_7^\rho V_8} = \alpha 1$	$\widehat{V_7^\rho V_4^\rho V_5} = \alpha 1$
$\widehat{V_4^\rho V_5 V_1^\rho} = \alpha 4$	$\widehat{V_7^\rho V_6 V_1^\rho} = \alpha 3$	$\widehat{V_7^\rho V_8 V_2^\rho} = \alpha 3$	$\widehat{V_4^\rho V_5 V_1^\rho} = \alpha 3$

Table 2. Edge and angle measures of $\mathfrak{P}_{(\mathcal{C},\rho)}$

The case of $\mathfrak{P}_{(\mathcal{C},\rho)}$ with $\rho = \arccos\left(-\frac{1}{\sqrt{3}}\right)$ corresponds to the tetrahedral spherical tiling and the cases corresponding to $\rho \in \{0,\pi\}$ are lunes.

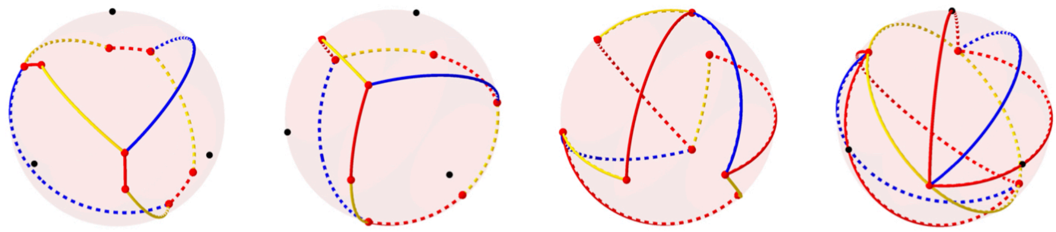

Figure 5. (a) $\mathfrak{P}_{(\mathcal{C},\frac{\pi}{8})}$, (b) $\mathfrak{P}_{(\mathcal{C},\frac{1}{2}\arccos(-\frac{1}{3}))}$, (c) $\mathfrak{P}_{\left(\mathcal{C},\arccos\left(-\frac{1}{\sqrt{3}}\right)\right)}$, (d) $\mathfrak{P}_{(\mathcal{C},\pi)}$.

For each $\rho \in]0,\pi[\backslash\{\frac{1}{2}\arccos\left(-\frac{1}{3}\right)\}$, $\mathfrak{P}_{(\mathcal{C},\rho)}$ is a monohedral tiling with four non-convex pentagonal faces and eight vertices, six of them of valence 3 surrounded by angles $(\alpha_1,\alpha_1,\alpha_2)$ being the other two of valence 2, surrounded by angles (α_3,α_4).

If $\rho = \arccos\left(-\frac{1}{\sqrt{3}}\right)$ the tiling $\mathfrak{P}_{(\mathcal{C},\rho)}$ defines a known dihedral tiling of the sphere by eight spherical right triangles.

5. Conclusions and future works

In this work, we present classes of monohedral tilings of the sphere obtained with the aid of GeoGebra. The use of special tools created in GeoGebra, for the study of spherical tilings, have proved to be quite useful for the search of new ones. In future works we intend to generalise the strategy described here, to be apllied to more generic *cells*, hoping to give a contribution to the current knowledge on this subject.

Acknowledgement

This work was supported in part by the Portuguese Foundation for Science and Technology (FCT— Fundação para a Ciência e a Tecnologia), through CIDMA — Centre for Research and Development in Mathematics and Applications, within project UID/MAT/04106/2013.

References

[1] D. Austin and W. Dickinson. "Spherical easel. A spherical drawing program." (2009).

[2] A.M. Breda, "A class of tilings of S2." Geometriae Dedicata 44:3 (1992), 241-253.

[3] J. Brooks and J. Strantzen, "Spherical triangles of area π and isosceles tetrahedra." Mathematics Magazine 78:4 (2005),311-314.

[4] H. L. Davies, "Packings of spherical triangles and tetrahedra." Proc. Colloquium on Convexity (Copenhagen, 1965). 1965.

[5] R.J. Dawson, "Some New Tilings of the Sphere with Congruent Triangles." Renaissance Banff: Mathematics, Music, Art, Culture. Bridges Conference, 2005.

[6] R.J. Dawson, "Tilings of the sphere with isosceles triangles." Discrete & Computational Geometry 30:3 (2003), 467-487.

[7] J. M. Dos Santos, and A. M. Breda. "Spherical Geometry and Spherical Tilings with GeoGebra" (2017). Manuscript submitted for publication.

[8] J. Erdős, "Sphaerica: Interactive Spherical Geometry Software." Proceedings of Bridges 2010: Mathematics, Music, Art, Architecture, Culture. Tessellations Publishing, 2010.

[9] H. Gao, N. Shi, and M. Yan, "Spherical tiling by 12 congruent pentagons." Journal of Combinatorial Theory, Series A 120:4 (2013), 744-776.

[10] M. Hohenwarter and K. Fuchs. "Combination of dynamic geometry, algebra and calculus in the software system GeoGebra." Computer Algebra Systems and Dynamic Geometry Systems in Mathematics Teaching Conference. 2004.

[11] D. M. Y. Sommerville, "VI.—Division of Space by Congruent Triangles and Tetrahedra." Proceedings of the Royal Society of Edinburgh 43 (1924), 85-116.

[12] G. Y. Panina, "Planar pseudo-triangulations, spherical pseudo-tilings and hyperbolic virtual polytopes." arXiv preprint math/0607171 (2006).

[13] G. Y. Panina, "Pointed spherical tilings and hyperbolic virtual polytopes." Journal of Mathematical Sciences 175:5 (2011), 591-599.

[14] Y. Ueno and Y. Agaoka, "Tilings of the 2-dimensional sphere by congruent right triangles." Memoirs of the Faculty of Integrated Arts and Sciences, Hiroshima University. IV, Science reports: studies of fundamental and environmental sciences 22 (1996), 1-23.

[15] Y. Ueno and Y. Agaoka, "Classification of tilings of the 2-dimensional sphere by congruent triangles." Hiroshima Mathematical Journal 32:3 (2002), 463-540.

Received Received October 25, 2017; revision received November 24, 2017

Ana Maria D'Azevedo Breda, Departamento de Matemática, Universidade de Aveiro, Campus Universitário de Santiago, 3810-193 Aveiro, Portugal.

E-mail: ambreda@ua.pt

José Manuel Dos Santos Dos Santos, Universidade Aberta, Rua da Escola Politécnica 141-147, 1269-001 Lisboa, Portugal

E-mail: dossantosdossantos@gmail.com

Chapter 5

Two classes of dihedral spherical pentagonal tilings.

In this paper we present two classes of dihedral spherical pentagonal tilings. We begin by showing how to generate new classes of dihedral pentagonal spherical tilings, changing the side gluing rules of the regular spherical hexahedral tiling, by means of a local action of particular subgroups of spherical isometries. In relation to these classes of pentagonal tilings, we will describe some of their combinatorial and topological properties. These classes of spherical tilings emerged as a result of an interative construction process, only possible, as previously stated by the use of newly produced GeoGebra tools and the dynamic interaction capabilities of this software.

Here we extend the knowledge of the set of pentagonal spherical tilings. A proper adaptation to the procedure described in chapter 4 to characterise the one-parameter family of tilings, $\mathfrak{P}_{(\mathcal{C},\tau)}$ $\tau \in]0,\pi[\setminus\{\frac{1}{2}\arccos\left(-\frac{1}{3}\right)\}$, by four congruent spherical non convex pentagons [22], determines two distinct one-parameter families composed by 12 pentagons:

$$\mathfrak{P}^{*}_{(\mathcal{C}_1,\tau^*)}, \tau^* \in]0, \arccos(\tfrac{\sqrt{3}}{3})[\setminus\{\arctan(\tfrac{\sqrt{2}}{2})\};$$

$$\mathfrak{P}^{**}_{(\mathcal{C}_2,\tau^{**})}, \tau^{**} \in]0, \tfrac{\pi}{2}[\setminus\{\arccos(\left(\tfrac{1}{8409}\left(41\sqrt{2803}+58\sqrt{5606}\right)\right)\}.$$

In the section 4, some topological properties of $\mathfrak{P}^{*}_{(\mathcal{C}_1,\tau^*)}$ and $\mathfrak{P}^{**}_{(\mathcal{C}_2,\tau^{**})}$ are given. We will show that the set composed by the union of these two families is arcwise-connected.

Two Classes of Dihedral Spherical Pentagonal Tilings, Searching Spherical Tilings with GeoGebra

Ana Maria d'Azevedo Breda

José Manuel Dos Santos Dos Santos

May 2018

Abstract

By a dihedral spherical tiling we mean a decomposition of the sphere by two non congruent spherical polygons. Making use of GeoGebra, a well known free interactive mathematics software, we will show how to generate new classes of dihedral pentagonal spherical tilings, changing the side gluing rules of the regular spherical hexahedral tiling, by means of a local action of particular subgroups of spherical isometries. In relation to these classes of pentagonal tilings, we will describe some of their combinatorial and topological properties. These classes of spherical tilings emerged as a result of an interative construction process, only possible by the use of newly produced GeoGebra tools and the dynamic interaction capabilities of this software.

keywords: Spherical Geometry, Spherical Tilings, GeoGebra.

1 Introduction

Spherical tilings by right triangles were obtained by Yukako Ueno and Yoshio Agaoka in 1996 [22]. Later, in 2002, the complete classification of monohedral edge-to-edge triangular spherical tilings was achieved by the same authors [23]. They have extended the classification of triangular f-spherical foldings, studied and characterized by Ana Breda, in 1992 [12].

The classification of spherical tilings by triangles is not yet completed. In fact, little is known when the condition of being monohedral or edge-to-edge is dropped out.

The combinatorial study of spherical tilings by twelve pentagons considering all vertices of valence greater than or equal to three has been also done, see [17] for details. Very little is known about spherical tilings involving non-convex spherical polygons, that is, tilings where the possibility of vertices of valence equal to two should not be dismissed. Recently, a family of spherical monohedral tiles by four congruent and non-convex spherical pentagons has been characterised [9].

Moving now to the dihedral case, it is worth mention that, the classification of dihedral f-tilings of the sphere whose prototiles are a kite and an equilateral or isosceles triangle has been achieved [3, 6, 4, 5]. Great strides were also made in the study of spherical f-tilings by kites and scalene triangles [2, 1]. In this paper we present two families of dihedral spherical tilings, by twelve spherical pentagons, characterising an infinite family of non-convex spherical pentagons.

Besides the theoretical mathematical aspects involved in the study of spherical tilings, they are also object of interest in other areas of knowledge and in technological applications. In fact, the study of spherical tiling has applications to chemistry, for instance, in the study of periodic nanostructures [16], emerging new forms of association of molecules, notably fullerenes [15], lwading to a deeper study of spherical tilings by triangles, squares, pentagons, and hexagons [19]. In the same line of reasoning other tilings including heptagons [21] and heptagon and octagons [20] had emerged. Applications to new possibilities for new molecular patterns are exposed in [24, 13]. Nowadays, in engineering there is a need to merge the computer aided design and computer aided engineering into a single approach, contributing to an increasing interest in studying relationships between spherical tilings and spherical Bezier curves [14]. The knowledge of spherical tilings can also be useful for the development of some issues in computational algebra [18]. The facility location problems, spherical designs and minimal energy point configurations on spheres [7, 8] are other fields where the study of spherical tilings is quite useful.

In ours first works we prepared several tools to work with spherical geometry in GeoGebra, namely two searching new spherical tilings [11]. With this new tools, we extend the knowledge of the antiprismatic spherical tiling family and by this way get new families of polyhedrons [10].

In this article we intend to extend the knowledge of the set of spherical tilings, here denoted by $\mathfrak{T}$, presenting and characterising subsets of $\mathfrak{T}_5$, the set of all pentagonal spherical tilings.

A proper adaptation to the procedure recently described to characterise the one-paramete family of tilings, $\mathfrak{P}_{(\mathscr{C},\tau)}$ $\tau \in]0,\pi[\setminus\{\frac{1}{2}\arccos(-\frac{1}{3})\}$, by four congruent spherical non convex pentagons, see [9], determines two distinct one-parameter families of spherical dihedral pentagona (convex and non convex) tilings with 12 faces.

$$\mathfrak{P}^*_{(\mathscr{C}_1,\tau^*)},\ \tau^* \in]0,\arccos(\tfrac{\sqrt{3}}{3})[\setminus\{\arctan(\tfrac{\sqrt{2}}{2})\};$$

$$\mathfrak{P}^{**}_{(\mathscr{C}_2,\tau^{**})},\ \tau^{**} \in]0,\tfrac{\pi}{2}[\setminus\{\arccos((\tfrac{1}{8409}\left(41\sqrt{2803}+58\sqrt{5606}\right))\}.$$

As we shall see, the set composed by the union of these two families is arcwise-connected in $\mathfrak{T}_5$.

2 The family of monohedral spherical tiling $\mathfrak{P}_{(\mathscr{C},\tau)}$

Let us explain, briefly, the procedure carried out to generate the one-parameter family of spherical tilings, $\mathfrak{P}_{(\mathscr{C},\tau)}, \tau \in]0,\pi[\setminus\{\frac{1}{2}\arccos(-\frac{1}{3})\}$, each one of which composed by four congruent pentagons.

First, consider the following subset of spherical points,

$$\mathscr{C} = \{X \in S^2 : X \in \widehat{PS} \vee X \in \widehat{PR} \vee X \in \widehat{PQ}\},$$

where A and B are two distinct points in the sphere such that $\widehat{AOB} = \arcsin(\frac{1}{3}) + \frac{\pi}{2}$ and C is a point in the sphere such that $[ABC]$ defines an equilateral triangle of angles $\frac{2\pi}{3}$, see fig. 1(a), and the points Q, S and R are the midpoints of the spherical segments $\widehat{AB}, \widehat{BC}$ and $\widehat{CA}$, respectively.

Consider, now, the orbit of $\mathscr{C}$ under the action of $\mathscr{I}$, the subgroup of the isometry group of the tetrahedrical spherical tiling generated by the rotations $\mathscr{R}_{(S,\pi)}$ and $\mathscr{R}_{(C,\frac{2\pi}{3})}$. Notice that, any element of $\mathscr{I}$ has A, B, C, Q, S, R as fixed points.

For each value of $\tau \in]0,\pi[\setminus\{\frac{1}{2}\arccos(-\frac{1}{3})\}$, the action of $\mathscr{I}$ on $\mathscr{C}$ defines a class of

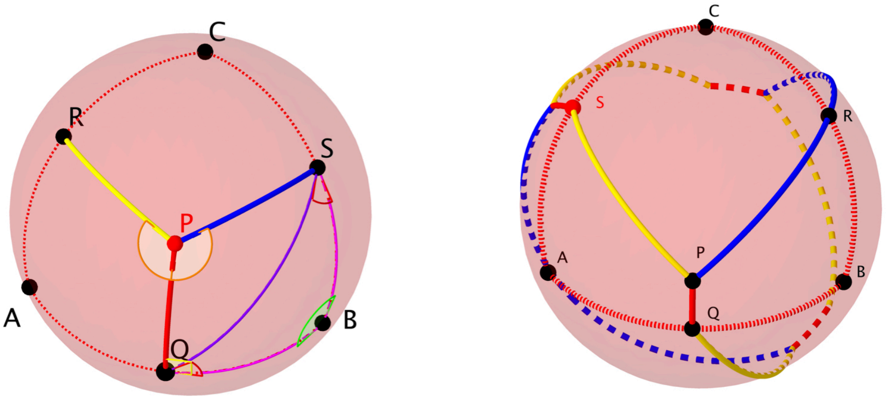

(a) $\mathscr{C}$ (b) $\mathfrak{P}_{(\mathscr{C},\frac{\pi}{10})}$

Figure 1: Generating cell and the corresponding tiling for $\tau = \pi/10$.

spherical monohedral pentagonal tilings denoted by $\mathfrak{P}_{(\mathscr{C},\tau)}$, see [9].

For each $\tau \in]0,\pi[\setminus\{\frac{1}{2}\arccos(-\frac{1}{3})\}$, $\mathfrak{P}_{(\mathscr{C},\tau)}$ is a monohedral tiling composed by four non-convex pentagons, each one of area π and whose length edges are, in cyclic order, given by $(b,a,2a,b,a)$, with $b=\tau$ and $a=\arccos(\frac{\sqrt{2}}{2}\sin(\tau))$. Besides, $\mathfrak{P}_{(\mathscr{C},\tau)}$ has eight vertices, six of them of valence 3, being the other two of valence 2, see some of the representatives of this family in figures 2(a) and 2(c).

The case of $\mathfrak{P}_{(\mathscr{C},\tau)}$ with $\tau = \frac{1}{2}\arccos(-\frac{1}{3})$ corresponds to the tetrahedral spherical tiling, see figure 2(b), and the cases $\tau \in \{0,\pi\}$ correspond to tilings composed by spherical lunes, see figure 2(d).

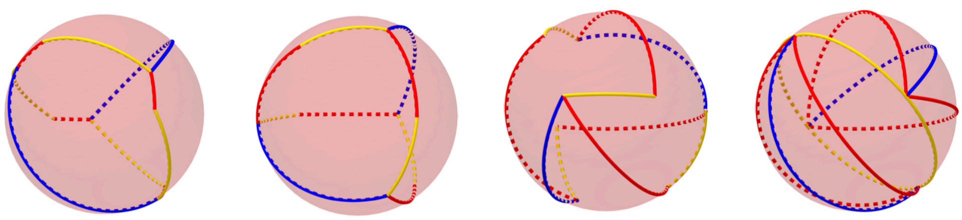

(a) $\mathfrak{P}_{(\mathscr{C},\frac{\pi}{8})}$ (b) $\mathfrak{P}_{(\frac{1}{2}\arccos(-\frac{1}{3}))}$ (c) $\mathfrak{P}_{(\mathscr{C},\arccos(-\frac{1}{\sqrt{3}}))}$ (d) $\mathfrak{P}_{(\mathscr{C},\pi)}$

Figure 2: Some elements of $\mathfrak{P}_{(\mathscr{C},\tau)}$

These results led to the the natural question.

What do we get by means of a similar procedure but starting from the other monohedral regular tilings of the sphere?

In the next section we will tackle this question taking the monohedral hexahedric tiling of the sphere as the starting point.

3 Two one-parameter families of spherical dihedral tilings by spherical pentagons

Consider one of the quadrangular faces, $[A,B,C,D]$, of the regular hexahedric spherical tiling. Without loss of generality we may assume that the isosceles, non equilateral, spherical triangle $[A,B,C]$ has as corresponding angles $\frac{\pi}{3}, \frac{\pi}{3}, \frac{2\pi}{3}$. Let Q, R and S be the midpoints of the arcs $\widehat{AB}$, $\widehat{BC}$ and $\widehat{CA}$, respectively.

Having in mind, the use of a similar procedure as the one indicated in the previous section, we should study separately two cases according to the dynamic generated by the displacement of a point P, in one case, in the arc $\widehat{QC}$, and make an angle of $\dfrac{\pi}{2}$ with the arc $\widehat{AB}$, and in the other case, in the arc $\widehat{AR}$ and make an angle of $\dfrac{\pi}{6}$ with the arc $\widehat{AB}$, see table 1.

In the first case consider the set,

$$\mathscr{C}_1 = \{X \in S^2 : X \in \widehat{PS} \vee X \in \widehat{PR} \vee X \in \widehat{PQ} \vee X \in \widehat{SA}\}$$

and in the second case consider the set,

$$\mathscr{C}_2 = \{X \in S^2 : X \in \widehat{PS} \vee X \in \widehat{PR} \vee X \in \widehat{PQ} \vee X \in \widehat{RB}\}.$$

Using GeoGebra to make some explorations and making use of some of the symmetries of the hexahedral tiling, we end up with the tiling, $\mathfrak{P}^*_{(\mathscr{C}_1,\tau^*)}$, in the first case and with the tiling $\mathfrak{P}^{**}_{(\mathscr{C}_1,\tau^{**})}$, see table 1. The details will be given in the following sections.

From now on and without loss of generality, let's consider: $A = (\frac{\sqrt{3}}{3}, -\frac{\sqrt{6}}{3}, 0)$, $B = (\frac{\sqrt{3}}{3}, \frac{\sqrt{6}}{3}, 0)$, $C = (\frac{\sqrt{3}}{3}, 0, \frac{\sqrt{6}}{3})$, $Q = (1,0,0)$, $R = (\frac{\sqrt{2}}{2}, \frac{1}{2}, \frac{1}{2})$, $S = (\frac{\sqrt{2}}{2}, -\frac{1}{2}, \frac{1}{2})$.

	Tilings.	Cell, $\mathscr{C}_i, i \in \{1,2\}$.	Planar Graph.
1st Case $\mathfrak{P}^*_{(\mathscr{C}_1,\frac{\pi}{4})}$	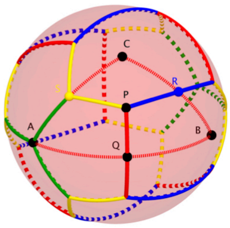	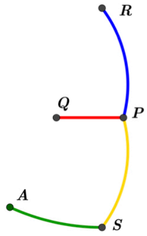	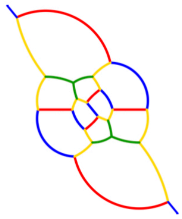
2nd Case $\mathfrak{P}^{**}_{(\mathscr{C}_2,\frac{\pi}{4})}$	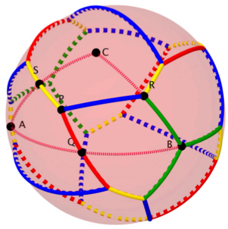	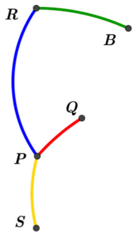	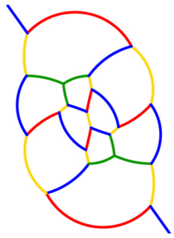

Table 1: Elements of dihedral pentagonal tilings, for $\widehat{QOP} = \frac{\pi}{4}$, in first case, and $\widehat{AOP} = \frac{\pi}{4}$, in the second case, the "generator" cell, $\mathscr{C}_1$ and $\mathscr{C}_2$, and the planar graph by stereographic projection in plane $z = -1$.

3.1 Elements of $\mathfrak{P}^*_{(\mathscr{C}_1,\tau^*)}$

The construction of the one parameter family of tilings $\mathfrak{P}^*_{(\mathscr{C}_1,\tau^*)}$, is based on the case where $P \in \widehat{QC}$, $\widehat{QOP} = \tau^*$, $\tau^* \in [0, \arccos\left(\frac{\sqrt{3}}{3}\right)]$. These conditions imply that $P = (\cos(\tau^*), 0, \sin(\tau^*))$.

First we note that for $\tau^* \in \{0, \arctan\left(\frac{\sqrt{2}}{2}\right), \arccos\left(\frac{\sqrt{3}}{3}\right)\}$, $\mathfrak{P}^*_{(\mathscr{C},\tau^*)}$ does not correspond to a pentagonal tiling. In fact, for $\tau = 0$ we have a dihedral tiling with six equilateral spherical triangle and six spherical rombus (fig 3(a)); if $\tau^* = \arctan\left(\frac{\sqrt{2}}{2}\right)$ we get a tiling, not edge to edge, composed by six spherical pentagons and six isosceles spherical triangles (fig 3(b)). For $\tau^* = \arccos\left(\frac{\sqrt{3}}{3}\right)$, we end up with a monohedral spherical tiling composed by twelve isosceles spherical triangle (fig 3(b)).

Looking at the illustration given in table 1, we notice that in the second row of this table, the points A, S and P are vertices of the tiling and the points Q and R are exactly the midpoints of edges of the tiling. The arc measure of the elements of $\mathscr{C}_1$ are:

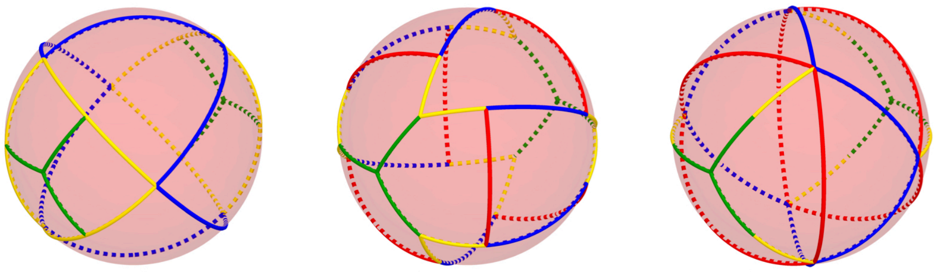

(a) $\mathfrak{P}^*_{(\mathscr{C}_1,0)}$ (b) $\mathfrak{P}^*_{\left(\mathscr{C}_1,\arctan\left(\frac{\sqrt{2}}{2}\right)\right)}$ (c) $\mathfrak{P}^*_{\left(\mathscr{C}_1,\arccos\left(\frac{\sqrt{3}}{3}\right)\right)}$

Figure 3: Degenerated cases of $\mathfrak{P}^*_{(\mathscr{C}_1,\tau^*)}$, $\tau^* \in \{0, \arctan\left(\frac{\sqrt{2}}{2}\right), \arccos\left(\frac{\sqrt{3}}{3}\right)\}$.

$$\widehat{PQ} = \tau^* = c$$
$$\widehat{PR} = \widehat{PS} = \arccos\left(\tfrac{1}{2}\sin(\tau^*) + \tfrac{\sqrt{2}}{2}\cos(\tau^*)\right) = b$$
$$\widehat{SA} = \arccos\left(\tfrac{\sqrt{6}}{3}\right) = a.$$

Each element of this family of tilings has two non congruent pentagonal prototiles, with the following edge cyclic configurations $(a,b,2c,b,a)$ and $(b,2b,2c,2b,b)$.

The angles of the arcs, bellow specified, are:

$$\widehat{QPS} = \arccos\left(\frac{\sqrt{\sin^2(\tau^*)}\left(2-\sqrt{2}\cot(\tau^*)\right)}{\sqrt{-2\sqrt{2}\sin(2\tau^*)-\cos(2\tau^*)+5}}\right)$$
$$\widehat{PSA} = \arccos\left(-\frac{2\sin(\tau^*)}{\sqrt{-2\sqrt{2}\sin(2\tau^*)-\cos(2\tau^*)+5}}\right)$$
$$\widehat{CSP} = \arccos\left(\frac{2\sin(\tau^*)}{\sqrt{-2\sqrt{2}\sin(2\tau^*)-\cos(2\tau^*)+5}}\right)$$
$$\widehat{RPQ} = \arccos\left(\frac{\sqrt{\sin^2(\tau^*)}\left(2-\sqrt{2}\cot(\tau^*)\right)}{\sqrt{-2\sqrt{2}\sin(2\tau^*)-\cos(2\tau^*)+5}}\right)$$
$$\widehat{SAQ} = \frac{\pi}{3}$$
$$\widehat{SPR} = 2\pi - (\widehat{QPS} + \widehat{RPQ}) = 2(\pi - \widehat{QPS})$$

In order to obtain the spherical tilings, $\mathfrak{P}^*_{(\mathscr{C}_1,\tau^*)}$, we consider the following set of spherical isometries, $\mathscr{I} = \{\mathscr{R}_{(R,\pi)}, \mathscr{R}_{(AOQ1)}, \mathscr{R}_{(R_2,\pi)}, \mathscr{R}_{(A,\frac{2\pi}{3})}\}$, composed by three rotations, identified by its center and angle, and a reflection identified by the plane of reflection, where $Q_1 = \mathscr{R}_{(R,\pi)}(Q), R_2 = \mathscr{R}_{(AOQ1)}(R)$.

The matricial representation of the element of $\mathscr{I}$ is given by:

$$\mathscr{R}_{(R,\pi)}=\begin{pmatrix}0&\frac{1}{\sqrt{2}}&\frac{1}{\sqrt{2}}\\ \frac{1}{\sqrt{2}}&-\frac{1}{2}&\frac{1}{2}\\ \frac{1}{\sqrt{2}}&\frac{1}{2}&-\frac{1}{2}\end{pmatrix};\quad \mathscr{R}_{(AOQ1)}=\begin{pmatrix}0&-\frac{1}{\sqrt{2}}&\frac{1}{\sqrt{2}}\\ -\frac{1}{\sqrt{2}}&\frac{1}{2}&\frac{1}{2}\\ \frac{1}{\sqrt{2}}&\frac{1}{2}&\frac{1}{2}\end{pmatrix};$$
$$\mathscr{R}_{(R2,\pi)}=\begin{pmatrix}-1&0&0\\ 0&-1&0\\ 0&0&1\end{pmatrix};\quad \mathscr{R}_{(A,\frac{2\pi}{3})}=\begin{pmatrix}0&-\frac{1}{\sqrt{2}}&-\frac{1}{\sqrt{2}}\\ -\frac{1}{\sqrt{2}}&\frac{1}{2}&-\frac{1}{2}\\ \frac{1}{\sqrt{2}}&\frac{1}{2}&-\frac{1}{2}\end{pmatrix}.$$

Consider $\mathscr{C}_1^0=\mathscr{C}_1$ (graphically represented in the second row and third column of table 1), $\mathscr{C}_1^1=\mathscr{R}_{(R,\pi)}(\mathscr{C}_1^0)$ $\mathscr{C}_1^2=\mathscr{R}_{(AOQ1)}(\mathscr{C}_1^1)$, $\mathscr{C}_1^3=\mathscr{R}_{(R_2,\pi)}(\mathscr{C}_1^2)$, $\mathscr{C}_1^4=\mathscr{R}_{(A,\frac{2\pi}{3})}(\bigcup_{i=0}^{3}\mathscr{C}_1^i)$, and $\mathscr{C}_1^5=\mathscr{R}_{(A,\frac{2\pi}{3})}(\mathscr{C}_1^4)$.

Under these conditions the set $\mathscr{C}_1^5$ defines the spherical tiling $\mathfrak{P}^*_{(\mathscr{C}_1,\tau^*)}$.

Thus, for each angle $\tau^*\in]0,\arccos(\frac{\sqrt{3}}{3})[\setminus\{\arctan(\frac{\sqrt{2}}{2})\}$, the process described above, defines a spherical dihedral tiling with: twenty vertices; thirty edges; and the faces are twelve spherical classes of non congruent pentagons, equally distributed, see fig. 4.

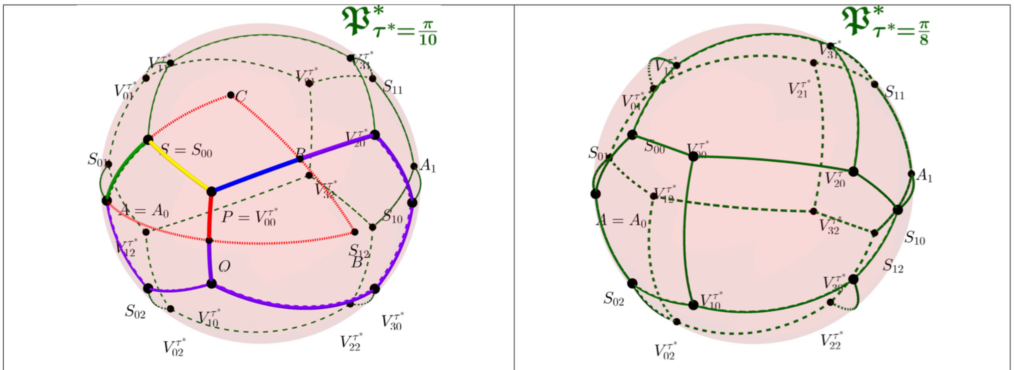

$A0=(\frac{\sqrt{3}}{3},-\frac{\sqrt{6}}{3},0)$	$A1=\mathscr{R}_O(A0)=(-\frac{\sqrt{3}}{3},\frac{\sqrt{6}}{3},0)$
$S00=(\frac{\sqrt{2}}{2},-\frac{1}{2},\frac{1}{2})$	$S10=\mathscr{R}_O(S01)=(0,1,0)$
$S01=(0,-1,0)$	$S11=\mathscr{R}_{(A0,\frac{2\pi}{3})}(S10)=(-\frac{\sqrt{2}}{2},\frac{1}{2},\frac{1}{2})$
$S02=\mathscr{R}_{(A0,\frac{4\pi}{3})}(S00)=(\frac{\sqrt{2}}{2},-\frac{1}{2},-\frac{1}{2})$	$S12=\mathscr{R}_{(A0,\frac{4\pi}{3})}(S10)=(-\frac{\sqrt{2}}{2},\frac{1}{2},-\frac{1}{2})$
$V_{00}^{\tau^*}=(\cos\tau^*,0,\sin\tau^*)$	$V_{20}^{\tau^*}=(\frac{\sqrt{2}}{2}\sin\tau^*,\frac{\sqrt{2}}{2}\cos\tau^*+\frac{1}{2}\sin\tau^*,\frac{\sqrt{2}}{2}\cos\tau^*-\frac{1}{2}\sin\tau^*)$
$V_{01}^{\tau^*}=(-\frac{\sqrt{2}}{2}\sin\tau^*,-\frac{\sqrt{2}}{2}\cos\tau^*-\frac{1}{2}\sin\tau^*,\frac{\sqrt{2}}{2}\cos\tau^*-\frac{1}{2}\sin\tau^*)$	$V_{21}^{\tau^*}=(-\cos\tau^*,0,\sin\tau^*)$
$V_{02}^{\tau^*}=(\frac{\sqrt{2}}{2}\sin\tau^*,\frac{\sqrt{2}}{2}\cos\tau^*-\frac{1}{2}\sin\tau^*,-\frac{\sqrt{2}}{2}\cos\tau^*-\frac{1}{2}\sin\tau^*)$	$V_{22}^{\tau^*}=(-\frac{\sqrt{2}}{2}\sin\tau^*,\frac{\sqrt{2}}{2}\cos\tau^*-\frac{1}{2}\sin\tau^*,-\frac{\sqrt{2}}{2}\cos\tau^*-\frac{1}{2}\sin\tau^*)$
$V_{10}^{\tau^*}=(\cos\tau^*,0,-\sin\tau^*)$	$V_{30}^{\tau^*}=(\frac{\sqrt{2}}{2}\sin\tau^*,\frac{\sqrt{2}}{2}\cos\tau^*+\frac{1}{2}\sin\tau^*,-\frac{\sqrt{2}}{2}\cos\tau^*+\frac{1}{2}\sin\tau^*)$
$V_{11}^{\tau^*}=(\frac{\sqrt{2}}{2}\sin\tau^*,-\frac{\sqrt{2}}{2}\cos\tau^*+\frac{1}{2}\sin\tau^*,\frac{\sqrt{2}}{2}\cos\tau^*+\frac{1}{2}\sin\tau^*)$	$V_{31}^{\tau^*}=(-\frac{\sqrt{2}}{2}\sin\tau^*,\frac{\sqrt{2}}{2}\cos\tau^*-\frac{1}{2}\sin\tau^*,\frac{\sqrt{2}}{2}\cos\tau^*+\frac{1}{2}\sin\tau^*)$
$V_{12}^{\tau^*}=(-\frac{\sqrt{2}}{2}\sin\tau^*,-\frac{\sqrt{2}}{2}\cos\tau^*+\frac{1}{2}\sin\tau^*,-\frac{\sqrt{2}}{2}\cos\tau^*+\frac{1}{2}\sin\tau^*)$	$V_{32}^{\tau^*}=(-\cos\tau^*,0,-\sin\tau^*)$

Figure 4: Vertices of $\mathfrak{P}^*_{(\mathscr{C}_1,\tau^*)}$, and images of $\mathfrak{P}^*_{(\mathscr{C}_1,\frac{\pi}{10})}$ and $\mathfrak{P}^*_{(\mathscr{C}_1,\frac{\pi}{8})}$.

3.2 Elements of $\mathfrak{P}^{**}_{(\mathscr{C}_2,\tau^{**})}$

The construction of the one parameter family of tilings $\mathfrak{P}^{**}_{(\mathscr{C}_2,\tau^{**})}$, is based on the case where $P \in \widehat{AR}$, $\widehat{AOP} = \tau^{**}$, $\tau^{**} \in [0, \frac{\pi}{2}]$. These conditions imply that:

$$P = \left(\tfrac{\sqrt{3}}{3}\cos(\tau^{**}) + \tfrac{\sqrt{2}}{2}\sin(\tau^{**}), -\tfrac{\sqrt{6}}{3}\cos(\tau^{**}) + \tfrac{1}{2}\sin(\tau^{**}), \tfrac{1}{2}\sin(\tau^{**})\right).$$

First we note that for $\tau^{**} \in \{0, \arccos\left(\left(\frac{1}{8409}\left(41\sqrt{2803} + 58\sqrt{5606}\right)\right), \frac{\pi}{2}\right\}$, $\mathfrak{P}^{**}_{(\mathscr{C},\tau^{**})}$ does not correspond a pentagonal tiling. In fact, for $\tau^{**} = 0$ we get a dihedral spherical tiling, with six spherical scalene triangles and six spherical pentagons (fig 5(a)); if $\tau^{**} = \tau_1^{**} = \arccos\left(\left(\frac{1}{8409}\left(41\sqrt{2803} + 58\sqrt{5606}\right)\right)\right)$ we get a dihedral tiling, not edge to edge, composed by twelve spherical rombus (fig 5(b)); for $\tau^{**} = \frac{\pi}{2}$, we end up with a dihedral spherical tiling, composed by six scalene spherical triangles and six spherical rombus (fig 5(c)).

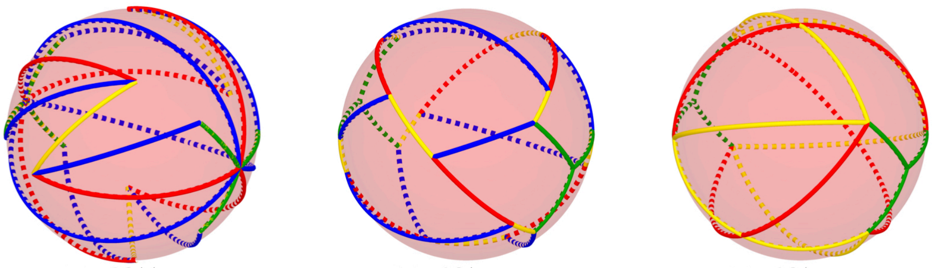

(a) $\mathfrak{P}^{**}_{(\mathscr{C}_2,0)}$ (b) $\mathfrak{P}^{*}_{(\mathscr{C}_2,\tau_1)}$ (c) $\mathfrak{P}^{*}_{(\mathscr{C}_2,\frac{\pi}{2})}$

Figure 5: Degenerated cases of $\mathfrak{P}^{**}_{(\mathscr{C}_2,\tau^{**})}$, $\tau^{**} \in \{0, \tau_1^{**}, \frac{\pi}{2}\}$.

Looking at the illustration given in table 1, we notice that in the third row of this table, the points P, R and B are vertices of the tiling and the points Q and S are exactly the midpoints of edges of the tiling. The arc measure of the elements of $\mathscr{C}_2$ are:

$$\widehat{PQ} = \arccos\left(\tfrac{1}{6}\left(2\sqrt{3}\cos(\tau^{**}) + 3\sqrt{2}\sin(\tau^{**})\right)\right) = d$$
$$\widehat{PR} = \tfrac{\pi}{2} - \tau^{**} = c$$
$$\widehat{PS} = \arccos\left(\tfrac{1}{6}\left(3\sin(\tau^{**}) + 2\sqrt{6}\cos(\tau^{**})\right)\right) = b$$
$$\widehat{RB} = \arccos\left(\tfrac{\sqrt{6}}{3}\right) = a.$$

Each element of this family of tilings has two non congruent pentagonal prototiles, with the following edge cyclic configurations $(a, c, 2d, b, a)$ and $(b, 2c, 2d, 2b, c)$.

The angles of the arcs, bellow specified, are:

$$\widehat{SPR} = \arccos\left(\frac{\sqrt{\cos^2(\tau^{**})}\left(\sqrt{6}-4\tan(\tau^{**})\right)}{\sqrt{-4\sqrt{6}\sin(2\tau^{**})-5\cos(2\tau^{**})+13}}\right)$$
$$\widehat{RPQ} = \arccos\left(\frac{\sqrt{\cos^2(\tau^{**})}\left(\sqrt{6}-2\tan(\tau^{**})\right)}{\sqrt{-2\sqrt{6}\sin(2\tau^{**})+\cos(2\tau^{**})+7}}\right)$$
$$\widehat{BRP} = \arccos\left(-\frac{2\left(\sqrt{6}\cos(\tau^{**})-6\sin(\tau^{**})\right)}{3\sqrt{-4\sqrt{6}\sin(2\tau^{**})-5\cos(2\tau^{**})+13}}\right)$$
$$\widehat{QPS} = 2\pi - (\widehat{RPQ}+\widehat{SPR})$$
$$\widehat{QBR} = \frac{\pi}{3}$$

In order to obtain the spherical tilings, $\mathfrak{P}^{**}_{(\mathscr{C}_2,\tau^{**})}$, we consider the following set of spherical isometries, $\mathscr{I}_2 = \{\mathscr{R}_{(S,\pi)}, \mathscr{R}_{(Q_1,\pi)}, \mathscr{R}_{(R_2,\pi)}, \mathscr{R}_{(B,\frac{2\pi}{3})}\}$, composed by four rotations, identified by its center and angle, where $Q_1 = \mathscr{R}_{(S,\pi)}(Q)$, $R_1 = \mathscr{R}_{(S,\pi)}(R)$, $R_2 = \mathscr{R}_{(Q_1,\pi)}(R_1)$.

The matricial representation of the element of $\mathscr{I}_2$ is given by:

$$\mathscr{R}_{(S,\pi)} = \begin{pmatrix} 0 & -\frac{1}{\sqrt{2}} & \frac{1}{\sqrt{2}} \\ -\frac{1}{\sqrt{2}} & -\frac{1}{2} & -\frac{1}{2} \\ \frac{1}{\sqrt{2}} & -\frac{1}{2} & -\frac{1}{2} \end{pmatrix}; \quad \mathscr{R}_{(Q_1,\pi)} = \begin{pmatrix} -1 & 0 & 0 \\ 0 & 0 & -1 \\ 0 & -1 & 0 \end{pmatrix};$$
$$\mathscr{R}_{(R_2,\pi)} = \begin{pmatrix} 0 & \frac{1}{\sqrt{2}} & -\frac{1}{\sqrt{2}} \\ \frac{1}{\sqrt{2}} & -\frac{1}{2} & -\frac{1}{2} \\ -\frac{1}{\sqrt{2}} & -\frac{1}{2} & -\frac{1}{2} \end{pmatrix}; \quad \mathscr{R}_{(B,\frac{2\pi}{3})} = \begin{pmatrix} 0 & \frac{1}{\sqrt{2}} & \frac{1}{\sqrt{2}} \\ \frac{1}{\sqrt{2}} & \frac{1}{2} & -\frac{1}{2} \\ -\frac{1}{\sqrt{2}} & \frac{1}{2} & -\frac{1}{2} \end{pmatrix}.$$

Consider, $\mathscr{C}_2^0 = \mathscr{C}_2 \setminus \{\widehat{RB}\}$ (graphically represented in the third row and third column of table 1), $\mathscr{C}_2^1 = \mathscr{R}_{(S,\pi)}(\mathscr{C}_2^0)$, $\mathscr{C}_2^2 = \mathscr{R}_{(Q_1,\pi)}(\mathscr{C}_2^1)$, $\mathscr{C}_2^3 = \mathscr{R}_{(R_2,\pi)}(\mathscr{C}_2^2)$, considering $B' = \mathscr{R}_{(O,\pi)}(B)$, $\mathscr{C}_2^4 = \mathscr{R}_{(B,\frac{2\pi}{3})}(\bigcup_{i=0}^{3}\mathscr{C}_1^i) \cup \{\widehat{RB}, \widehat{R_1B'}\}$, $\mathscr{C}_2^5 = \mathscr{R}_{(B,\frac{2\pi}{3})}(\mathscr{C}_2^4)$.

Under these conditions the set $\mathscr{C}_2^5$ define the spherical tiling $\mathfrak{P}^{**}_{(\mathscr{C}_2,\tau)}$.

Thus, for each angle $\tau^{**} \in]0, \frac{\pi}{2}[\setminus \{\arccos((\frac{1}{8409}(41\sqrt{2803}+58\sqrt{5606}))\}$, the process described above, defines a spherical dihedral tiling with: twenty vertices; thirty edges; and the faces are twelve spherical classes of non congruent pentagons, equally distributed, see fig. 6.

3.3 From the prototile to the construction of $\mathfrak{P}^{*}_{(\mathscr{C}_1,\tau)}$ and $\mathfrak{P}^{**}_{(\mathscr{C}_2,\tau)}$

In each of the tilings, of $\mathfrak{P}^{*}_{(\mathscr{C}_1,\tau^{*})}$ $\mathfrak{P}^{**}_{(\mathscr{C}_2,\tau^{**})}$, there is a set of four spherical pentagons, $\mathscr{P}$, that generate it, applying rotations, of angles $\frac{2\pi}{3}$ and $\frac{4\pi}{3}$, around the axis OB, see figure 7. We can

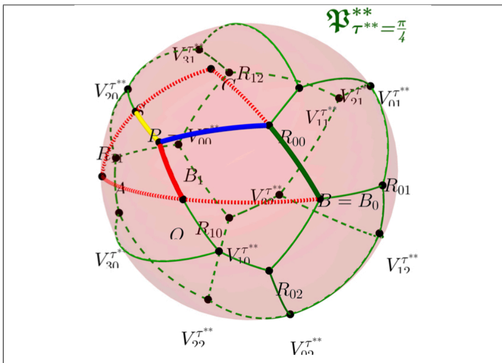	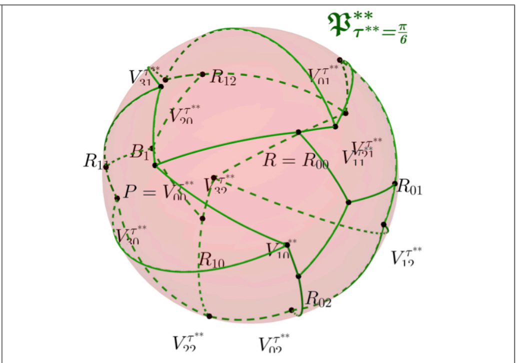
$B=V_1=(\frac{\sqrt{3}}{3},\frac{\sqrt{6}}{3},0)$ $R=(\frac{\sqrt{2}}{2},\frac{1}{2},\frac{1}{2})$ $R_{01}=\mathscr{R}_{(B,\frac{4\pi}{3})}(R)=(0,1,0)$ $R_{02}=\mathscr{R}_{(B,\frac{2\pi}{3})}(R)=(\frac{\sqrt{2}}{2},\frac{1}{2},-\frac{1}{2})$ $V_{00}^{\tau^{**}}=(\frac{\sqrt{3}}{3}\cos\tau^{**}+\frac{\sqrt{2}}{2}\sin\tau^{**},-\frac{\sqrt{6}}{3}\cos\tau^{**}+\frac{1}{2}\sin\tau^{**},\frac{1}{2}\sin\tau^{**})$ $V_{01}^{\tau^{**}}=(-\frac{\sqrt{3}}{3}\cos\tau^{**},\sin\tau^{**},\frac{\sqrt{6}}{3}\cos\tau^{**})$ $V_{02}^{\tau^{**}}=(-\frac{\sqrt{3}}{3}\cos\tau^{**}+\frac{\sqrt{2}}{2}\sin\tau^{**},\frac{1}{2}\sin\tau^{**},-\frac{\sqrt{6}}{3}\cos\tau^{**}-\frac{1}{2}\sin\tau^{**})$ $V_{10}^{\tau^{**}}=(\frac{\sqrt{3}}{3}\cos\tau^{**}+\frac{\sqrt{2}}{2}\sin\tau^{**},\frac{\sqrt{6}}{3}\cos\tau^{**}-\frac{1}{2}\sin\tau^{**},-\frac{1}{2}\sin\tau^{**})$ $V_{11}^{\tau^{**}}=(\frac{\sqrt{3}}{3}\cos\tau^{**},\frac{\sqrt{6}}{3}\cos\tau^{**},\sin\tau^{**})$ $V_{12}^{\tau^{**}}=(\frac{\sqrt{3}}{3}\cos\tau^{**}-\frac{\sqrt{2}}{2}\sin\tau^{**},\frac{\sqrt{6}}{3}\cos\tau^{**}+\frac{1}{2}\sin\tau^{**},-\frac{1}{2}\sin\tau^{**})$	$V_{11}=\mathscr{R}_O(B)=(-\frac{\sqrt{3}}{3},-\frac{\sqrt{6}}{3},0)$ $R'=\mathscr{R}_{1O}(R)=(-\frac{\sqrt{2}}{2},-\frac{1}{2},-\frac{1}{2})$ $R_{11}=\mathscr{R}_{(B,\frac{4\pi}{3})}(R')=(0,-1,0)$ $R_{12}=\mathscr{R}_{(B,\frac{2\pi}{3})}(R')=(-\frac{\sqrt{2}}{2},-\frac{1}{2},\frac{1}{2})$ $V_{20}^{\tau^{**}}=(\frac{\sqrt{3}}{3}\cos\tau^{**},-\sin\tau^{**},\frac{\sqrt{6}}{3}\cos\tau^{**})$ $V_{21}^{\tau^{**}}=(-\frac{\sqrt{3}}{3}\cos\tau^{**}-\frac{\sqrt{2}}{2}\sin\tau^{**},\frac{\sqrt{6}}{3}\cos\tau^{**}-\frac{1}{2}\sin\tau^{**},\frac{1}{2}\sin\tau^{**})$ $V_{22}^{\tau^{**}}=(\frac{\sqrt{3}}{3}\cos\tau^{**}-\frac{\sqrt{2}}{2}\sin\tau^{**},-\frac{1}{2}\sin\tau^{**},-\frac{\sqrt{6}}{3}\cos\tau^{**}-\frac{1}{2}\sin\tau^{**})$ $V_{30}^{\tau^{**}}=(-\frac{\sqrt{3}}{3}\cos\tau^{**}+\frac{\sqrt{2}}{2}\sin\tau^{**},-\frac{\sqrt{6}}{3}\cos\tau^{**}-\frac{1}{2}\sin\tau^{**},-\frac{1}{2}\sin\tau^{**})$ $V_{31}^{\tau^{**}}=(-\frac{\sqrt{3}}{3}\cos\tau^{**},-\frac{\sqrt{6}}{3}\cos\tau^{**},\sin\tau^{**})$ $V_{32}^{\tau^{**}}=(-\frac{\sqrt{3}}{3}\cos\tau^{**}-\frac{\sqrt{2}}{2}\sin\tau^{**},-\frac{\sqrt{6}}{3}\cos\tau^{**}+\frac{1}{2}\sin\tau^{**},-\frac{1}{2}\sin\tau^{**})$

Figure 6: Vertices of $\mathfrak{P}^{**}_{(\mathscr{C}_2,\tau^{**})}$, and images of $\mathfrak{P}^{**}_{(\mathscr{C}_2,\frac{\pi}{4})}$ and $\mathfrak{P}^{**}_{(\mathscr{C}_2,\frac{\pi}{6})}$.

also note that the set $\mathscr{P}$ is invariant by rotations of angle π around the axis OS, so there is a set, $\mathscr{P}_t$, of two non congruent pentagons of $\mathscr{P}$, which generate all the tiling. In fact, the protoile of the tiling, $\mathscr{P}_t$, corresponds to two adjacent and non-congruent spherical pentagons of the tiling. An illustration of the set $\mathscr{P}$ corresponds to the four visible pentagons in figure 7(a), for $\mathfrak{P}^{*}_{\frac{\pi}{7}}$, and in figure 7(b), for $\mathfrak{P}^{**}_{\frac{\pi}{7}}$.

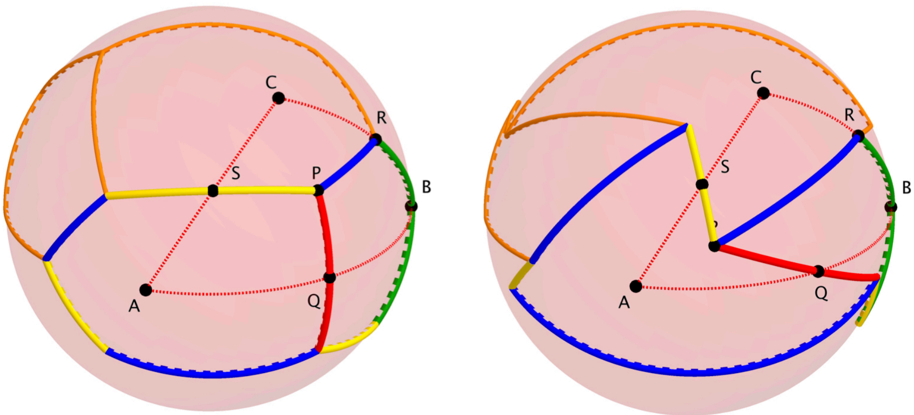

(a) $\mathfrak{P}^{*}_{\frac{\pi}{7}}$ (b) $\mathfrak{P}^{**}_{\frac{\pi}{7}}$

Figure 7: Representation of spherical Pentagons of the tiles prototiles.

4 Topological properties of $\mathfrak{P}^*_{(\mathscr{C}_1,\tau)}$ and $\mathfrak{P}^{**}_{(\mathscr{C}_2,\tau)}$

Let $\mathfrak{T}$ be the set of all tilings of S^2. Denote by ρ the metric in S^2, induced by the usual metric of $\mathbb{R}^3$ and by d_H the Hausdorff metric in $\mathfrak{T}$. Recall that, for any $X,Y \subset \mathfrak{T}$,

$$d_H(X,Y) = \max\{\sup_{x\in X}[\inf_{y\in Y} \rho(x,y)], \sup_{y\in Y}[\inf_{x\in X} \rho(x,y)]\}.$$

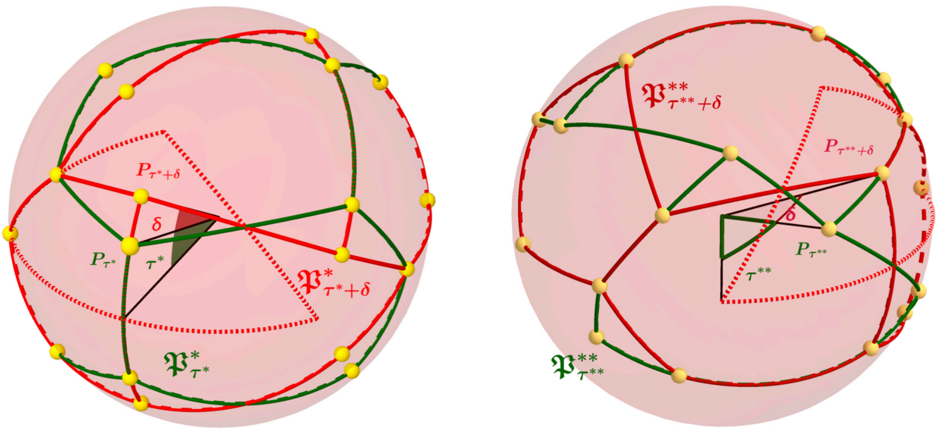

(a) $\mathfrak{P}^*_{\tau^*}$ and $\mathfrak{P}^*_{\tau^*+\delta}$ (b) $\mathfrak{P}^{**}_{\tau^{**}}$ and $\mathfrak{P}^{**}_{\tau^{**}+\delta}$

Figure 8: Representation of the tilings prototiles.

Consider the tilings: $\mathfrak{P}^*_{\tau^*}$; $\mathfrak{P}^*_{\tau^*+\delta}$; $\mathfrak{P}^{**}_{\tau^{**}}$; $\mathfrak{P}^{**}_{\tau^{**}+\delta}$. Having into account the geometric properties of the respective prototiles (see figure 8), it is straightforward to conclude that: $d_H(\mathfrak{P}^*_{\tau^*}, \mathfrak{P}^*_{\tau^*+\delta}) = \delta$ and $d_H(\mathfrak{P}^{**}_{\tau^{**}}, \mathfrak{P}^{**}_{\tau^{**}+\delta}) = \delta$. [1]

Let $\mathfrak{P}^* = \{\mathfrak{P}^*_{(\mathscr{C}_1,\tau^*)}, \tau^* \in [0, \arccos(\frac{\sqrt{3}}{3})]\}$ and $\mathfrak{P}^{**} = \{\mathfrak{P}^{**}_{(\mathscr{C}_2,\tau^{**})}, \tau^{**} \in [0, \frac{\pi}{2}]\}$, and consider the maps:

$$\varphi^* : [0, \arccos\left(\frac{\sqrt{3}}{3}\right)] \longrightarrow \mathfrak{P}^* \subset \mathfrak{T}(S^2); \qquad \varphi^{**} : [0, \frac{\pi}{2}] \longrightarrow \mathfrak{P}^{**} \subset \mathfrak{T}(S^2).$$

$$\tau^* \longmapsto \mathfrak{P}^*_{\tau^*} \qquad \tau^{**} \longmapsto \mathfrak{P}^{**}_{\tau^{**}}$$

Next we will prove that these maps are continuous at any element τ^*_0 and τ^{**}_0 in the

[1] It is worthwhile to mention that GeoGebra allows dynamic illustration of these propertie. Besides, we may obtain an approximation for the Hausdorff metric.

domain of φ^* and φ^{**}, respectively.

Let $\varepsilon \in \mathbf{R}^+$ and take $\delta < \varepsilon$, if $|\tau^* - \tau_0^*| \leq \delta$ and $|\tau^{**} - \tau_0^{**}| \leq \delta$, then:

$$d_H(\mathfrak{P}^*_{\tau^*}, \mathfrak{P}^*_{\tau_0^*}) = |\tau^* - \tau_0^*| \leq \delta < \varepsilon \text{ and } d_H(\mathfrak{P}^{**}_{\tau^{**}}, \mathfrak{P}^{**}_{\tau_0^{**}}) = |\tau^{**} - \tau_0^{**}| \leq \delta < \varepsilon.$$

Therefore we can conclude that φ^* and φ^{**} are both continuous and injective.

As stated in figures 4 and 6, the tilings $\mathfrak{P}^*_{(\mathscr{C}_1,\tau^*)}$ and $\mathfrak{P}^{**}_{(\mathscr{C}_2,\tau^{**})}$ are defined by the positions of their vertices. Accordingly, we may define a continuous path joining a tiling of $\mathfrak{P}^*_{(\mathscr{C}_1,\tau^*)}$ to a tiling of $\mathfrak{P}^{**}_{(\mathscr{C}_2,\tau^{**})}$, as we will show in 4.2.

A summary of properties of the elements of the families $\mathfrak{P}^*_{(\mathscr{C}_1,\tau^*)}$ and $\mathfrak{P}^{**}_{(\mathscr{C}_2,\tau^{**})}$ can be seen in figure 9.

Let us give a characterisation of the set of all tilings of these families that belong to $\mathfrak{T}_5$. We shall represent this set by $\mathfrak{P}_{\mathfrak{D}}$ which can be seen as

$$\mathfrak{P}_{\mathfrak{D}} = \mathfrak{P}^*_{\mathfrak{J}} \cup \mathfrak{P}^{**}_{\mathfrak{J}\mathfrak{J}}$$

where

$$\mathfrak{P}^*_{\mathfrak{J}} = \{\mathfrak{P}^*_{(\mathscr{C}_1,\tau^*)}, \tau^* \in]0, \arccos(\tfrac{\sqrt{3}}{3})[\setminus\{\arctan(\tfrac{\sqrt{2}}{2})\}\}$$

and

$$\mathfrak{P}^{**}_{\mathfrak{J}\mathfrak{J}} = \{\mathfrak{P}^{**}_{(\mathscr{C}_2,\tau^{**})}, \tau^{**} \in]0, \tfrac{\pi}{2}[\setminus\{\arccos((\tfrac{1}{8409}(41\sqrt{2803}+58\sqrt{5606}))\}\}.$$

4.1 The door tiling $\mathfrak{P}_{\mathfrak{d}}$

The tilings $\mathfrak{P}^*_{\left(\mathscr{C}_1,\arccos\left(\frac{3\sqrt{11}}{11}\right)\right)}$ and $\mathfrak{P}^{**}_{\left(\mathscr{C}_2,\arccos\left(\frac{\sqrt{33}}{11}\right)\right)}$ correspond to the same tiling, $\mathfrak{P}_{\mathfrak{d}}$, which we call door tiling. In fact, taking the point P as being the point of intersection of the spherical segments $\widehat{QC}$ and $\widehat{AR}$ then its coordinates are $\left(\frac{3\sqrt{11}}{11}, 0, \frac{\sqrt{22}}{11}\right)$, the angle of $\widehat{QOP} = \arccos\left(\frac{3\sqrt{11}}{11}\right) = \tau^*$ and $\widehat{AOP} = \arccos\left(\frac{\sqrt{33}}{11}\right) = \tau^{**}$. Therefore all vertices of the tilings coincide in both families.

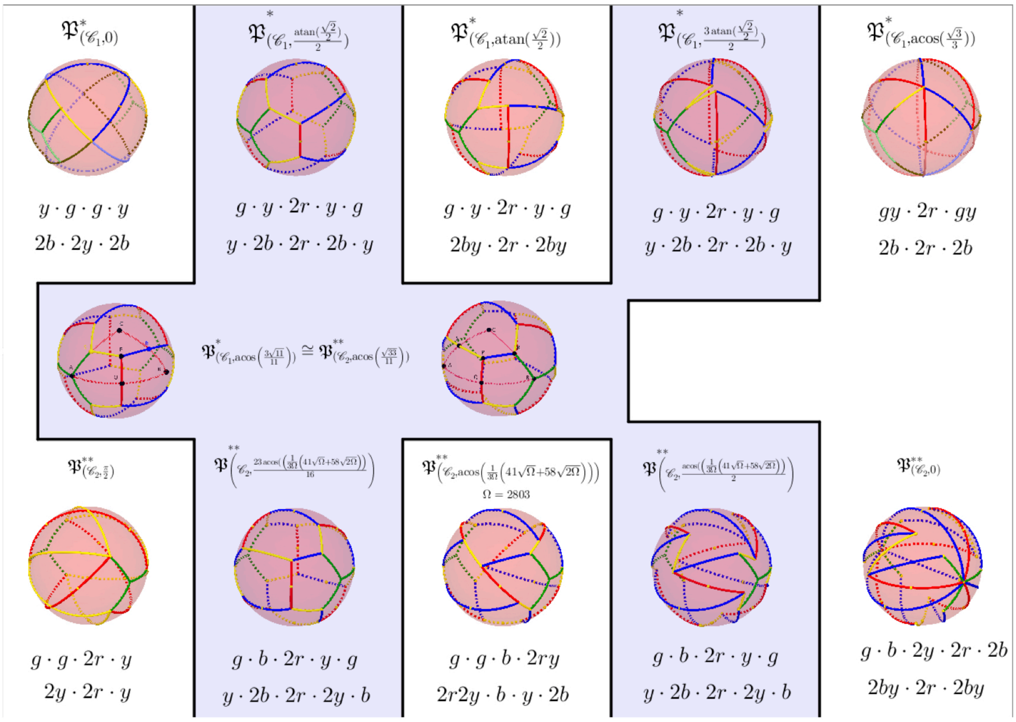

Figure 9: Geanalogy of $\mathfrak{P}_{\mathfrak{D}}$.

4.2 $\mathfrak{P}_{\mathfrak{D}}$ as a arcwised set of $\mathfrak{T}$

Now, we will show that $\mathfrak{P}_{\mathfrak{D}}$ is a arcwised subset of $\mathfrak{T}_5$, and therefore also of $\mathfrak{T}$.

Let $\mathfrak{E}_1$ and $\mathfrak{E}_2$ be two tilings of $\mathfrak{P}_{\mathfrak{D}}$ we have four cases to consider:

i) $\mathfrak{E}_1$ and $\mathfrak{E}_2$ belong to $\mathfrak{P}^*_{\mathfrak{J}}$;

ii) $\mathfrak{E}_1$ and $\mathfrak{E}_2$ belong to $\mathfrak{P}^{**}_{\mathfrak{J}\mathfrak{J}}$;

iii) $\mathfrak{E}_1 \in \mathfrak{P}^*_{\mathfrak{J}}$ and $\mathfrak{E}_2 \in \mathfrak{P}^{**}_{\mathfrak{J}\mathfrak{J}}$;

iv) $\mathfrak{E}_1 \in \mathfrak{P}^{**}_{\mathfrak{J}\mathfrak{J}}$ and $\mathfrak{E}_2 \in \mathfrak{P}^*_{\mathfrak{J}}$;

In the first case there exist t_1, t_2 in $[0, \arccos\left(\frac{\sqrt{3}}{3}\right)]$ such as $\mathfrak{E}_1 = \mathfrak{P}^*_{t_1}$ and $\mathfrak{E}_2 = \mathfrak{P}^*_{t_2}$. The map $\varphi^i(t) = \varphi^*(t_1 + (t_2 - t_1)t)$ is a continuous map for $t \in [0,1]$, with $\varphi^i(0) = \varphi^*(t_1) = \mathfrak{E}_1$ and $\varphi^i(1) = \varphi^*(t_2) = \mathfrak{E}_2$. The second case is analogous to the first case, in fact there exist t_1, t_2 in $[0, \frac{\pi}{2}]$ such as $\mathfrak{E}_1 = \mathfrak{P}^{**}_{t_1}$ and $\mathfrak{E}_2 = \mathfrak{P}^{**}_{t_2}$ and we can consider the continuous map $\varphi^{ii}(t) = \varphi^{**}(t_1 + (t_2 - t_1)t),\ t \in [0,1]$.

For the third case, the tiling $\mathfrak{P}_{\mathfrak{d}}$ plays a relevant role. Since $\mathfrak{E}_1$ and $\mathfrak{E}_2$ belongs, respectively, to $\mathfrak{P}^*_{\mathfrak{J}}$ and $\mathfrak{P}^{**}_{\mathfrak{J}\mathfrak{J}}$, there exist $t_1 \in [0, \arccos\left(\frac{\sqrt{3}}{3}\right)]$ and $t_2 \in [0, \frac{\pi}{2}]$ such as $\mathfrak{E}_1 = \mathfrak{P}^*_{t_1}$ and $\mathfrak{E}_2 = \mathfrak{P}^{**}_{t_2}$. Considering the map

$$\varphi^{iii}(t) = \begin{cases} \varphi^*\left(t_1 + 2t\left(\arccos\left(\frac{3\sqrt{11}}{11}\right) - t_1\right)\right) & 0 \le t \le \frac{1}{2} \\ \varphi^{**}\left(\arccos\left(\frac{\sqrt{33}}{11}\right) + 2\left(t - \frac{1}{2}\right)\left(t_2 - \arccos\left(\frac{\sqrt{33}}{11}\right)\right)\right) & \frac{1}{2} < t \le 1 \end{cases},$$

one has, $\varphi^{iii}(0) = \mathfrak{P}^*_{t_1}$, $\varphi^{iii}(\frac{1}{2}) = \mathfrak{P}_{\mathfrak{d}} = \mathfrak{P}^*_{\arccos\left(\frac{3\sqrt{11}}{11}\right)} = \mathfrak{P}^{**}_{\arccos\left(\frac{\sqrt{33}}{11}\right)}$ and $\varphi^{iii}(1) = \mathfrak{P}^{**}_{t_2}$.

As we shall see,

$$\forall_{t_0 \in [0,1]} \forall_{\varepsilon > 0} \exists_{\delta > 0} \, |t - t_0| < \delta \implies |\varphi^{iii}(t) - \varphi^{iii}(t_0)| < \varepsilon,$$

which means that φ^{iii} is continuous.

If $t_0 \in [0, \frac{1}{2}[$ or $t_0 \in]\frac{1}{2}, 1]$ the map φ^{iii} is continuous in t_0 by the continuity of the maps φ^* and φ^{**}.

Let us show the continuity φ^{iii} at $t_0 = \frac{1}{2}$.

Let $\varepsilon > 0$.

For any $t \in [0, \frac{1}{2}[$,

$d_H(\varphi^{iii}(t), \varphi^{iii}(\frac{1}{2})) = d_H(\varphi^*(t), \varphi^*(\frac{1}{2}))$, i.e.,

$d_H(\varphi^{iii}(t), \varphi^{iii}(\frac{1}{2})) = d_H(\mathfrak{P}_{t_1 + 2t(\arccos\left(\frac{3\sqrt{11}}{11}\right) - t_1)}, \mathfrak{P}_{\arccos\left(\frac{3\sqrt{11}}{11}\right)})$,

$d_H(\varphi^{iii}(t), \varphi^{iii}(\frac{1}{2})) = 2|t - \frac{1}{2}| \, |\arccos\left(\frac{3\sqrt{11}}{11}\right) - t_1|$.

For $t \in]\frac{1}{2}, 1]$,

$d_H(\varphi^{iii}(t), \varphi^{iii}(\frac{1}{2})) = d_H(\varphi^{**}(t), \varphi^{**}(\frac{1}{2})) = 2\left|t - \frac{1}{2}\right| \left|t_2 - \arccos\left(\frac{\sqrt{33}}{11}\right)\right|$.

Considering $\delta < min\{\frac{\varepsilon}{2\left|\arccos\left(\frac{3\sqrt{11}}{11}\right) - t_1\right|}, \frac{\varepsilon}{2\left|t_2 - \arccos\left(\frac{\sqrt{33}}{11}\right)\right|}\}$ we then have that

$|t - \frac{1}{2}| < \delta \implies |\varphi^{iii}(t) - \varphi^{iii}(\frac{1}{2})| < \varepsilon$,

therefore φ^{iii} is a continuous map.

Finaly, if $\mathfrak{E}_2$ and $\mathfrak{E}_1$ belongs, respectively, to $\mathfrak{P}_{\mathfrak{J}\mathfrak{J}}$ and $\mathfrak{P}_{\mathfrak{J}}$, there exist $t_1 \in [0, \frac{\pi}{2}]$ and $t_2 \in [0, \arccos\left(\frac{\sqrt{3}}{3}\right)]$ such as $\mathfrak{E}_1 = \mathfrak{P}^{**}_{t_1}$ and $\mathfrak{E}_2 = \mathfrak{P}^{*}_{t_2}$.Now, considering the map:

$$\varphi^{iv}(t) = \begin{cases} \varphi^{**}\left(t_1 + 2t\left(\arccos\left(\frac{\sqrt{33}}{11}\right) - t_1\right)\right) & 0 \leq t \leq \frac{1}{2} \\ \varphi^{*}\left(\arccos\left(\frac{3\sqrt{11}}{11}\right) + 2\left(t - \frac{1}{2}\right)\left(t_2 - \arccos\left(\frac{3\sqrt{11}}{11}\right)\right)\right) & \frac{1}{2} < t \leq 1 \end{cases},$$

one has $\varphi^{iv}(0) = \mathfrak{P}^{**}_{t_1}$, $\varphi^{iv}(\frac{1}{2}) = \mathfrak{P}_{\mathfrak{d}} = \mathfrak{P}^{**}_{\arccos\left(\frac{3\sqrt{33}}{11}\right)} = \mathfrak{P}^{*}_{\arccos\left(\frac{3\sqrt{11}}{11}\right)}$ and $\varphi^{iv}(1) = \mathfrak{P}^{*}_{t_2}$.

To proof that φ^{iv} is a continuous map, it suffices to show that φ^{iv} is continuous at $\frac{1}{2}$.

Let $\varepsilon > 0$. Considering $\delta < min\left\{\frac{\varepsilon}{2\left|\arccos\left(\frac{\sqrt{33}}{11}\right) - t_1\right|}, \frac{\varepsilon}{2\left|t_2 - \arccos\left(\frac{3\sqrt{11}}{11}\right)\right|}\right\}$ we may conclude that $d_H(\varphi^{iv}(t), \varphi^{iv}(\frac{1}{2})) < \varepsilon$. Therefore, φ^{iv} is continuous path in $\mathfrak{P}_{\mathfrak{D}}$.

In each one of the four cases, given two elements of $\mathfrak{P}_{\mathfrak{D}}$, $\mathfrak{E}_1$ and $\mathfrak{E}_2$, we have a continuous path, φ, joinning $\mathfrak{E}_1$ and $\mathfrak{E}_2$. Thus, $\mathfrak{P}_{\mathfrak{D}}$ is an arcwise connected set of $\mathfrak{T}_5$.

5 Conclusions

In this work, we present two new classes of dihedral tiling of the sphere $\mathfrak{P}^{*}_{\mathfrak{J}}$ and $\mathfrak{P}^{*}_{\mathfrak{J}\mathfrak{J}}$, by spherical pentagons, whose union is an arcwised connected set.

We also add some new knowledge about dihedrical spherical tilings by twelve pentagons namely topological characterisation of a special subset of these families of pentagonal tilings. The use of special tools created in GeoGebra, for the study of spherical tilings, has proved, once again, to be very useful in the search of new results. An important advantage of the applications created for this research is their interactivity capabilities and visualisation, promoting conjectures which where stated using formal proofs. One of the created applications enable us to get the Hausdorff measure between any two spherical pentagons of this family. The conjectures were also tested using the GeoGebra CAS capabilities. In future works we intend to generalise the strategy here described and apply it to other *cells* immersed in other spherical triangles, hoping to give some relevant contributions to the current knowledge of this subject.

Author Affiliation

Ana Maria D'Azevedo Breda

Departamento de Matemática, Universidade de Aveiro

Campus Universitário de Santiago

3810-193 Aveiro, Portugal

ambreda@ua.pt

José Manuel Dos Santos Dos Santos

Universidade Aberta

Rua da Escola Politécnica 141-147

1269-001 Lisboa, Portugal

dossantosdossantos@gmail.com

Acknowledgement

This work was supported in part by the Portuguese Foundation for Science and Technology (FCT — Fundação para a Ciência e a Tecnologia), through CIDMA — Centre for Research and Development in Mathematics and Applications, within project UID/MAT/04106/2013.

References

[1] Catarina P Avelino and Altino F Santos. 'Geometric and combinatorial structure of a class of spherical folding tesselations—II'. In: *AUSTRALASIAN JOURNAL OF COMBINATORICS* 70.1 (2018), pp. 104–122. URL: http://ajc.maths.uq.edu.au/pdf/70/ajc_v70_p104.pdf.

[2] Catarina P. Avelino and Altino F. Santos. 'Geometric and combinatorial structure of a class of spherical folding tessellations — I'. In: *Czechoslovak Mathematical Journal* 67.4 (2017), pp. 891–918. ISSN: 1572-9141. DOI: 10.21136/CMJ.2017.0610-15. URL: https://doi.org/10.21136/CMJ.2017.0610-15.

[3] Catarina P Avelino and Altino F Santos. 'Spherical and planar folding tessellations by kites and equilateral triangles'. In: *Australas. J. Combin* 53 (2012), pp. 109–125.

[4] Catarina Pina Avelino and Altino Manuel Folgado dos Santos. 'Spherical folding tessellations by kites and isosceles triangles: a case of adjacency'. In: *Mathematical Communications* 19.1 (2014), pp. 1–28. URL: https://http://www.mathos.unios.hr/mc/index.php/mc/article/download/483/141.

[5] Catarina Avelino and Altino Santos. 'Spherical folding tessellations by kites and isosceles triangles IV'. In: *ARS MATHEMATICA CONTEMPORANEA* 11.1 (2015), pp. 59–78. URL: https://amc-journal.eu/index.php/amc/article/download/703/852.

[6] CP Avelino and AF Santos. 'Spherical Folding Tessellations by Kites and Isosceles Triangles II'. In: *International Journal of Pure and Applied Mathematics* 85.1 (2013), pp. 45–67.

[7] Carlos Beltrán. 'A facility location formulation for stable polynomials and elliptic Fekete points'. In: *Foundations of Computational Mathematics* 15.1 (2015), pp. 125–157. URL: https://perswww.kuleuven.be/~u0017946/publications/Papers97/art97a-Saff-Kuijlaars-MI/Saff-Kuijlaars-MathIntel97.pdf.

[8] Johann S Brauchart and Peter J Grabner. 'Distributing many points on spheres: minimal energy and designs'. In: *Journal of Complexity* 31.3 (2015), pp. 293–326. URL: https://arxiv.org/pdf/1407.8282.pdf.

[9] Ana M d'Azevedo Breda and José M Dos Santos Dos Santos. 'A new class of monohedral pentagonal spherical tilings with GeoGebra'. In: *Portugaliae Mathematica* 74.3 (2018), pp. 257–266. DOI: 10.4171/PM/2006.

[10] Ana M d'Azevedo Breda and José M Dos Santos Dos Santos. 'Spherical Geometry and Spherical Tilings with GeoGebra'. In: *Journal for Geometry and Graphics* 22.2 (2018), pp. 283–299. ISSN: 1433-8157.

[11] Ana M d'Azevedo Breda and José M Dos Santos Dos Santos. 'Spherical tiling with GeoGebra - New results, challenges and open problems.' In: (2019in press).

[12] Ana MR Azevedo Breda. 'A class of tilings of S^2'. In: *Geometriae Dedicata* 44.3 (1992), pp. 241–253. URL: https://rd.springer.com/article/10.1007/BF00181393.

[13] Bart De Nijs et al. 'Entropy-driven formation of large icosahedral colloidal clusters by spherical confinement'. In: *Nature materials* 14.1 (2015), p. 56. URL: web.science.uu.nl/SCM/Articles/2015/de%20Nijs_NatureMater_2015.pdf.

[14] Sander Dedoncker et al. 'Bézier tilings of the sphere and their applications in benchmarking multipatch isogeometric methods'. In: *Computer Methods in Applied Mechanics and Engineering* 332 (2018), pp. 255–279. ISSN: 0045-7825. DOI: https://doi.org/10.1016/j.cma.2017.12.013. URL: http://www.sciencedirect.com/science/article/pii/S004578251730765X.

[15] Michel Deza et al. 'Fullerenes as tilings of surfaces'. In: *Journal of chemical information and computer sciences* 40.3 (2000), pp. 550–558. URL: http://citeseerx.ist.psu.edu/viewdoc/download?doi=10.1.1.105.5973&rep=rep1&type=pdf.

[16] Mircea V Diudea and Csaba L Nagy. *Periodic nanostructures*. Vol. 7. Springer Science & Business Media, 2007. DOI: 10.1007/978-1-4020-6020-5.

[17] Honghao Gao, Nan Shi and Min Yan. 'Spherical tiling by 12 congruent pentagons'. In: *Journal of Combinatorial Theory, Series A* 120.4 (2013), pp. 744–776. ISSN: 0097-3165. DOI: https://doi.org/10.1016/j.jcta.2012.12.006. URL: http://www.sciencedirect.com/science/article/pii/S0097316512001896.

[18] Joachim König, Arielle Leitner and Danny Neftin. 'Almost-regular Dessins d'Enfant on a torus and sphere'. In: *Topology and its Applications* 243 (2018), pp. 78–99. ISSN: 0166-8641. DOI: https://doi.org/10.1016/j.topol.2018.05.002. URL: http://www.sciencedirect.com/science/article/pii/S0166864118303250.

[19] Ali Asghar Rezaei. 'Polygonal tiling of some surfaces containing fullerene molecules'. In: *Iranian Journal of Mathematical Chemistry* 5.2 (2014), pp. 99–105. URL: http://ijmc.kashanu.ac.ir/article_7375_490966fb9747f786985dfc15d4bc6a1a.pdf.

[20] Ali Asghar Rezaei. 'Tiling Fullerene Surface with Heptagon and Octagon'. In: *Fullerenes, Nanotubes and Carbon Nanostructures* 23.12 (2015), pp. 1033–1036. DOI: 10.1080/1536383X.2015.1057817. eprint: https://doi.org/10.1080/1536383X.2015.1057817. URL: https://doi.org/10.1080/1536383X.2015.1057817.

[21] Yuan-Zhi Tan et al. 'Carbon arc production of heptagon-containing fullerene [68]'. In: *Nature communications* 2 (2011), ncomms1431. URL: http://dx.doi.org/10.1038/ncomms1431.

[22] Yukako Ueno and Yoshio Agaoka. 'Tilings of the 2-dimensional sphere by congruent right triangles'. In: *Memoirs of the Faculty of Integrated Arts and Sciences, Hiroshima University. IV, Science reports: studies of fundamental and environmental sciences* 22 (1996), pp. 1–23. URL: http://ir.lib.hiroshima-u.ac.jp/files/public/0/673/20141016120323365034/KJ00000197303.pdf.

[23] Yukako Ueno, Yoshio Agaoka et al. 'Classification of tilings of the 2-dimensional sphere by congruent triangles'. In: *Hiroshima Mathematical Journal* 32.3 (2002), pp. 463–540. URL: http://www.math.sci.hiroshima-u.ac.jp/hmj/v32.3/P463-540.PDF.

[24] Zhi Wang et al. 'Assembly of silver Trigons into a buckyball-like Ag180 nanocage'. In: *Proceedings of the National Academy of Sciences* 114.46 (2017), pp. 12132–12137.

Chapter 6

New classes of monohedral spherical tilings by non-convex spherical hexagons and non-convex spherical pentagons with GeoGebra [23]

Once again, we will make use of GeoGebra to show how to generate new classes of monohedral non-convex hexagonal and pentagonal spherical tilings.

The one parameter class of monohedral non-convex hexagonal tilings, $\mathfrak{H}_{(\mathcal{C},\tau)}$, was obtained changing the side gluing rules of the regular spherical octahedral tiling, by local actions of particular subgroups of spherical isometries. The description of this family is given.

We also show the existence of a new family of monohedral non-convex pentagonal tiling, $\mathfrak{P}_{(\mathcal{SC},\theta_1,\theta_2)}$, which arises as a degenerated case associated to the family $\mathfrak{H}_{(\mathcal{C},0)}$. The geometrical and combinatorial properties of these families are described.

New classes of monohedral spherical tilings by non-convex spherical hexagons and non-convex spherical pentagons with GeoGebra

Ana Maria D'Azevedo Breda[1] and José Manuel Dos Santos Dos Santos[2]

[1] Universidade de Aveiro, Departamento de Matemática, Aveiro, Portugal
ambreda@ua.pt
[2] Universidade Aberta, Departamento de Ciências e Tecnologia, Lisboa, Portugal
dossantosdossantos@gmail.com

Abstract

In previous works we have illustrate a procedure to obtain spherical tiling with GeoGebra. We have found new classes of monohedral spherical tilings by four spherical pentagons, and new class of dihedral spherical tiling by twelve spherical pentagons. One again, we will make use of GeoGebra to show how we can generate new classes of monohedral non-convex hexagonal spherical tilings, $\mathfrak{H}_{(\mathscr{C},\tau)}$, changing the side gluing rules of the regular spherical octahedral tiling, by local action of particular subgroups of spherical isometries.

In relation to one of the new classes, by hexagonal tiles, we describe some of its properties. We also show the existence of a new family of monohedral pentagonal tiling which arises as a degenerated case associated to the family $\mathfrak{H}_{(\mathscr{C},0)}$. All these classes of spherical tilings have emerged as a result of an interactive construction process, only possible by the use of newly produced GeoGebra tools and the dynamic interaction capabilities of this software.

1 Introduction

Spherical tilings by right triangles were obtained by Yukako Ueno and Yoshio Agaoka in 1996 [20]. Later, in 2002, the complete classification of monohedral edge-to-edge triangular spherical tilings was achieved by the same authors [21]. They have extended the classification of triangular f-spherical foldings, studied and characterised by Ana Breda, in 1992 [3].

The classification of spherical tilings by triangles is not yet completed. In fact, little is known when the condition of being monohedral or edge-to-edge is dropped out.

The combinatorial study of spherical tilings by twelve pentagons considering all vertices of valence greater than or equal to three has been also achieved, see [11] for details. Very little is known about spherical tilings involving non-convex spherical polygons, namely, tilings where the possibility of vertices of valence two should not be dismissed. Recently, a family of spherical monohedral tiles by four congruent and non-convex spherical pentagons has been characterised [6].

Besides the theoretical mathematical aspects involved in the study of spherical tilings, they are also object of interest in other areas of knowledge and in technological applications. Walter Kohn report that the year 1984 brought a big surprise in the field of crystallography. He refers the work of:

> "D. Schechtman and co-workers that reported a beautiful x-ray pattern with unequivocal icosahedral symmetry for rapidly quenched AlMn compounds. The appropriate theory was independently developed by D. Levine and P. Steinhardt, who coined the words quasicrystal and quasiperiodic. Even more curious was the fact that R. Penrose (1984) had anticipated these concepts in purely geometric [terms], so-called Penrose tilings" [13, p. s70].

Findings of this kind reinforce the need to continue studying geometric patterns and their properties. Spherical tiling has also applications to chemistry. For instance, in the study of periodic nanostructures [10], emerging new forms of association of molecules, notably fullerenes [9], leading to a deeper study of spherical tilings by triangles, squares, pentagons [17]. In the same line of reasoning other tilings including heptagons[19] and heptagons and octagons[18] had emerged. Applications to new possibilities for new molecular patterns are exposed in [22, 15, 16, 12, 7]. Nowadays, in engineering there is a need to merge the computer aided design and computer aided engineering into a single approach, contributing to an increasing interest in studying relationships between spherical tilings and spherical Bezier curves [8]. The knowledge of spherical tilings can also be useful for the developed of some issues in computational algebra [14]. The facility location problems, spherical designs and minimal energy point configurations on spheres [1, 2] are other fields where the study of spherical tilings is quite useful.

In this article we intend to extend the knowledge of the set of spherical tilings, here denoted by $\mathfrak{T}$, presenting and characterising subsets of hexagonal spherical tilings, as well as new patterns of pentagonal tilings.

2 Related Work

It is a well-known fact that it is not possible to find a monohedral tiling of the sphere by convex spherical hexagons whose vertices have valence equal to three. However, we are interested in study of tilings of the sphere by non-convex spherical polygons, namely the existence of monohedral tilings by non-convex spherical hexagons, with some vertices with valence equal to two. In a tiling of the sphere by spherical polygons, at vertices of valence two are associated two angles whose sum is 2π, a situation that posed further problems to the investigation of the existence of such tilings. These situations may be solved making use of the dynamic capabilities of GeoGebra that have been proved to be interesting for our research.

We had created tools in GeoGebra to spherical geometry, initially we use these tools to obtain some well known spherical tilings and provide illustrations of some new spherical tilings [5]. Namely, we found a new family of tilings of the sphere, $\widehat{\mathfrak{B}_{\frac{p}{q}}}$, $p,q \in \mathbb{N}$. This family contains the well known antiprismatic tilings, which are identified and obtained by a global action of a subgroup of spherical isometries, see [4] .

A proper adaptation to the procedure previously described to characterise the one-parameter family of tilings, $\mathfrak{P}_{(\mathscr{C},\tau)}$ with $\tau \in]0,\pi[\setminus\{\frac{1}{2}\arccos(-\frac{1}{3})\}$, by four congruent spherical non convex pentagons, see [6], determines a one-parameter family of monohedral spherical hexagonal tilings with six faces, $\mathfrak{H}_{(\mathscr{C},\tau)}, \tau \in \left]0, \arcsin\left(\frac{\sqrt{6}}{3}\right)+\frac{\pi}{2}\right[\setminus \{\arctan\left(\frac{\sqrt{2}}{2}\right)\}$.

3 Methodology

Consider one of the triangular faces, $[A,B,C]$, of the regular octahedrical spherical tiling. Without loss of generality we may assume that the equilateral, spherical triangle $[ABC]$ of angles $\frac{\pi}{2}$, has as vertices the points A,B,C whose coordinates are respectively $(1,0,0),(0,1,0),(0,0,1)$. Let Q, S and R be the midpoints of the arcs $\widehat{AB}$, $\widehat{BC}$ and $\widehat{CA}$, respectively.

Having in mind, the use of a similar procedure as the one indicated in the end of the previous section, we study the tilings arising from the dynamic displacement of a point P, in the arc $\widehat{QC}$ making an angle of $\frac{\pi}{2}$ with the arc $\widehat{AB}$, and the spherical point $D = (\frac{\sqrt{3}}{3}, -\frac{\sqrt{3}}{3}, \frac{\sqrt{3}}{3})$, crucial to the definition of the set

$$\mathscr{C} = \{X \in S^2 : X \in \widehat{PS} \vee X \in \widehat{PR} \vee X \in \widehat{PQ} \vee X \in \widehat{DR}\},$$

which is the starting cell for the generation of the tilings, see figure 1.

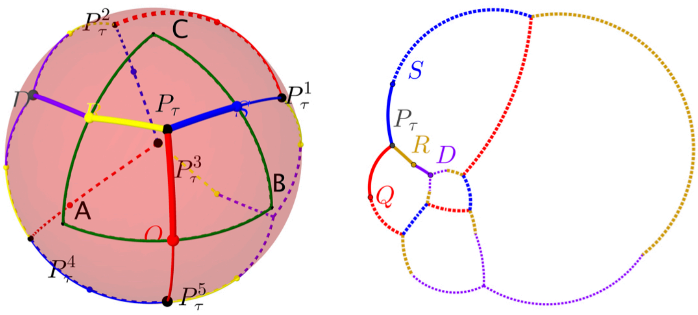

(a) $\mathfrak{H}_{(\mathscr{C},\frac{\pi}{4})}$ (b) Cell $\mathscr{C}$ in the and planar graph.

Figure 1: Monohedral spherical tiling $\mathfrak{H}_{(\mathscr{C},\frac{\pi}{4})}$ and one of its planar graph.

It should be pointed out that without the dynamic properties of GeoGebra, the approach here described would not be possible. The number of simulations to be performed to have some insights about the behaviour of the created spherical patterns would be behind the imagination.

As we will see the use of GeoGebra for making explorations and the use of some of the symmetries of the octahedral tiling end up in the one parameter family of tilings $\mathfrak{H}_{(\mathscr{C},\tau)}$. The details will be given in the following section.

4 Experimental Results

The construction of the one parameter family of tilings $\mathfrak{H}_{(\mathscr{C},\tau)}, \tau \in \left]0, \arcsin\left(\frac{\sqrt{6}}{3}\right)+\frac{\pi}{2}\right[\setminus \left\{\arctan\left(\frac{\sqrt{2}}{2}\right)\right\}$ is based in the case where $P \in \widehat{QC}$ and $\widehat{QOP} = \tau$.

The points defining the cell $\mathscr{C}$ have respectively the coordinates:

$Q = (\cos(\frac{\pi}{4}), \sin(\frac{\pi}{4}), 0);$
$R = (\cos(\frac{\pi}{4}), 0, \sin(\frac{\pi}{4}));$
$S = (0, \cos(\frac{\pi}{4}), \sin(\frac{\pi}{4}));$
$D = (\frac{\sqrt{3}}{3}, -\frac{\sqrt{3}}{3}, \frac{\sqrt{3}}{3});$
$P = (\cos(\frac{\pi}{4})\cos(\tau), \sin(\frac{\pi}{4})\cos(\tau), \sin(\tau)).$

First we note that there are three cases where $\mathfrak{H}_{(\mathscr{C},\tau)}$ does not correspond to a hexagonal tiling. In fact, for $\tau = 0$ we have a monohedral tiling with six spherical pentagons (fig 2(a)). This spherical tiling belongs to a family of two parameters not yet studied. In fact it corresponds to a family of spherical tilings, by six non-convex spherical pentagons, defined starting from eleven vertex points: six of valence two; two of valence three; and four of valence four.

If τ is equal to $\arctan\left(\frac{\sqrt{2}}{2}\right)$ we get a tiling by six congruents spherical "squares", this tiling correspond to the monohedral hexahedral tiling of the sphere (fig 2(b)). For τ equal to $\arcsin\left(\frac{\sqrt{6}}{3}\right)+\frac{\pi}{2}$, we end up with a dihedral spherical tiling composed by six congruent spherical pentagons and six congruent spherical digons (fig 2(c)).

For values of $\tau^* \in \left]0, \arcsin\left(\frac{\sqrt{6}}{3}\right)+\frac{\pi}{2}\right[\setminus \{\arctan(\frac{\sqrt{2}}{2})\}$ we have tilings of the sphere by six spherical non-convex hexagons, with fourteen vertices, six vertices with valence two and the other eighth vertices of valence three.

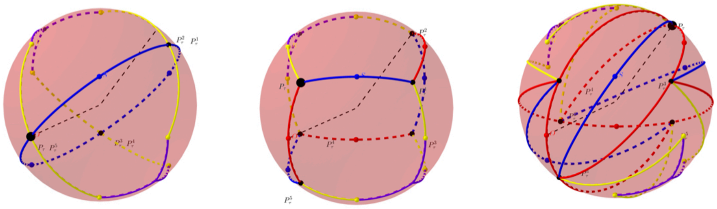

(a) $\mathfrak{H}_{(\mathscr{C},0)}$ (b) $\mathfrak{H}_{\left(\mathscr{C},\arctan\left(\frac{\sqrt{2}}{2}\right)\right)}$ (c) $\mathfrak{H}_{\left(\mathscr{C},\arcsin\left(\frac{\sqrt{6}}{3}\right)+\frac{\pi}{2}\right)}$

Figure 2: Degenerated cases of $\mathfrak{H}_{(\mathscr{C},\tau)}$.

Looking at the illustration given in figure 1(a), the points P_τ^i are vertices of the tiling and the points Q and S are exactly the midpoints of two edges of the tiling. The arc measure of the elements of $\mathscr{C}$ are:

$\widehat{PQ} = \tau = c$

$\widehat{PR} = \widehat{PS} = \arccos\left(\frac{1}{2}\cos(\tau) + \frac{\sqrt{2}}{2}\sin(\tau)\right) = b$

$\widehat{DR} = \arccos\left(\frac{\sqrt{6}}{3}\right) = a.$

Each element of this family of tilings has one non-convex hexagonal prototile, with the following edge cyclic configurations $(a,b,2b,2c,b,a)$.

The angles defined by the arcs specified bellow are:

$$\widehat{SPQ} = \arccos\left(\frac{\frac{1}{2} - \cos x\left(\frac{\cos x}{2} + \frac{\sin x}{\sqrt{2}}\right)}{\sqrt{1-\cos^2(x^2)}\sqrt{1-\left(\frac{\cos x}{2}+\frac{\sin x}{\sqrt{2}}\right)^2}}\right)$$

$\widehat{SPQ} = \widehat{QPR}$

$\widehat{RPS} = 2\pi - 2\widehat{SPQ}$

$$\widehat{PRD} = \arccos\left(\frac{\sqrt{3}\left(\frac{\sin x}{\sqrt{3}} - \sqrt{\frac{2}{3}}\left(\frac{\cos x}{2}+\frac{\sin x}{\sqrt{2}}\right)\right)}{\sqrt{1-\left(\frac{\cos x}{2}+\frac{\sin x}{\sqrt{2}}\right)^2}}\right)$$

$\widehat{RD\mathscr{R}_{(D,\frac{2\pi}{3})}(R)} = \frac{2\pi}{3}$

For obtaining the spherical tilings, $\mathfrak{H}_{(\mathscr{C},\tau)}$, we consider the following set of spherical isometries, $\mathscr{I} = \{\mathscr{R}_{(S,\pi)}, \mathscr{R}_{(Q_1,\pi)}, \mathscr{R}_{(S_2,\pi)}, \mathscr{R}_{(Q_3,\pi)}, \mathscr{R}_{(S_3,\pi)}\}$ composed by five rotations, identified by its center and angle, where $Q_1 = \mathscr{R}_{(S,\pi)}(Q)$, $S_2 = \mathscr{R}_{(S,\pi)}(Q_1)$, $Q_3 = \mathscr{R}_{(S_2,\pi)}(Q_1)$, $S_3 = \mathscr{R}_{(S_2,\pi)}(Q_3)$.

The matricial representation of the element of $\mathscr{I}$ is given by:

$$\mathscr{R}_{(S,\pi)} = \mathscr{R}_{(Q_3,\pi)} = \begin{pmatrix} -1 & 0 & 0 \\ 0 & 0 & 1 \\ 0 & 1 & 0 \end{pmatrix}, \mathscr{R}_{(S_2,\pi)} = \begin{pmatrix} 0 & 1 & 0 \\ 1 & 0 & 0 \\ 0 & 0 & 1 \end{pmatrix}, \mathscr{R}_{(Q_1,\pi)} = \mathscr{R}_{(S_3,\pi)} = \begin{pmatrix} 0 & 0 & -1 \\ 0 & -1 & 0 \\ -1 & 0 & 0 \end{pmatrix}$$

Consider $\mathscr{C}^0 = \mathscr{C}$ (graphically represented in figure 1(b)), $\mathscr{C}^1 = \mathscr{R}_{(S,\pi)}(\mathscr{C}^0)$, $\mathscr{C}^2 = \mathscr{R}_{(Q_1,\pi)}(\mathscr{C}^1)$, $\mathscr{C}^3 = \mathscr{R}_{(S_2,\pi)}(\mathscr{C}^2)$, $\mathscr{C}^4 = \mathscr{R}_{(Q_3,\pi)}(\mathscr{C}^3)$, and $\mathscr{C}^5 = \mathscr{R}_{(S_3,\pi)}(\mathscr{C}^4)$.

Under these conditions the set $\bigcup_{i=0}^{5}\mathscr{C}^i$ define the spherical tiling $\mathfrak{H}_{(\mathscr{C},\tau)}$.

Thus, for each $\tau \in \left]0, \arcsin\left(\frac{\sqrt{6}}{3}\right) + \frac{\pi}{2}\right[\setminus \{\arctan\left(\frac{\sqrt{2}}{2}\right)\}$,
the procedure described above, defines a spherical monohedral tiling with: fourteen vertices; eighteen edges; and the faces are six congruent non-convex spherical hexagons, see fig. 3.

When $\tau = 0$, $\mathfrak{H}_{(\mathscr{C},0)}$ is a spherical tiling by six spherical non-convex pentagons (the arc $\widehat{PQ}$ "dis-appeared"). We define a new cell $\mathscr{SC}$ in order to obtain the family $\mathfrak{P}_{(\mathscr{SC},\theta_1,\theta 2)}$, the details are given next. We would like to pointed out that all tiles of these tilings have one angle of measure $\frac{2\pi}{3}$, angle that is defined by to edges, congruent to $\widehat{DR}$. In these conditions we search families of tilings by six

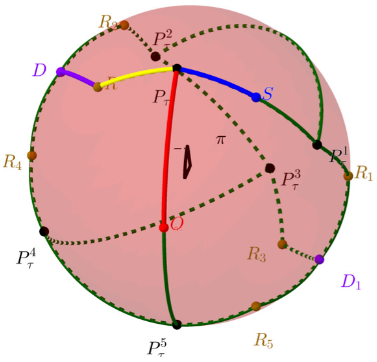

$D = (\frac{\sqrt{3}}{3}, -\frac{\sqrt{3}}{3}, \frac{\sqrt{3}}{3})$
$D_1 = (-\frac{\sqrt{3}}{3}, \frac{\sqrt{3}}{3}, -\frac{\sqrt{3}}{3})$
$R = (cos(\frac{\pi}{4}), 0, sin(\frac{\pi}{4}))$
$R_1 = (-cos(\frac{\pi}{4}), sin(\frac{\pi}{4}), 0)$
$R_2 = (0, -cos(\frac{\pi}{4}), sin(\frac{\pi}{4}))$
$R_3 = (-cos(\frac{\pi}{4}), 0, -sin(\frac{\pi}{4}))$
$R_4 = (cos(\frac{\pi}{4}), -sin(\frac{\pi}{4}), 0)$
$R_5 = (0, cos(\frac{\pi}{4}), -sin(\frac{\pi}{4}))$
$P_\tau = (\cos(\frac{\pi}{4})\cos(\tau), \sin(\frac{\pi}{4})\cos(\tau), \sin(\tau))$
$P_\tau^1 = (-\cos(\frac{\pi}{4})\cos(\tau), \sin(\tau), \sin(\frac{\pi}{4})\cos(\tau))$
$P_\tau^2 = (-\cos(\frac{\pi}{4})\cos(\tau), -\sin(\tau), \sin(\frac{\pi}{4})\cos(\tau))$
$P_\tau^3 = (-sin(\tau), -cos(\frac{\pi}{4})cos(\tau), -sin(\frac{\pi}{4})cos(\tau))$
$P_\tau^4 = (sin(\tau), -cos(\frac{\pi}{4})cos(\tau), -sin(\frac{\pi}{4})cos(\tau))$
$P_\tau^5 = (\cos(\frac{\pi}{4})\cos(\tau), \sin(\frac{\pi}{4})\cos(\tau), \sin(\tau))$

Figure 3: The tiling $\mathfrak{H}_{(\mathscr{C},\frac{\pi}{3})}$ and vertices coordinates of $\mathfrak{H}_{(\mathscr{C},\tau)}$.

non-convex spherical pentagons: with eleven vertices, six of them with valence two, two other vertices with valence three, and three vertices with valence four; each element of the tile has $(a,b,2b,b,a)$ edge cyclic configurations.

Using GeoGebra, with a procedure described in listing 1, we easily find the family $\mathfrak{P}_{(\mathscr{SC},\theta_1,\theta_2)}$ where $\mathfrak{H}_{(\mathscr{C},0)}$ is equal to $\mathfrak{P}_{(\mathscr{SC},\frac{\pi}{2}-\arccos\left(\frac{\sqrt{6}}{3}\right),\frac{\pi}{4})}$.

```
s:=x^2+y^2+z^2=1
t1=Slider(0, pi/2, pi/100, 1, 50, false, false, false, false)
t2=Slider(0, pi/2, pi/100, 1, 50, false, false, false, false)
V1=(0,0,1)
V2=(cos(t1),0,sin(t1))
V3=(cos(t2),sin(t2),0)
V4=(cos(t2+pi/4),sin(t2+pi/4),0)
a12=CircularArc(Centre(s),V1,V2,Plane((0,0,0),V1,V2))
a23=CircularArc(Centre(s),V2,V3,Plane((0,0,0),V2,V3))
a34=CircularArc(Centre(s),V3,V4,Plane((0,0,0),V3,P4))
SC10={a12,a23,a34}
SC11=Rotate(SC10,pi,Ray(Centre(s),V3))
SC12=Rotate({SC10,SC11},2pi/3,Ray(Centre(s),V1))
SC13=Rotate(SC12,2pi/3,Ray(Centre(s),V1))
```

Listing 1: GeoGebra commands to obtain $\mathfrak{P}_{(\mathscr{SC},\theta_1,\theta_2)}$.

Now, considering the vertices V^1, $V^2_{\theta_1}$ and $V^3_{\theta_2}$ and
$P = (\cos(\theta_2 + \frac{\pi}{4}), \sin(\theta_2 + \frac{\pi}{4}), 0)$, see fig. 4, our new cell is the set:
$\mathscr{SC} = \{X \in S^2 : X \in \widehat{V_1 V^2_{\theta_1}} \vee X \in \widehat{V^2_{\theta_1} V^3_{\theta_2}} \vee X \in \widehat{V^3_{\theta_2} P_4}\}$.

In the procedure described in listing 1, the set of spherical isometries to be considered for the local action is
$\mathscr{I}_1 = \{\mathscr{R}_{(V^3_{\theta_2},\pi)}, \mathscr{R}_{(V_1,\frac{2\pi}{3})}\}$
composed by two rotations. The matricial representation of the elements of $\mathscr{I}_1$ are given by:

$$\mathscr{R}_{(V^3_{\theta_2},\pi)} = \begin{pmatrix} 2\cos^2(\theta_2)-1 & 2\cos(\theta_2)\sin(\theta_2) & 0 \\ 2\cos(\theta_2)\sin(\theta_2) & 2\sin^2(\theta_2)-1 & 0 \\ 0 & 0 & -1 \end{pmatrix}; \quad \mathscr{R}_{(V_1,\frac{2\pi}{3})} = \begin{pmatrix} -\frac{1}{2} & -\frac{1}{2}\sqrt{3} & 0 \\ \frac{1}{2}\sqrt{3} & -\frac{1}{2} & 0 \\ 0 & 0 & 1 \end{pmatrix}.$$

So, let $\mathscr{SC}^0 = \mathscr{SC}$ (see figure 4), $\mathscr{SC}^1 = \mathscr{R}_{(V^3_{\theta_2},\pi)}(\mathscr{C}^0)$, $\mathscr{SC}^2 = \mathscr{R}_{(V_1,\frac{2\pi}{3})}(\mathscr{SC}^0 \cup \mathscr{SC}^1)$, $\mathscr{SC}^3 = \mathscr{R}_{(V_1,\frac{2\pi}{3})}(\mathscr{SC}^2)$.

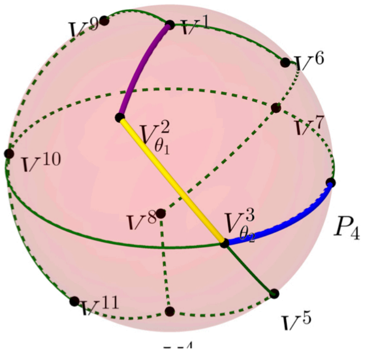

$$V^1 = (0,0,1)$$
$$V^2_{\theta_1} = (\cos(\theta_1), 0, \sin(\theta_1))$$
$$V^3_{\theta_2} = (\cos(\theta_2), \sin(\theta_2), 0)$$
$$V^4 = (0,0,-1)$$
$$V^5 = (\cos(2\theta_2)\cos(\theta_1), \cos(\theta_1)\sin(2\theta_2), -\sin(\theta_1))$$
$$V^6 = \left(\frac{-\cos(\theta_1)}{2}, \frac{\sqrt{3}\cos(\theta_1)}{2}, \sin(\theta_1)\right)$$
$$V^7 = \left(\frac{-\cos(\theta_2)}{2} - \frac{\sqrt{3}\sin(\theta_2)}{2}, \frac{\sqrt{3}\cos(\theta_2)}{2} - \frac{\sin(\theta_2)}{2}, 0\right)$$
$$V^8 = \left(-\cos(\theta_1)\sin\left(2\theta_2 + \frac{\pi}{6}\right), \cos(\theta_1)\cos\left(2\theta_2 + \frac{\pi}{6}\right), -\sin(\theta_1)\right)$$
$$V^9 = \left(\frac{-\cos(\theta_1)}{2}, -\frac{\sqrt{3}\cos(\theta_1)}{2}, \sin(\theta_1)\right)$$
$$V^{10} = \left(-\frac{1}{2}\cos(\theta_2) + \frac{\sqrt{3}}{2}\sin(\theta_2), -\frac{\sqrt{3}}{2}\cos(\theta_2) - \frac{1}{2}\sin(\theta_2), 0\right)$$
$$V^{11} = \left(\cos(\theta_1)\sin\left(2\theta_2 - \frac{\pi}{6}\right), -\cos(\theta_1)\cos\left(\frac{\pi}{6} - 2\theta_2\right), -\sin(\theta_1)\right)$$

Figure 4: The tiling $\mathfrak{P}_{(\mathscr{SC},\frac{\pi}{4},\frac{\pi}{4})}$ and vertices coordinates of $\mathfrak{P}_{(\mathscr{SC},\theta_1,\theta_2)}$.

Under these conditions the set $\bigcup_{i=0}^{3} \mathscr{SC}^i$ defines the family of monohedral spherical tiling by non-convex spherical pentagons $\mathfrak{P}_{(\mathscr{SC},\theta_1,\theta_2)}$.

5 Conclusion

In this work, we present two new classes of monohedral tilings of the sphere $\mathfrak{H}_{(\mathscr{C},\tau)}$ and $\mathfrak{P}_{(\mathscr{SC},\theta_1,\theta_2)}$, by spherical hexagons and by spherical pentagons, respectively, extending the knowledge in this topic. It should be noted that the degenerated case $\mathfrak{H}_{(\mathscr{C},0)}$ put in evidence a monohedral tiling of the sphere by six spherical pentagons, which is part of another two parameters family of spherical tiles by non-convex spherical pentagons, that had not yet been studied. This fact reinforces the interest of GeoGebra in the study of spherical tilings.

The use of special tools created in GeoGebra, for the study of spherical tilings, have proven to be very useful in the search of new results. An important advantage of the applications created for this research is their interactivity capabilities and visualisation, promoting conjectures which where starting points for the search of formal proofs. The conjectures were also tested using the GeoGebra CAS capabilities. In future works we intend to generalise the strategy here described and apply it to other type of *cells* immersed in other spherical triangles.

6 Acknowledgments

This research was supported by the Portuguese national funding agency for science, research and technology (FCT), within the Center for Research and Development in Mathematics and Applications (CIDMA), project UID/MAT/04106/2019.

References

[1] Carlos Beltrán. A facility location formulation for stable polynomials and elliptic fekete points. *Foundations of Computational Mathematics*, 15(1):125–157, 2015.

[2] Johann S Brauchart and Peter J Grabner. Distributing many points on spheres: minimal energy and designs. *Journal of Complexity*, 31(3):293–326, 2015.

[3] Ana MR Azevedo Breda. A class of tilings of s^2. *Geometriae Dedicata*, 44(3):241–253, 1992.

[4] Ana M d'Azevedo Breda and José M Dos Santos Dos Santos. Spherical geometry and spherical tilings with geogebra. *Journal for Geometry and Graphics*, 22(2):283–299, 2018.

[5] Ana M d'Azevedo Breda and José M Dos Santos Dos Santos. Spherical tiling with geogebra - new results, challenges and open problems. *Resonance-journal of science education*, 2019in press.

[6] Ana M d'Azevedo Breda and José M Dos Santos Dos Santos. A new class of monohedral pentagonal spherical tilings with geogebra. *Portugaliae Mathematica*, 74(3):257–266, 2018.

[7] Bart De Nijs, Simone Dussi, Frank Smallenburg, Johannes D Meeldijk, Dirk J Groenendijk, Laura Filion, Arnout Imhof, Alfons Van Blaaderen, and Marjolein Dijkstra. Entropy-driven formation of large icosahedral colloidal clusters by spherical confinement. *Nature materials*, 14(1):56, 2015.

[8] Sander Dedoncker, Laurens Coox, Florian Maurin, Francesco Greco, and Wim Desmet. Bézier tilings of the sphere and their applications in benchmarking multipatch isogeometric methods. *Computer Methods in Applied Mechanics and Engineering*, 332:255 – 279, 2018.

[9] Michel Deza, Patrick W Fowler, A Rassat, and Kevin M Rogers. Fullerenes as tilings of surfaces. *Journal of chemical information and computer sciences*, 40(3):550–558, 2000.

[10] Mircea V Diudea and Csaba L Nagy. *Periodic nanostructures*, volume 7. Springer Science & Business Media, 2007.

[11] Honghao Gao, Nan Shi, and Min Yan. Spherical tiling by 12 congruent pentagons. *Journal of Combinatorial Theory, Series A*, 120(4):744 – 776, 2013.

[12] Giuliana Indelicato, Newton Wahome, Philippe Ringler, Shirley A Müller, Mu-Ping Nieh, Peter Burkhard, and Reidun Twarock. Principles governing the self-assembly of coiled-coil protein nanoparticles. *Biophysical journal*, 110(3):646–660, 2016.

[13] Walter Kohn. An essay on condensed matter physics in the twentieth century. *Reviews of Modern Physics*, 71(2):S59, 1999.

[14] Joachim König, Arielle Leitner, and Danny Neftin. Almost-regular dessins d'enfant on a torus and sphere. *Topology and its Applications*, 243:78 – 99, 2018.

[15] Majid Mosayebi, Deborah K Shoemark, Jordan M Fletcher, Richard B Sessions, Noah Linden, Derek N Woolfson, and Tanniemola B Liverpool. Beyond icosahedral symmetry in packings of proteins in spherical shells. *Proceedings of the National Academy of Sciences*, 114(34):9014–9019, 2017.

[16] Manica Negahdaripour, Nasim Golkar, Nasim Hajighahramani, Sedigheh Kianpour, Navid Nezafat, and Younes Ghasemi. Harnessing self-assembled peptide nanoparticles in epitope vaccine design. *Biotechnology advances*, 35(5):575–596, 2017.

[17] Ali Asghar Rezaei. Polygonal tiling of some surfaces containing fullerene molecules. *Iranian Journal of Mathematical Chemistry*, 5(2):99–105, 2014.

[18] Ali Asghar Rezaei. Tiling fullerene surface with heptagon and octagon. *Fullerenes, Nanotubes and Carbon Nanostructures*, 23(12):1033–1036, 2015.

[19] Yuan-Zhi Tan, Rui-Ting Chen, Zhao-Jiang Liao, Jia Li, Feng Zhu, Xin Lu, Su-Yuan Xie, Jun Li, Rong-Bin Huang, and Lan-Sun Zheng. Carbon arc production of heptagon-containing fullerene [68]. *Nature communications*, 2:ncomms1431, 2011.

[20] Yukako Ueno and Yoshio Agaoka. Tilings of the 2-dimensional sphere by congruent right triangles. *Memoirs of the Faculty of Integrated Arts and Sciences, Hiroshima University. IV, Science reports: studies of fundamental and environmental sciences*, 22:1–23, 1996.

[21] Yukako Ueno, Yoshio Agaoka, et al. Classification of tilings of the 2-dimensional sphere by congruent triangles. *Hiroshima Mathematical Journal*, 32(3):463–540, 2002.

[22] Zhi Wang, Hai-Feng Su, Yuan-Zhi Tan, Stan Schein, Shui-Chao Lin, Wei Liu, Shu-Ao Wang, Wen-Guang Wang, Chen-Ho Tung, Di Sun, et al. Assembly of silver trigons into a buckyball-like ag180 nanocage. *Proceedings of the National Academy of Sciences*, 114(46):12132–12137, 2017.

Chapter 7

Conclusions

The GeoGebra tools and applications built, so far, allow the visualization and the establishment of relationships among crucial elements related with spherical tilings, greatly contribute to the research in this topic. It is in the generation of a great variety of spherical configurations / relationships that we believe GeoGebra can make a substantial contribution for the description and construction of spherical tilings, not yet explored, besides being a resource of great utility in the study of spherical geometry, in general.

Here, we have presented several new GeoGebra tools, namely in the Chapters 2 and 3, that may be used to explore spherical geometry and to explore spherical tilings. An important advantage of these applications is the interactivity and the visualisation of the created objects, promoting conjectures and the respective formal proofs. The conjectures can also be tested by the GeoGebra CAS capabilities. These capabilities allow the description of the combinatorial and geometric characterisation of the two parameter spherical tiling families $\widehat{\mathfrak{B}_{\frac{p}{q}}}$, $p, q \in \mathbb{N}$ with $gcd(p, q) = 1$, obtaining $n-$hedral spherical tilings, and expanding the well known antiprismatic dihedrical one.

In this work, we found several classes of spherical tilings, some monohedrals ($\mathfrak{T}_{(\mathcal{C},\rho)}$, $\mathfrak{P}_{(\mathcal{C},\rho)}$, $\mathfrak{H}_{(\mathcal{C},\tau)}$, $\mathfrak{P}_{(\mathcal{SC},\theta_1,\theta_2)}$), others dihedrals ($\mathfrak{P}_{\mathfrak{D}}$), with the aid of GeoGebra. The use of the tools created in GeoGebra have proved, as showed, to be quite useful for the search of new spherical tilings.

Considering the dihedral tilings here presented we got, among others, two new classes of dihedral tilings of the sphere $\mathfrak{P}^*_{\mathfrak{J}}$ and $\mathfrak{P}^*_{\mathfrak{J}\mathfrak{J}}$, by pentagons, whose union, $\mathfrak{P}_{\mathfrak{D}}$, is an arcwised connected set.

It should be noted that the degenerated case $\mathfrak{H}_{(\mathcal{C},0)}$, see chapter 6, provides an example of a monohedral tiling of the sphere by six spherical pentagons, $\mathfrak{P}_{(\mathcal{SC},\theta_1,\theta_2)}$, which is part of another two parameters family of spherical tiles by non-convex spherical pentagons, that had not yet been studied. This fact reinforces the interest of GeoGebra in the study of spherical tilings.

It is well known that there is a unique monohedral spherical tiling by convex pentagons, with twelve tile. Besides, all spherical tilings by twelve pentagons with vertices of valence three have been classified. However, admiting tilings with vertices of valence two, we found two more families of monohedral tilings by non-convex pentagons, one of them with four tiles, $\mathfrak{P}_{(\mathcal{C},\rho)}$, and the other one, $\mathfrak{P}_{(\mathcal{SC},\theta_1,\theta_2)}$, with six.

Recalling the notes made in the introduction about the tilings of the plane by pentagons, and considering our findings regarding families of monohedral spherical tilings by non-convex pentagons, the following questions remain open:

> Are there other families of monohedral tilings of the sphere by non-convex pentagons?
>
> If so, is it possible to characterize all these families?

It should also be noted that these questions can be also placed in relation to the families of monohedral tilings of the sphere by non-convex $n-$gons, with $n \in \mathbb{N}$ and $n \leq 5$.

The work presented here is a contribution to the construction of more knowledge about spherical tilings. The process here described can be applied to other types of *cells* immersed in other spherical triangles. Our strategy was applied to the cells that emerged from the tetrahedral, hexahedral and octahedral monohedral spherical tiling. Note that we only study, by these processes, cases of edge-to-edge monohedral tilings of the sphere. We still need to apply similar processes to the study of monohedral tilings that are not edge-to-edge, which as far as we know is a subject where there are still few studies.

We still need to study the configurations associated with the monohedral spherical tilings by 12 pentagonal and 20 spherical triangles. Although GeoGebra acts as an instrument of analysis and conjecture generation, which facilitates the research work, the proofs of the result have some complexity. It should also be noted that despite the use of processes involving simple concepts, the methods of proof are complex, in addition to a great difficulty in obtaining easily realisable results.

Finally, our end will be a (re) beginning ...

"Wanderer, your footsteps are
the road and nothing more;
wanderer, there is no road,
the road is made by walking."
Antonio Cipriano José María Machado Ruiz

Bibliography

[1] Y. Akama et al. Classification of spherical tilings by congruent quadrangles over pseudo-double wheels (i)–a special tiling by congruent concave quadrangles. *Hiroshima Mathematical Journal*, 43(3):285–304, 2013.

[2] D. Austin and W. Dickinson. Spherical easel. A spherical drawing program., 2009. Available online at http://merganser.math.gvsu.edu/easel/.

[3] C. P. Avelino and A. M. F. d. Santos. Spherical f-tilings by triangles and r-sided regular polygons, r$\geq$ 5. *Electron. J. Combin*, 15(1):R22, 2008.

[4] C. P. Avelino and A. M. F. d. Santos. Spherical and planar folding tessellations by kites and equilateral triangles. *Australas. J. Combin*, 53:109–125, 2012.

[5] C. P. Avelino and A. M. F. d. Santos. Spherical folding tessellations by kites and isosceles triangles ii. *International Journal of Pure and Applied Mathematics*, 85(1):45–67, 2013.

[6] C. P. Avelino and A. M. F. d. Santos. Spherical folding tessellations by kites and isosceles triangles: a case of adjacency. *Mathematical Communications*, 19(1):1–28, 2014. URL https://http://www.mathos.unios.hr/mc/index.php/mc/article/download/483/141.

[7] C. P. Avelino and A. M. F. d. Santos. Spherical folding tessellations by kites and isosceles triangles iv. *ARS MATHEMATICA CONTEMPORANEA*, 11(1):59–78, 2015. URL https://amc-journal.eu/index.php/amc/article/download/703/852.

[8] C. P. Avelino and A. M. F. d. Santos. Geometric and combinatorial structure of a class of spherical folding tessellations — i. *Czechoslovak Mathematical Journal*, 67(4): 891–918, Dec 2017. ISSN 1572-9141. doi: 10.21136/CMJ.2017.0610-15. URL https://doi.org/10.21136/CMJ.2017.0610-15.

[9] C. P. Avelino and A. M. F. d. Santos. Geometric and combinatorial structure of a class of spherical folding tesselations—ii. *AUSTRALASIAN JOURNAL OF COMBINATORICS*, 70(1):104–122, 2018. URL http://ajc.maths.uq.edu.au/pdf/70/ajc_v70_p104.pdf.

[10] C. Beltrán. A facility location formulation for stable polynomials and elliptic fekete points. *Foundations of Computational Mathematics*, 15(1):125–157, 2015. URL https://perswww.kuleuven.be/~u0017946/publications/Papers97/art97a-Saff-Kuijlaars-MI/Saff-Kuijlaars-MathIntel97.pdf.

[11] N. Bourbaki. *Elements of the History of Mathematics*. Springer Science & Business Media, 1998.

[12] J. S. Brauchart and P. J. Grabner. Distributing many points on spheres: minimal energy and designs. *Journal of Complexity*, 31(3):293–326, 2015. URL https://arxiv.org/pdf/1407.8282.pdf.

[13] A. M. R. d. Breda. A class of tilings of S^2. *Geometriae Dedicata*, 44(3):241–253, 1992.

[14] A. M. R. d. Breda. A note on octahedral spherical foldings. *Portugaliae Math*, 53, 1996.

[15] A. M. R. d. Breda and J. M. D. S. Dos Santos. Dihedral antiprismatic spherical tilings - *GeoGebra App*, 2018. URL https://ggbm.at/vybwsjm4.

[16] A. M. R. d. Breda and J. M. D. S. Dos Santos. Dihedral spherical tilings by twelve pentagons - *GeoGebra App*, 2018. URL https://ggbm.at/pppzxfcn.

[17] A. M. R. d. Breda and J. M. D. S. Dos Santos. Evolution of nets of equilateral spherical triangles - *GeoGebra App*, 2018. URL https://ggbm.at/z6qsuwzj.

[18] A. M. R. d. Breda and J. M. D. S. Dos Santos. Monohedral spherical tilings by four triangles and four pentagons - *GeoGebra App*, 2018. URL https://ggbm.at/jhvbxbhp.

[19] A. M. R. d. Breda and J. M. D. S. Dos Santos. Monohedral spherical tilings by six non-convex hexagons - *GeoGebra App*, 2018. URL https://ggbm.at/gxqnvuzr.

[20] A. M. R. d. Breda and J. M. D. S. Dos Santos. Monohedral spherical tilings by six non-convex pentagons - *GeoGebra App*, 2018. URL https://ggbm.at/hyhecte3.

[21] A. M. R. d. Breda and J. M. D. S. Dos Santos. Spherical geometry and spherical tilings with geogebra. *Journal for Geometry and Graphics*, 22(2):283–299, 2018. ISSN 1433-8157.

[22] A. M. R. d. Breda and J. M. D. S. Dos Santos. A new class of monohedral pentagonal spherical tilings with geogebra. *Portugaliae Mathematica*, 74(3):257–266, 2018. doi: 10.4171/PM/2006. URL https://ria.ua.pt/bitstream/10773/22148/1/PM_74-3_06%20257.pdf.

[23] A. M. R. d. Breda and J. M. D. S. Dos Santos. New classes of monohedral spherical tilings by non-convex spherical hexagons and non-convex spherical pentagons with geogebra. In G. Lee and Y. Jin, editors, *Proceedings of 34th International Conference on Computers and Their Applications*, volume 58 of *EPiC Series in Computing*, pages 75–82. EasyChair, 2019. doi: 10.29007/qk2k. URL https://easychair.org/publications/paper/gxVJ.

[24] A. M. R. d. Breda and J. M. D. S. Dos Santos. Spherical tiling with geogebra: New results, challenges and open problems. *Resonance-journal of science education*, 2019a. Article submitted in May, 16, 2018 and has been accepted for publication in October, 10, 2018 . The authors wait the proofs, once the article will be scheduled for publication in 2019.

[25] A. M. R. d. Breda and A. M. F. d. Santos. Dihedral f-tilings of the sphere by spherical triangles and equiangular well-centered quadrangles. *Beiträge zur Algebra und Geometrie*, 45:447–461, 2004.

[26] J. Brooks and J. Strantzen. Spherical triangles of area π and isosceles tetrahedra. *Mathematics Magazine*, 78(4):311–314, 2005.

[27] H. S. M. Coxeter. Discrete groups generated by reflections. *Annals of Mathematics*, pages 588–621, 1934.

[28] H. S. M. Coxeter. *Twelve geometric essays*. Southern Illinois Univ Pr, 1968.

[29] H. S. M. Coxeter. *Regular Complex Polytopes. Coxeter*. Cambridge University, 1974.

[30] H. Davies. Packings of spherical triangles and tetrahedra. In *Proc. Colloquium on Convexity (Copenhagen, 1965)*, pages 42–51, 1967.

[31] R. Dawson and B. Doyle. Tilings of the sphere with right triangles i: the asymptotically right families. *JOURNAL OF COMBINATORICS*, 13(2):R48, 2006. URL http://emis.ams.org/journals/EJC/Volume_13/PDF/v13i1r48.pdf.

[32] R. J. M. Dawson. An isosceles triangle that tiles the sphere in exactly three ways. *Discrete & Computational Geometry*, 30(3):459–466, 2003.

[33] R. J. M. Dawson. Tilings of the sphere with isosceles triangles. *Discrete & Computational Geometry*, 30(3):467–487, 2003.

[34] R. J. M. Dawson et al. Some new tilings of the sphere with congruent triangles. In *Renaissance Banff: Mathematics, Music, Art, Culture*, pages 489–496. Bridges Conference, 2005.

[35] B. De Nijs, S. Dussi, F. Smallenburg, J. D. Meeldijk, D. J. Groenendijk, L. Filion, A. Imhof, A. Van Blaaderen, and M. Dijkstra. Entropy-driven formation of large icosahedral colloidal clusters by spherical confinement. *Nature materials*, 14(1):56, 2015. URL web.science.uu.nl/SCM/Articles/2015/deNijs_NatureMater_2015.pdf.

[36] S. Dedoncker, L. Coox, F. Maurin, F. Greco, and W. Desmet. Bézier tilings of the sphere and their applications in benchmarking multipatch isogeometric methods. *Computer Methods in Applied Mechanics and Engineering*, 332:255 – 279, 2018. ISSN 0045-7825. doi: https://doi.org/10.1016/j.cma.2017.12.013. URL http://www.sciencedirect.com/science/article/pii/S004578251730765X.

[37] M. Deza, P. W. Fowler, A. Rassat, and K. M. Rogers. Fullerenes as tilings of surfaces. *Journal of chemical information and computer sciences*, 40(3):550–558, 2000. URL http://citeseerx.ist.psu.edu/viewdoc/download?doi=10.1.1.105.5973&rep=rep1&type=pdf.

[38] M. V. Diudea and C. L. Nagy. *Periodic nanostructures*, volume 7. Springer Science & Business Media, 2007.

[39] J. Erdős. Sphaerica: Interactive spherical geometry software. In G. W. Hart and R. Sarhangi, editors, *Proceedings of Bridges 2010: Mathematics, Music, Art, Architecture, Culture*, pages 443–446, Phoenix, Arizona, 2010. Tessellations Publishing. ISBN 978-0-98460-420-3. Available online at http://archive.bridgesmathart.org/2010/bridges2010-443.html.

[40] H. Gao, N. Shi, and M. Yan. Spherical tiling by 12 congruent pentagons. *Journal of Combinatorial Theory, Series A*, 120(4):744 – 776, 2013. ISSN 0097-3165. doi: https://doi.org/10.1016/j.jcta.2012.12.006. URL http://www.sciencedirect.com/science/article/pii/S0097316512001896.

[41] A. Goebel. Archimedes geo3d, 2008. URL http://spatialgeometry.com/drupal/en.

[42] B. Grunbaum and G. C. Shephard. Tilings by regular polygons. *Mathematics Magazine*, 50(5):227–247, 1977. URL https://www.maa.org/sites/default/files/pdf/upload_library/22/Allendoerfer/1978/0025570x.di021102.02p0230f.pdf.

[43] F. Hausdorff. Dimension und äußeres Maß. *Mathematische Annalen*, 79(1-2):157–179, 1918. URL http://www.springerlink.com/content/j3x1t373233w4713.

[44] F. Hausdorff. Set theory (reprint). *Chelsea, New York*, 1978.

[45] M. Hohenwarter and K. Fuchs. Combination of dynamic geometry, algebra and calculus in the software system geogebra. In *Computer Algebra Systems and Dynamic Geometry Systems in Mathematics Teaching Conference*, 2004. Available online at http://archive.geogebra.org/static/publications/pecs_2004.pdf.

[46] M. Hohenwarter et al. Geogebra, interactive geometry, algebra, statistics and calculus software, 2001. Available online at https://www.geogebra.org/.

[47] W. R. Inc. Wolfram programming lab, Version 12.0. Champaign, IL, 2019.

[48] G. Indelicato, N. Wahome, P. Ringler, S. A. Müller, M.-P. Nieh, P. Burkhard, and R. Twarock. Principles governing the self-assembly of coiled-coil protein nanoparticles. *Biophysical journal*, 110(3):646–660, 2016.

[49] B. Kahr and A. G. Shtukenberg. Histories of crystallography by Shafranovskii and Schuh. In *Recent advances in crystallography*. InTech, 2012.

[50] J. Kepler. *The harmony of the world*, volume 209. American Philosophical Society, 1997.

[51] W. Kohn. An essay on condensed matter physics in the twentieth century. *Reviews of Modern Physics*, 71(2):S59, 1999.

[52] J. König, A. Leitner, and D. Neftin. Almost-regular dessins d'enfant on a torus and sphere. *Topology and its Applications*, 243:78 – 99, 2018. ISSN 0166-8641. doi: https://doi.org/10.1016/j.topol.2018.05.002. URL http://www.sciencedirect.com/science/article/pii/S0166864118303250.

[53] J. M. Lee. *Riemannian manifolds: an introduction to curvature*, volume 176. Springer Science & Business Media, 2006.

[54] C. Löh. Geometric group theory, an introduction. *Universität Regensburg*, 2011.

[55] C. Mann, J. McLoud-Mann, and D. Von Derau. Convex pentagons that admit i-block transitive tilings. *Geometriae Dedicata*, 194(1):141–167, 2018.

[56] G. Maxwell. The crystallography of Coxeter groups. *Journal of Algebra*, 35(1-3):159–177, 1975.

[57] M. Mosayebi, D. K. Shoemark, J. M. Fletcher, R. B. Sessions, N. Linden, D. N. Woolfson, and T. B. Liverpool. Beyond icosahedral symmetry in packings of proteins in spherical shells. *Proceedings of the National Academy of Sciences*, 114(34):9014–9019, 2017.

[58] M. Negahdaripour, N. Golkar, N. Hajighahramani, S. Kianpour, N. Nezafat, and Y. Ghasemi. Harnessing self-assembled peptide nanoparticles in epitope vaccine design. *Biotechnology advances*, 35(5):575–596, 2017.

[59] G. Panina. Planar pseudo-triangulations, spherical pseudo-tilings and hyperbolic virtual polytopes. *arXiv preprint math/0607171*, 2006.

[60] G. Y. Panina. Pointed spherical tilings and hyperbolic virtual polytopes. *Journal of Mathematical Sciences*, 175(5):591–599, 2011.

[61] G. Polya. XII. Über die Analogie der Kristallsymmetrie in der Ebene. *Zeitschrift für Kristallographie-Crystalline Materials*, 60(1-6):278–282, 1924.

[62] M. Rao. Exhaustive search of convex pentagons which tile the plane. *arXiv preprint arXiv:1708.00274*, 2017.

[63] A. A. Rezaei. Polygonal tiling of some surfaces containing fullerene molecules. *Iranian Journal of Mathematical Chemistry*, 5(2):99–105, 2014. URL http://ijmc.kashanu.ac.ir/article_7375_490966fb9747f786985dfc15d4bc6a1a.pdf.

[64] A. A. Rezaei. Tiling fullerene surface with heptagon and octagon. *Fullerenes, Nanotubes and Carbon Nanostructures*, 23(12):1033–1036, 2015.

[65] P. S. Ribeiro. *D-pavimentações esféricas diedrais triangulares*. PhD thesis, Departamento de Matemática, 2012.

[66] S. A. Robertson. *Polytopes and symmetry*, volume 90. Cambridge University Press, 1984. URL http://catdir.loc.gov/catdir/samples/cam031/83015171.pdf.

[67] E. B. Saff and A. B. Kuijlaars. Distributing many points on a sphere. *The mathematical intelligencer*, 19(1):5–11, 1997. URL https://perswww.

kuleuven.be/~u0017946/publications/Papers97/art97a-Saff-Kuijlaars-MI/Saff-Kuijlaars-MathIntel97.pdf.

[68] Y. Sakano and Y. Akama. Classification of spherical tilings by congruent kites, darts, and rhombi–spherical hilbert's eighteenth problem. *preprint*, 2013.

[69] D. Salunke, D. Caspar, and R. Garcea. Polymorphism in the assembly of polyomavirus capsid protein vp1. *Biophysical journal*, 56(5):887, 1989.

[70] R. Schwartz, P. W. Shor, and B. Berger. Local rule simulations of capsid assembly. *Journal of Theoretical Medicine*, 6(2):81–85, 2005. ISSN 10273662. doi: 10.1080/10273660500149257. URL https://www.tandfonline.com/doi/abs/10.1080/10273660500149257.

[71] D. Sommerville. Vi.—division of space by congruent triangles and tetrahedra. *Proceedings of the Royal Society of Edinburgh*, 43:85–116, 1924.

[72] R. Stein. A new pentagon tiler. *Mathematics magazine*, 58(5):308, 1985.

[73] Y.-Z. Tan, R.-T. Chen, Z.-J. Liao, J. Li, F. Zhu, X. Lu, S.-Y. Xie, J. Li, R.-B. Huang, and L.-S. Zheng. Carbon arc production of heptagon-containing fullerene [68]. *Nature communications*, 2:ncomms1431, 2011. URL http://dx.doi.org/10.1038/ncomms1431.

[74] The Sage Developers. Sagemath, the Sage Mathematics Software System, 2017. https://www.sagemath.org.

[75] R. Twarock. Mathematical virology: a novel approach to the structure and assembly of viruses. *Philosophical Transactions of the Royal Society of London A: Mathematical, Physical and Engineering Sciences*, 364(1849):3357–3373, 2006.

[76] Y. Ueno and Y. Agaoka. Tilings of the 2-dimensional sphere by congruent right triangles. *Memoirs of the Faculty of Integrated Arts and Sciences, Hiroshima University. IV, Science reports: studies of fundamental and environmental sciences*, 22:1–23, 1996.

[77] Y. Ueno, Y. Agaoka, et al. Classification of tilings of the 2-dimensional sphere by congruent triangles. *Hiroshima Mathematical Journal*, 32(3):463–540, 2002.

[78] Z. Wang, H.-F. Su, Y.-Z. Tan, S. Schein, S.-C. Lin, W. Liu, S.-A. Wang, W.-G. Wang, C.-H. Tung, D. Sun, et al. Assembly of silver trigons into a buckyball-like ag180 nanocage. *Proceedings of the National Academy of Sciences*, 114(46):12132–12137, 2017.